

The nature and significance of the Faroe-Shetland Terrane: linking Archaean basement blocks across the North Atlantic

Holdsworth, R.E.¹, Morton, A.², Frei, D.³, Gerdes, A.⁴, Strachan, R.A.⁵, Dempsey, E.⁶, Warren, C.⁷ & Whitham, A.⁸

¹ = Department of Earth Sciences, Durham University, Durham, DH1 3LE, UK

2 = HM Research, Giddanmu, St Ishmaels SA62 3TJ, UK and CASP, University of Cambridge, Madingley Rise, Cambridge CB3 0UD, UK.

3 = Department of Earth Sciences, University of the Western Cape, 7530 Bellville, Western Cape, South Africa.

4 = Goethe-Universität Frankfurt, Institut für Geowissenschaften, Petrologie und Geochemie,
Altenhöferallee 1, 60438 Frankfurt am Main, Germany.

5 = School of Earth and Environmental Sciences, University of Portsmouth, Portsmouth, PO1 3QL, UK.

6 = School of Environmental Sciences, University of Hull, Hull, HU6 7RX, UK

7 = School of Environment, Earth and Ecosystem Sciences, The Open University, Walton Hall, Kents Hill, Milton Keynes MK7 6AA, UK.

8 = CASP, University of Cambridge, Madingley Rise, Cambridge CB3 0UD, UK.

Abstract: Core samples of the continental basement rocks that underlie the eastern Faroe-Shetland Basin (FSB) and its inshore margins west of Shetland reveal a suite of predominantly granodioritic to granitic orthogneisses (including TTG), together with lesser volumes of foliated granitoids and subordinate dioritic to mafic gneisses and amphibolites. A small area of lithologically similar gneisses also crops out onshore at North Roe/Uyea west of the Caledonian front in Shetland. In the core samples, coarse grained gneissose textures and mineralogies consistent with upper amphibolite facies metamorphism are overprinted by a weak, but ubiquitous, static greenschist facies retrogression. Later structures include widespread epidote-quartz veining, and local developments of mylonite, cataclasite, pseudotachylite and phyllonite. Regions associated with the Rona Ridge oil fields (e.g. Clair, Lancaster) also preserve extensive brittle fracturing and associated low temperature hydrothermal mineralization (quartz, adularia, calcite, pyrite/chalcopyrite) with significant fracture-hosted hydrocarbons. New and published U-Pb zircon analyses from the gneisses offshore give a relatively narrow range of Neoarchaean protolith ages (ca 2.7-2.8 Ga) spread over a geographic area of 60,000 km² west of Shetland. Detrital zircon data from overlying Triassic-Cretaceous sedimentary sequences in the FSB suggest an equivalent limited range of Neoarchaean source materials. Hf isotopic data indicate involvement of Palaeo- to Mesoarchaean crustal sources. Overall, our findings suggest that a major phase of Neoarchaean crustal formation and associated high grade metamorphism dominates basement rocks in the region. They are similar in age and lithology to the protoliths of the nearest onshore Lewisian Complex of NW Scotland (Rhiconich Terrane). However, they lack geochronological or textural evidence for the widespread Proterozoic Laxfordian events (ca 1.7-1.8 Ga) which are widespread in Scotland. This suggests that the Precambrian rocks west of Shetland - the Faroe-Shetland Terrane - can be correlated with the Archaean rocks of the

42 Central Greenland-Rae Craton and that a northern limit of Proterozoic reworking lies just
43 offshore from the north coast of Scotland.

44 **Keywords:** Lewisian; Faroe-Shetland; Neoarchaean; Nagssugtoqidian; Laxfordian; U-Pb
45 geochronology.

46

47 **Introduction**

48 The nature, age and affinities of the onshore continental basement terranes in the circum-
49 North Atlantic region are now fairly well understood (e.g. Park 2005, Wheeler et al. 2010;
50 Mason 2015 and references therein). In contrast, our knowledge of the basement in many
51 of the intervening offshore areas is relatively sparse since relatively few wells have
52 penetrated through the overlying Palaeozoic to Recent sedimentary cover sequences. Even
53 in wells where core materials exist, these have commonly not been studied in any great
54 detail. An improved understanding of the age and affinities of basement in offshore regions
55 will allow better constraints on the likely locations of major tectonic and terrane boundaries
56 across the North Atlantic. It also better constrains which onshore areas are best used as
57 surface analogues along the continental margins to investigate the potential influences of
58 basement inheritance on the structural development of the Atlantic margins.

59 In this paper, we present new lithological descriptions and the results of U-Pb and Lu-Hf
60 zircon geochronological studies from a range of basement rocks sampled in offshore
61 borehole cores taken in the region west of Shetland and north of Scotland and the Outer
62 Hebrides. These data supplement a small amount of information provided by Ritchie et al.
63 (2011), which was largely based on a more detailed unpublished report by Chambers et al.
64 (2005).

65

66 **Location and Regional Setting**

67 Geophysical evidence and geological sampling from the seabed and borehole cores suggests
68 that continental basement rocks underlie a large region north of Scotland and west of
69 Shetland. Precambrian basement rocks are exposed onshore in Shetland and on small
70 islands north of Scotland and west of Orkney (notably Foula, Sule Skerry, Stack Skerry, Rona,
71 Sula Sgeir; Fig. 1; Ritchie et al. 2011). West of the Walls Boundary Fault, most of these rocks
72 are assigned to the Lewisian Gneiss Complex (Fig. 1), although some in Shetland are thought
73 to be of younger Moine or Dalradian (i.e. Neoproterozoic) affinities (Flinn 1985). Offshore,
74 the affinities of the basement are less certain, although the rocks are generally viewed as
75 being correlatives of the Lewisian. Two prominent elongate basement ridges known as the
76 Rona Ridge and Solan Bank High are buried beneath mainly Mesozoic and younger
77 sedimentary rocks and define the southeastern margin of the Faroe-Shetland Basin. They

78 trend NE-SW running from north of Shetland to the NW tip of Scotland and lie in the
79 uplifted footwalls of Mesozoic normal faults. A basement ridge of this trend continues to
80 the south forming the Outer Hebrides island chain (Fig. 1).

81 In Scotland, the Archaean-Palaeoproterozoic Lewisian Gneiss Complex forms the basement
82 of the foreland of the Ordovician-Silurian Caledonide orogen (Fig. 1). The western limit of
83 the orogen is defined by the easterly-dipping Moine Thrust (Fig. 1), although Neoarchaean
84 basement inliers within the Caledonian hinterland have been broadly correlated with the
85 Lewisian (Friend et al. 2008). The gneiss complex represents a fragment of Laurentian crust
86 that was juxtaposed with the European plate during the Early Palaeozoic Caledonian
87 orogenic cycle, and subsequently separated from North America during the late Mesozoic to
88 early Cenozoic opening of the North Atlantic Ocean. It is dominated by orthogneisses, the
89 protoliths of which were emplaced between ca. 3.1 Ga and ca. 2.7 Ga. They were then
90 subject to high-grade metamorphism at 2.7 and 2.5 Ga, dyke intrusion at ca. 2.4 and 2.0 Ga,
91 and variably intense Palaeoproterozoic reworking at ca. 1.8-1.7 Ga (e.g. Whitehouse 1993;
92 Kinny and Friend 1997; Friend and Kinny 2001; Whitehouse and Bridgewater 2001; Kinny et
93 al. 2005; Park 2005; Wheeler et al. 2010; Mason 2012, 2016; Goodenough et al. 2013;
94 Davies and Heaman 2014; Crowley et al. 2015). This geological history has strong similarities
95 to the Nagssugtoqidian belt of SE Greenland, and the two segments of crust are thought to
96 have been contiguous prior to opening of the North Atlantic (Kalsbeek et al. 1993; Friend
97 and Kinny 2001; Park 2005).

98 The Shetland Islands form the northernmost exposures of the Caledonide orogen in the
99 British Isles (Fig. 1). A large part of Shetland is underlain by Neoproterozoic to Cambrian
100 metasedimentary successions that were deformed and metamorphosed during the
101 Caledonian orogeny (Flinn 1985; 1988). In northwest Shetland, the easterly-dipping Uyea
102 Shear Zone in the North Roe-Uyea area is probably structurally analogous to the Moine
103 Thrust (Fig. 1; Walker et al. 2016). A suite of granitic orthogneisses and metagabbros in its
104 footwall have been correlated directly with the Lewisian Gneiss Complex (Pringle 1970; Flinn
105 et al. 1979; Flinn 1985, 2009).

106 Isolated U-Pb zircon data obtained from basement gneisses from offshore boreholes north
107 and west of Shetland give ages in the range 2.7-2.8 Ga and lack any evidence for
108 Palaeoproterozoic (Laxfordian) reworking (Chambers et al. 2005). This led Ritchie et al.
109 (2011) to tentatively suggest that the Lewisian-like basement rocks lying to the west of the
110 Walls Boundary fault could be assigned to a single Neoarchaean domain they termed the
111 'Faroe-Shetland Block'. This block, they suggested, is located northward of the eastwards
112 continuation of the Nagssugtoqidian belt through mainland Scotland.

113 The present study has looked in detail at over 70 thin sections of basement gneisses from
114 the offshore region west of Shetland. Some are existing sections held by the BGS or the Clair
115 Joint Venture Group, but many are new. The locations of all offshore borehole cores that
116 contain basement referred to in the present paper are shown in Figure 1.

117

118 **Lithologies and Contact Relationships**

119 *Basement rocks*

120 The most detailed description of basement lithologies to date is given in Chambers et al.
121 (2005), summarised in Ritchie et al. (2011). It covered material studied from 42 offshore
122 boreholes from a wide region extending from west of Shetland southwards to the Stanton
123 High (west of Mull) and offshore to Rockall. In addition to thin section descriptions of
124 lithologies, these authors also carried out major and trace element geochemistry on all
125 samples.

126 The basement rocks west of Shetland are dominated by quartzofeldspathic granodioritic
127 orthogneisses, with subordinate units of more granitic, intermediate and mafic
128 compositions. Most of these gneisses are thought to be of tonalitic-trondhjemitic-dioritic
129 affinity, although this has been proven using strict geochemical criteria in only a small
130 number of samples (Chambers et al. 2005). The rocks are mostly foliated and show evidence
131 for amphibolite facies regional metamorphism variably overprinted by a weak, but
132 persistent low-grade retrogression. Later fault rocks, including mylonites and
133 pseudotachylytes, are locally preserved but are very minor constituents.

134 The most complete set of basement cores come from the sub-horizontal 206/7a-2 well
135 drilled by Elf through the Clair basement ridge in a SE to NW direction (Fig. 2a). These
136 basement rocks are described in more detail below as it is possible to see some of the
137 contact relationships of the various constituent gneisses in the six more or less continuous
138 ca 9-10 m core sections (Fig. 2b). Furthermore, they exhibit a range of lithologies that are
139 highly representative of the region west of Shetland (e.g. Chambers et al. 2005; Ritchie et al.
140 2011). Where necessary, reference will be made to other cores in cases where other
141 features have been observed that are not seen in 206/7a-2 – logs of these additional cores
142 are shown in Figure 3. Core from 206/8-8 has been varnished, so some of the best images of
143 lithology are taken from that core, together with 206/7a-2 in Figure 4.

144 Medium to coarse grained, grey granodioritic gneiss (Fig. 4a) forms ca 55% of the 60 m of
145 core from 206/7a-2. Subordinate interlayered units include medium to coarse grained pink
146 granitic gneiss (15%, Fig. 4b) and foliated coarse grained porphyritic granite (15%, Fig. 4c –
147 see also 206/9-2, Fig. 3). The latter rock type occurs as sheets apparently subparallel to the
148 gneissic layering in most cases, although a single discordant example in 206/7a-2 is
149 associated with a local cm-scale high strain shear zone (Fig. 4d). Units of green mafic gneiss
150 (10%) and grey dioritic gneiss (5%) are also present locally and are commonly either
151 interlayered with the other gneisses, or occur as earlier foliated enclaves (Fig. 4e, see also
152 206/8-8, Fig. 3). About 20% of the gneisses comprise mm- to cm-scale interlayered units of
153 the various lithologies described above (Fig. 2b). In a few sections of core, metre-scale
154 folding of the gneissic layering is preserved (Fig. 4f).

155 In thin section, the gneisses are typically medium to coarse grained, with cuspatelobate
156 grain boundary textures between quartz, feldspar and variably retrogressed mafic minerals
157 (amphiboles, pyroxenes) consistent with high temperature regional metamorphism (Fig. 5a,
158 b; e.g. Passchier and Trouw 2005). Marginal myrmekites and perthitic textures are widely
159 preserved in rocks with more granitic compositions and are again consistent with moderate
160 to low intensity high temperature deformation (Simpson 1985). Lower temperature
161 subgrain rotation recrystallization textures are only very weakly developed, as are local
162 deformation lamellae and undulose extinction in quartz grains. Originally calcic plagioclase
163 grains are ubiquitous, but now commonly have more albitic compositions and are either
164 altered to sericite or seeded with numerous tiny grains of epidote/clinozoisite (Fig. 5c).
165 Likewise, pyroxenes are usually only preserved as local relict grains and are partially to
166 completely pseudomorphed by fine grained intergrown aggregates of chlorite ± green
167 biotite ± colourless amphibole ± epidote ± equigranular quartz ± calcite, titanite and ore;
168 chlorite and epidote often occur as distinctive overgrowing coronae (Fig. 5d).

169 Overall, the rocks preserve textural and mineralogical evidence for early amphibolite facies
170 regional metamorphism, which has then been variably overprinted by low temperature
171 greenschist facies retrogression and (mostly) very low intensity associated strains. Overall
172 finite strains are low and there is no compelling evidence pointing to more than one phase
173 of prograde amphibolite facies deformation and metamorphism. Chambers et al. (2005)
174 suggested that the preservation of rare examples of coarse-grained, two-pyroxene
175 assemblages indicated that metamorphism locally reached granulite facies. Fine to ultrafine
176 grained epidote-quartz veins are locally common cross-cutting the gneisses (Fig. 5e), as are
177 small (mm-to-cm thick) rare cross-cutting units of phyllonite (also seen in 206/12-1, Fig. 3),
178 cataclasite and pseudotachylite (e.g. 206/9-2, Fig. 3).

179 Cover sequences

180 The Rona Ridge and Solan Bank High basement ridges are overlain by diverse, but
181 volumetrically limited Late Palaeozoic-Mesozoic cover sequences. The impersistence of
182 these mainly fluvial-lacustrine to shallow marine deposits seems to reflect the long-term
183 persistence of the ridges, with many local unconformities developed (Ritchie et al. 2011;
184 Stoker et al. 2018). Basement - cover unconformities are sampled directly in several cores
185 (Fig. 3), e.g. 205/21-1A (Lancaster, basement overlain by Jurassic Rona Sandstone), 206/8-8
186 (Clair, basement overlain by Devonian Clair Group) and 206/12-1 (southern Clair Ridge,
187 basement overlain by possible upper Cretaceous breccia conglomerate – see below). In all
188 cases, there is very little evidence of deep weathering profiles developed in the basement
189 rocks underlying these unconformities. Clasts of all basement host and early fault rock types
190 – bar pseudotachylite – are found within the oldest overlying cover sequence in 206/8-8
191 (Fig. 5f, Devonian Clair Group). Later fractures and veins – which occur in both basement
192 and Devonian to Jurassic cover sequences – are associated with widespread sediment-filled

193 fractures, quartz-adularia-calcite-base metal sulphide mineralization and hydrocarbons
194 (bitumen, oil). These features will be described in separate publications.

195

196 Sample Locations and Descriptions

197 The core materials examined here are conveniently subdivided into four geographic groups,
198 here termed (from northeast to southwest): 'Victory', 'Greater Clair', 'Lancaster' and 'Sula
199 Sgeir-Orkney' (Table I; Fig. 1). From these sub-areas, 14 samples have been dated using U-Pb
200 zircon geochronology, complementing the three dates previously obtained from the study
201 area by Chambers et al. (2005). In addition, Lu-Hf isotopic analyses were undertaken on 9 of
202 the 14 zircon samples.

203 *Sula Sgeir-Orkney sub-area*

204 **Sample HM11705** comes from 13.00 m depth in BGS borehole 88/02. The succession encountered in
205 this borehole was described by Chambers et al. (2005) as comprising quartzo-feldspathic schist cut
206 by cataclasite bands. The analysed sample is a strongly deformed medium grained granitic rock
207 comprising quartz, K-feldspar, plagioclase, biotite and hornblende with minor titanite, epidote,
208 allanite, ore, clinozoisite, zircon and secondary chlorite (after biotite and hornblende). The foliation
209 is defined by a strong shape-preferred elongation of quartz, feldspar and mafic minerals. It is cut by
210 several foliation-parallel cataclasite bands and associated pseudotachylytes (Fig. 6a).

211 **Samples HM11709 and HM11711** come from BGS seabed cores (59-04/85DM and 59-04/186DM,
212 respectively). HM11709 is a granitic gneiss containing sericitised plagioclase, quartz, K-feldspar,
213 chlorite, biotite and muscovite, together with relict garnet, which is now mostly altered to chlorite,
214 biotite and plagioclase. HM11711 is a highly altered granite, consisting of quartz, sericitised
215 plagioclase, epidote, calcite and clay minerals.

216 *Lancaster sub-area*

217 **Sample HM11686** comes from exploration well 204/25-1 (depth 2870.43 m) and is a coarse grained
218 interbanded unit of granodioritic-dioritic gneiss (Fig. 6b). It comprises varying proportions of
219 plagioclase, quartz, green pyroxene and hornblende, ore minerals, secondary chlorite, and
220 accessories (allanite, apatite, zircon). It is cut by small fractures with associated calcite veining.

221 **Sample HM11687**, from exploration well 204/26-1A (depth 2648.68 m), is a medium to coarse
222 grained granodioritic gneiss. It comprises sericitized plagioclase, quartz and altered mafics (after
223 amphibole or pyroxene), which are now mainly fine-grained chlorite, epidote and ore minerals.
224 Apatite and zircon are accessory phases.

225 **Sample HM11688** comes from exploration well 204/27-1 (depth 2136.20 m) and is a medium to
226 coarse grained granitic gneiss comprising plagioclase, K-feldspar, quartz, biotite and titanite, with
227 accessory ore, allanite and secondary chlorite. Other than fracturing, there is little evidence for low
228 temperature overprinting in quartz grains.

229 **Sample HM11689** comes from exploration well 204/28-1 (depth 1941.55 m) and is a granodioritic
230 gneiss comprising sericitized plagioclase, quartz, K-feldspar, biotite and sparse grains of green
231 amphibole, both of which are altered to secondary chlorite. Accessories include ore, allanite and
232 zircon. Quartz grains show minor development of undulose extinction but otherwise preserve high
233 temperature coarse grain sizes and cuspatelobate boundaries with feldspars.

234 *Greater Clair sub-area*

235 **Sample HM11691** comes from exploration well 205/20-1 (depth 2017.50 m) and is a coarse grained
236 granitic gneiss. It comprises plagioclase, K-feldspar, quartz, brown-green hornblende, altered
237 pyroxene, and accessories (ore, allanite, zircon, epidote, titanite, apatite). The rock is weakly foliated
238 with well-developed marginal myrmekite development (Fig. 6c). Some minor subgrain development
239 and fine subgrain rotation recrystallization is preserved in quartz with numerous microcracks filled
240 with epidote.

241 **Samples HM11692** and **HM11694** are both taken from exploration well 206/7a-2, at depths 2141.40
242 m and 2593.30 m respectively. They are medium to coarse grained granodioritic gneisses comprising
243 plagioclase, quartz, K-feldspar and mafics (amphibole, biotite, chlorite – possibly after pyroxene),
244 together with minor amounts of epidote, allanite, apatite, zircon, ore and titanite. Whilst dominated
245 by coarse grained high temperature fabrics, mm-wide zones of low temperature brittle-ductile
246 overprinting are evident and are associated with increased retrogression and breakdown of
247 plagioclase to fine grained aligned aggregates of white mica and epidote (Fig. 6d). Associated quartz
248 grains show evidence of limited marginal subgrain rotation recrystallization in these regions and
249 feldspar clasts have fibrous quartz-white mica tails consistent with the operation of solution-
250 precipitation creep (Fig. 6d).

251 **Sample HM22702** is a coarse grained granodioritic gneiss from exploration well 206/12-1 (depth
252 1716.65 m). It comprises highly sericitised plagioclase, quartz and fine-grained aggregates of brown
253 biotite together with accessory apatite, ore, epidote and zircon.

254 *Victory Sub-area*

255 **Sample HM11698** comes from exploration well 208/23-1 (depth 2071.26 m) and is a granitic gneiss
256 comprising plagioclase, K-feldspar, quartz and minor amounts of ore, epidote, titanite, limonite and
257 zircon. It preserves evidence of moderate deformation at high temperatures with elongate quartz
258 grains domains only locally overprinted by weak subgrain development and bulging recrystallization.
259 Plagioclase is heavily saussuritized and is substantially replaced by fine calcite-quartz intergrowths.

260 **Sample HM11699**, from exploration well 208/26-1 (depth 3741.31 m), is a medium to coarse grained
261 granodioritic gneiss containing plagioclase, quartz, brown biotite, brown-green hornblende, relict
262 clinopyroxene (2%) and accessories (ore, epidote). Fine aggregates of green amphibole, biotite and
263 epidote occur locally, possibly after orthopyroxene (Fig. 6e). Both hornblende and biotite are locally
264 altered to fine aggregates of secondary chlorite. Cuspatelobate quartz-feldspar grain boundaries are
265 well developed with very little low temperature recrystallization of quartz.

266 **Sample HM11700** comes from exploration well 208/27-2 (depth 1357.11 m) and is a mixture of
267 coarse grained granitic and more mafic granitic gneiss. The mafic unit comprises plagioclase, K
268 feldspar, quartz, brown partially altered pyroxene and accessories (ore, epidote, apatite, zircon) (Fig.

269 6f). The pyroxene is altered locally to blue-green amphibole and has prominent ore-rich alteration
270 rims. The more leucocratic unit comprises plagioclase, K-feldspar and quartz with minor biotite and
271 epidote.

272

273 **U-Pb and Lu-Hf Zircon Geochronology**

274 *Analytical methods*

275 The samples chosen for analysis (Table I) were collected from a larger sample set, some of
276 which did not yield minerals suitable for U-Pb dating. Following thin-section preparation,
277 the samples were crushed to < 250 µm at the Open University, Milton Keynes, UK. Zircons
278 were concentrated using a combination of magnetic separation and heavy liquid treatment.
279 The final separation step was made by hand-picking zircon grains from the heavy and non-
280 magnetic fraction using an optical microscope. The individual zircon grains were mounted
281 on double-sided, transparent adhesive tape and subsequently embedded in 1-inch diameter
282 circular epoxy mounts for polishing.

283 All U-Pb age data were obtained at the Central Analytical Facility (CAF), Stellenbosch
284 University, South Africa, by laser ablation - single collector - magnetic sectorfield -
285 inductively coupled plasma - mass spectrometry (LA-SF-ICP-MS) employing a Thermo
286 Finnigan Element2 mass spectrometer coupled to a NewWave UP213 laser ablation system.
287 All age data presented here were obtained by single spot analyses with a spot diameter of
288 30 µm and a crater depth of approximately 15-20 µm, corresponding to an ablated zircon
289 mass of approximately 150-200 ng. The methods employed for analysis and data processing
290 are described in detail by Gerdes and Zeh (2006) and Frei and Gerdes (2009). For quality
291 control, the Plešovice (Sláma et al. 2008) and M127 (Nasdala et al. 2008; Mattinson 2010)
292 zircon reference materials were analyzed, and the results were consistently in good
293 agreement with the published ID-TIMS ages. Full analytical details and the results for all
294 quality control materials analysed are given in Table II. The calculation of concordia ages and
295 plotting of concordia diagrams were performed using Isoplot/Ex 3.0 (Ludwig 2003). CL
296 (cathodoluminescence) imaging of the zircon grains was undertaken at the CAF using a Zeiss
297 Merlin SEM, with a beam current of 10 nA and a 15 mm working distance. Analyses used for
298 age calculations were screened for inheritance based on textures as revealed by CL images
299 and ^{207}Pb - ^{206}Pb age determinations, and are based on analyses that are 99-101%
300 concordant. For calculations of upper intercept ages, anchoring of regression lines was not
301 employed.

302 Also included in the U-Pb zircon geochronology study are four sandstone samples ranging in
303 age from Triassic to Cretaceous. The analytical protocol followed for the detrital zircon
304 study is identical to that for the basement samples described above, except that the grain
305 size fraction was that used routinely for conventional heavy mineral provenance
306 investigations (63-125 µm).

307 Hafnium isotope measurements were performed with a Thermo-Finnigan NEPTUNE multi
308 collector ICP-MS at Goethe University Frankfurt (GUF) coupled to RESolution M50 193nm
309 ArF Excimer (Resonetics) laser system following the method described in Gerdes and Zeh
310 (2006, 2009). Between 10 and 19 individual zircons per sample were analysed. Prior to Hf-
311 isotope analysis, the internal textures were investigated by cathodoluminescence imaging.
312 Only homogeneous growth zones in zircons yielding concordant or nearly concordant U-Pb
313 ages were targeted for Hf-isotope analysis. Spots of 40 µm in diameter were drilled with a
314 repetition rate of 5.5 Hz and an energy density of 6 J/cm² during 50s of data acquisition. The
315 instrumental mass bias for Hf isotopes was corrected using an exponential law and a
316 ¹⁷⁹Hf/¹⁷⁷Hf value of 0.7325. In case of Yb isotopes, the mass bias was corrected using the Hf
317 mass bias of the individual integration step multiplied by a daily $\beta_{\text{Hf}}/\beta_{\text{Yb}}$ offset factor
318 (Gerdes and Zeh 2009). All data were adjusted relative to the JMC475 of ¹⁷⁶Hf/¹⁷⁷Hf ratio =
319 0.282160 and quoted uncertainties are quadratic additions of the within run precision of
320 each analysis and the reproducibility of the JMC475 (2SD = 0.0028%, n = 8). Accuracy and
321 external reproducibility of the method was verified by repeated analyses of reference zircon
322 GJ-1 and Plesovice, which yielded a ¹⁷⁶Hf/¹⁷⁷Hf of 0.282010 ± 0.000025 (2 SD, n=7) and
323 0.0282475 ± 0.000020 (n=7), respectively. This is in excellent agreement with previously
324 published results (e.g. Gerdes and Zeh 2006; Slama et al. 2008) and with the LA-MC-ICPMS
325 long-term average of GJ-1 (0.282010 ± 0.000025; n > 800) and Plesovice (0.282483 ±
326 0.000025, n > 300) reference zircon at GUF.

327

328 The initial ¹⁷⁶Hf/¹⁷⁷Hf values are expressed as $\epsilon_{\text{Hf}}(t)$, which is calculated using:

329

- 330 (i) a decay constant value of $1.867 \times 10^{-11} \text{ year}^{-1}$
331 (ii) CHUR after Bouvier et al. (2008; ¹⁷⁶Hf/¹⁷⁷HfCHUR, today = 0.282785 and ¹⁷⁶Lu/¹⁷⁷Hf
332 CHUR,today = 0.0336), and
333 (iii) the apparent Pb-Pb ages obtained for the respective domains.

334

335 For the calculation of Hf two stage model ages (T_{DM}) in billions of years, the measured
336 ¹⁷⁶Lu/¹⁷⁷Hf of each spot (first stage = age of zircon), a value of 0.0113 for the average
337 continental crust, and a depleted mantle ¹⁷⁶Lu/¹⁷⁷Lu DM = 0.0384 and ¹⁷⁶Hf/¹⁷⁷Hf DM =
338 0.283165 (average MORB; Chauvel et al. 2008) were used.

339

340 Results: U-Pb ages from basement rocks

341 The 14 samples of crystalline basement rocks dated here yield a comparatively limited range
342 of zircon U-Pb ages within the Neoarchaean (Table III). These data lie in the same age range
343 as the 3 dates obtained by Chambers et al. (2005) in the same study area, which are also
344 listed in Table III.

345 Sula Sgeir-Orkney sub-area

346 **Sample HM11705** (BGS borehole 88/02, 13.00 m) contains elongate prismatic zircons with
347 typical oscillatory igneous zonation patterns (Figs 7a and b). Occasional zircons are strongly
348 metamict, but nevertheless retain remnant oscillatory zoning (Fig. 7b). They display a
349 discordant trend with an upper intercept age of 2754 ± 22 Ma with an MSWD of 0.88 (Fig.
350 8a).

351 **Sample HM11709** (BGS seabed core 59-04/85DM) has equant to elongate prismatic zircons
352 with indistinct oscillatory magmatic zoning. They are mostly dark under CL (high-U) with a
353 small number of grains having bright rims. The main zircon group yields a concordia age of
354 2747 ± 7 Ma with an MSWD of 0.42 and a probability of concordance of 0.99 (Figs 8b and c).
355 In addition, there is a small number of older zircons interpreted as inherited, together with
356 two zircons with younger ages (2621 ± 26 Ma and 2628 ± 28 Ma) probably related to Pb-loss
357 during a subsequent Neoarchaean thermal (possibly hydrothermal) event.

358 **Sample HM11711** (BGS seabed core 59-04/186DM) has a zircon population with a concordia
359 age of 2826 ± 5 Ma, with an MSWD of 0.45 and a probability of concordance of 1.00 (Figs 8d
360 and e), excluding a single younger zircon dated as 2681 ± 39 Ma.

361 Lancaster sub-area

362 **Sample HM11686** (204/25-1, 2870.43 m) contains equant to stubby subhedral to
363 subrounded zircons that show evidence of resorbtion. Grains show indistinct oscillatorily-
364 zoned centres that are dark under CL, with bright rims that also have magmatic textures
365 (Fig. 7c). Many of the zircons in this sample are moderately to highly fractured. On the
366 Wetherill concordia diagram, they show a discordant trend with an upper intercept age of
367 2729 ± 12 Ma with an MSWD of 0.52 (Figs 9a and 9b). In addition, there is an older less
368 precise analysis at ca 2850 Ma, interpreted as inherited, and a small number of slightly
369 younger zircons.

370 **Sample HM11687** (204/26-1A, 2648.68 m) contains zircons with indistinct oscillatory
371 magmatic zoning, with euhedral to subhedral relatively equant morphologies. They fall on a
372 discordant trend (Figs 9c and 9d) with an upper intercept age of 2733 ± 14 Ma (MSWD =
373 2.0), but there is one older grain dated as ca. 3100 Ma, interpreted as inherited. The four
374 zircons with 100% concordance yield a concordia age of 2744 ± 16 Ma with an MSWD of
375 0.41 and probability of concordance of 0.84 (Fig. 9e).

376 **Sample HM11688** (204/27-1, 2136.20 m) has prismatic zircons that range from stubby to
377 moderately elongate, and are euhedral to subrounded. Some display indistinct oscillatory
378 magmatic zoning (Fig. 7d) but many show metamictisation/recrystallisation owing to
379 relatively high U contents, which has partially or wholly destroyed the original igneous
380 zoning fabric. They display a discordant trend (Figs 9f and g) with an upper intercept age of
381 2745 ± 15 Ma (MSWD = 4.2). The concordant zircons yield a concordia age of 2739 ± 8 Ma

382 with an MSWD of 0.87 and probability of concordance of 0.62 (Fig. 9h). As with sample
383 HM11687, there is also evidence for a minor inherited component.

384 **Sample HM11689** (204/28-1, 1941.55 m) has zircons that display a discordant trend (Fig. 9i)
385 with an upper intercept age of 2762 ± 13 Ma (MSWD = 8.6). The concordant zircons yield a
386 concordia age of 2793 ± 10 Ma with an MSWD of 1.0 and probability of concordance of 0.45
387 (Fig. 9j).

388 Greater Clair sub-area

389 **Sample HM11691** (205/20-1, 2017.50 m) has equant to prismatic, euhedral, subhedral and
390 subrounded zircons with typical igneous dark oscillatory zoning, many of which are
391 surrounded by brighter oscillatorily-zoned rims that are also magmatic, produced by
392 resorbtion in the melt (Figs 7e and f). In some cases (Fig. 7e), there is evidence for several
393 phases of zircon growth and resorbtion. The zircons display a discordant trend (Fig. 10a)
394 with an upper intercept age of 2736 ± 12 Ma (MSWD = 0.96). There is no significant
395 difference in age between the dark grain centres and the brighter rims (Figs 7e and f).

396 **Sample HM11692** (206/7a-2, 2141.40 m) has mostly elongate euhedral to subhedral zircons
397 with relatively indistinct oscillatory magmatic zoning. Some of the zircons have bright
398 oscillatorily-zoned rims that are also magmatic. When plotted on a Wetherill concordia
399 diagram, the data reveal a degree of scatter along the concordia line, precluding
400 determination of an upper intercept age (Fig. 10b). However, the main group of zircons yield
401 a concordia age of 2806 ± 8 Ma with an MSWD of 0.41 and probability of concordance of
402 0.84 (Fig. 10c). There appears to be a subordinate younger cluster at ca 2750 Ma.

403 **Sample HM11694** (206/7a-2, 2593.30 m) has zircons that display a discordant trend (Fig.
404 10d) and yield an upper intercept age of 2753 ± 14 Ma (MSWD = 1.6) (Fig. 10e).

405 **Sample HM22702** (206/12-1, 1716.65 m) has mostly elongate prismatic euhedral to
406 subhedral zircons with typical magmatic oscillatory zoning patterns (Fig. 7g). There is
407 evidence for several phases of zircon growth with both dark and bright areas under CL, but
408 there is no significant difference in age between the two. The data define a discordant trend
409 with an upper intercept age of ca. 2748 Ma (Fig. 10f). There is some scatter in the ages
410 determined from the sample, which extend back to 2828 Ma. This is interpreted as
411 indicating the presence of inherited zircons and suggests a relatively prolonged history of
412 basement formation and stabilisation.

413 Victory Sub-area

414 **Sample HM11698** (208/23-1, 2071.26 m) has equant to prismatic euhedral to subhedral
415 zircons with typical igneous dark oscillatory zoning, many of which are surrounded by
416 brighter oscillatorily-zoned rims that are also magmatic. These textures indicate the zircons
417 underwent partial resorbtion in the melt prior to a later stage of crystallisation, but there is

418 no significant difference in age between the dark grain centres and the brighter rims (Fig.
419 7h). The zircon data display a discordant trend (Fig. 10g) with an upper intercept age of
420 2776 ± 12 Ma (MSWD = 2.6).

421 **Sample HM11699** (208/26-1, 3741.31 m) has zircons that are all close to concordia, but
422 show significant scatter that precludes meaningful determination of an upper intercept age
423 (Fig. 10h). The zircons have generally equant to stubby prismatic morphology and range
424 from euhedral to subrounded. Many of the zircons are dark under CL with oscillatory
425 magmatic zoning, but most of these have bright margins that display broad, mosaic-like
426 textures that are typically of anatetic origin (Figs 7i and j). Other zircons are entirely bright
427 under CL and show only anatetic textures. The probability density plot (Fig. 11a) shows the
428 presence of two main groups, one in the 2720-2760 Ma range and one (possibly bimodal) in
429 the 2800-2860 Ma range. This is the only sample in the data set that shows a significant
430 difference in age between the dark cores and the bright rims (Fig. 7j), and the bimodal age
431 distribution is believed to be a manifestation of at least two phases of zircon growth. The
432 earlier phase (ca 2800-2860 Ma) generated zircons with typical oscillatory magmatic zoning
433 that have dark CL (relatively high U), whereas the later phase (ca 2720-2760 Ma) generated
434 zircons with anatetic textures, either as rims on the older grains or as entirely new grains.

435 **Sample HM11700** (208/27-2, 1357 m) has zircons that are mostly concordant or near-
436 concordant (Fig.10i), and yield a concordia age of 2789 ± 8 Ma with an MSWD of 0.76 and
437 probability of concordance of 0.78 (Fig. 10j).

438 *Results: U-Pb ages of detrital zircons in cover sequences*

439 In addition to U-Pb zircon data that give direct measurement of basement ages, detrital
440 zircon data may provide additional information. Four sandstone samples from the eastern
441 part of the Faroe-Shetland Basin, ranging in age from Triassic to Early Cretaceous, have
442 yielded almost exclusively Neoarchaean age spectra consistent with the data presented
443 above. Three of these samples are located in reasonably close proximity to basement
444 penetrations: HM12189 (204/27-1, 2094.65 m) and HM12194 (202/3-1A, 1642.50 m), which
445 are located adjacent to the Lancaster sub-area, and HM12357 (206/4-1, 4115 m), which is
446 close to the Greater Clair sub-area (Fig. 1). The other sample (HM12172, 213/23-1, 3598.36
447 m) has greater areal significance, since it is located further west in the basin, close to the
448 Corona Ridge (Fig. 1), but it is nearest to the Victory sub-area.

449 Lancaster sub-area

450 Samples HM12189 (204/27-1, 2094.65 m) and HM12194 (202/3-1A, 1642.50 m) are both
451 from sandstones of the Upper Jurassic Rona Member (Kimmeridge Clay Formation). The
452 Rona sandstones were deposited by fan-deltas draining adjacent Archaean basement highs
453 as a result of footwall uplift on normal faults bounding the Rona and Judd Highs (Fig 1;
454 Verstralen et al. 1995). Both samples have detrital zircon populations that are
455 overwhelmingly dominated by a 2680-2820 Ma group (Fig. 11b, c), consistent with local

456 basement sourcing, although the sample from 202/3-1a contains a small number of younger
457 zircons ranging from Palaeoproterozoic to Early Palaeozoic, suggesting minor involvement
458 of other source materials.

459 Greater Clair sub-area

460 Sample HM12357 is from the Lower Cretaceous Royal Sovereign Formation at 4115 m depth
461 in well 206/4-1, located immediately to the northwest of the Clair Field area (Fig. 1). The
462 zircon population is almost exclusively Archaean, dominated by a Neoarchaean group
463 between 2660 Ma and 2780 Ma with three older zircons with scattered ages between 2940
464 Ma and 3040 Ma (Fig. 11d).

465 Well 213/23-1 (Victory sub-area)

466 Sample HM12172 is from a Triassic sandstone at 3598.36 m depth in well 213/23-1, located
467 significantly further basin-ward compared with all other samples in the study. Excluding two
468 younger zircons at 1096 Ma and 1751 Ma, the spectrum is exclusively Archaean. In this case,
469 however, the distribution is polymodal, with three main groups being apparent. The largest
470 group lies between 2760-2900 Ma, with smaller groups at 2640-2740 Ma and 2920-2980 Ma
471 (Fig. 11e).

472 *Results: Lu-Hf data from basement rocks*

473 The $\epsilon\text{Hf(t)}$ versus U-Pb crystallisation age diagram (Fig. 12) suggests the presence of three
474 distinct groups within the sample set. The two basement samples from the Victory sub-area
475 (HM11698: 208/23-1, 2071.26 m and HM11700: 208/27-2, 1357.11 m) have depleted
476 mantle model ages of 3200-3300 Ma. These data indicate recycling of older crustal
477 components of probable Palaeoarchaean age (extracted from the depleted mantle at ca
478 3200 to 3300 Ma) during the formation of new crust at ca 2750 to 2800 Ma.

479 In contrast, basement samples HM11686 (204/25-1, 2870.43 m, Lancaster sub-area),
480 HM11691 (205/20-1, 2017.50 m, Greater Clair sub-area) and HM11711 (59-04/186DM, Sula
481 Sgeir-Orkney sub-area) have younger model ages indicating extraction from the depleted
482 mantle at ca 2900 to 3000 Ma. Therefore, this group represents recycling of Mesoarchaean
483 crust during crustal formation events at ca 2750 to 2800 Ma. Crystalline basement samples
484 HM11694 (206/7a-2, 2593.30 m, Greater Clair sub-area) and HM11705 (88/02, 13.00 m,
485 Sula Sgeir-Orkney sub-area) have intermediate model ages, indicating they originated
486 through melting of crust extracted from the depleted mantle during the Palaeoarchaean to
487 Mesoarchaean.

488

489 **Discussion and conclusions**

490 The 17 basement age determinations presented here fall in a relatively narrow range
491 between 2729-2826 Ma, similar to the 2700-2829 Ma ages obtained from 3 samples in the
492 same area by Chambers et al. (2005). The geographic distribution of the 20 ages obtained is
493 shown in Figure 13 – there is no clear difference in age ranges in any of the 4 sub-areas
494 defined here.

495 By contrast, Hf isotope data from the Neoarchaean samples indicate that despite the
496 relatively limited range in their U-Pb crystallisation ages, there is evidence for significant
497 variation in their pre-crystallisation history (Figs 12 and 13). Extraction from the depleted
498 mantle varied in age from ca 3200 Ma to ca 2900 Ma. The oldest Hf T_{DM} ages are from the
499 Victory sub-area (wells 208/23-1 and 208/27-2), which is the most northeasterly segment in
500 the study. Therefore, although the data set is limited, there is evidence for lateral variations
501 in the Hf model age data that may indicate the existence of different crustal domains in the
502 Neoarchaean of the west of Shetland area.

503 The uniformity in U-Pb crystallization ages of basement is strikingly consistent with the
504 restricted range of Neoarchaean sources seen in detrital zircons preserved in sediments
505 from various stratigraphic levels and locations in cover sequences in the eastern part of the
506 Faroe-Shetland Basin. These include the Upper Jurassic Rona Formation in 202/3-1a and
507 204/27-1 and the Lower Cretaceous Royal Sovereign Formation in 206/4-1. The Triassic of
508 213/23-1 records two events in a similar but somewhat wider range (2640-2900 Ma),
509 together with an earlier event between 2920-2980 Ma. This earlier group partially overlaps
510 with one of the main zircon components (ca 2960-3020 Ma) seen in Archaean-sourced
511 Albian sandstones from Kangerlussuaq, East Greenland (Whitham et al. 2004). In none of
512 the cases described above is there any evidence for Proterozoic reworking of Archaean
513 crust.

514 It should be noted that the discordant arrays of data visible in some samples in Figures 9
515 and 10 trend downwards to mainly Mesozoic lower intercept ages. The significance of these
516 is not completely understood at present, but they most likely reflect lead loss during
517 thermal events associated with Phanerozoic basin development. Further investigations will
518 be aimed at clarifying the low temperature history of the basement during Mesozoic rifting.

519 *Neoarchaean events in the Faroe-Shetland basement rocks*

520 The U-Pb zircon analyses of intermediate to felsic basement gneisses from offshore
521 boreholes in the FST reported herein and by Chambers et al. (2005) reveal that the majority
522 of ages range from 2829 Ma to 2700 Ma. The analysed grains are primarily magmatic with
523 oscillatory zoning, and many show evidence of several phases of crystallisation. In most
524 cases, there is no significant difference in age between the different growth phases, but in
525 one sample there is clear evidence for two distinct events. A small number of samples
526 contain older outliers, interpreted as inherited. In contrast to Chambers et al. (2005), we
527 have found no compelling textural evidence within the zircon grains for granulite facies

metamorphism: the U-Pb ages are therefore believed to date the crystallisation of the igneous protoliths. The only clear example of complexity is seen in the zircons from 208/26-1, where the bimodal age distribution suggests at least two phases of zircon growth at ca 2800-2860 Ma and ca 2720-2760 Ma, with the latter group of zircons preserving evidence of anatexitic textures, either as rims on the older grains or as entirely new grains.

The majority of the crystallisation ages fall between ca 2720 Ma and ca 2750 Ma, but show a bimodal distribution with a subordinate group between ca 2790 Ma and ca 2840 Ma (Fig. 14). It therefore appears that the Faroe-Shetland Terrane underwent a prolonged phase of stabilisation between ca 2840 Ma and 2700 Ma, with the main phase taking place between 2720-2750 Ma. From the presently-available data, there does not appear to be any geographic trend in the crystallisation ages (Fig. 13), although the detrital zircon data from well 213/23-1, further west than all the basement penetrations, indicates some older events, a picture that is also inferred from cover sediments in Kangerlussuaq on the conjugate margin (Whitham et al., 2004) (Fig. 11f).

Comparison with the Lewisian Gneiss Complex

The new data reported here provide a firmer basis for assessing the proposed correlation of the basement rocks west of Shetland with the Lewisian Gneiss Complex of mainland Scotland and the Outer Hebrides. The U-Pb ages obtained fall within, although mainly at the lower end of, the broad range of emplacement ages that have been established for different components of the Lewisian Gneiss Complex (ca 3135-2680 Ma; Wheeler et al. 2010 and references therein). Sm-Nd model ages obtained by Chambers et al. (2005) lie in the range 3300-2830 Ma and are similar to those obtained from the Lewisian Gneiss Complex (3000-2700 Ma; Whitehouse 1989, Corfu et al. 1993). The Hf isotope data reported here from zircons in the basement west of Shetland indicate extraction from the depleted mantle from ca 3300 Ma to ca 2900 Ma. The igneous protoliths of the two gneiss complexes were therefore both emplaced during the same protracted period of Palaeo- to Neoarchaean crustal growth in the North Atlantic region (e.g. Garde et al. 2000; Nutman et al. 2010; Tappe et al. 2011; Dyck et al. 2015).

The main difference between the two gneiss complexes is that the basement gneisses west of Shetland show no sign in the U-Pb zircon analyses of the ca 2500 Inverian and ca 1800-1700 Ma Laxfordian amphibolite to granulite facies events that have been documented from different parts of the Lewisian Gneiss Complex (e.g. Kinny et al. 2005; Wheeler et al. 2010, Mason 2015 and references therein). The prolonged crustal history associated with the onshore Lewisian Complex is also reflected in detrital zircon ages from sediment in Abhainn Caslavat, which is a stream draining Lewisian TTG gneisses of the Tarbert Terrane (Outer Hebrides). The zircons in this stream sample identify both the ca 2850-3100 Ma and ca 1675 Ma events identified in the Tarbert Terrane by Kinny et al. (2005), as well as a large group of zircons between ca 2550 Ma and ca. 2850 Ma (Morton et al. 2012).

566 *Regional correlations with Greenland*

567 It is widely believed that the Lewisian Gneiss Complex of mainland Scotland was continuous
568 with the Nagssugtoqidian mobile belt of SE Greenland prior to opening of the North Atlantic
569 Ocean (Fig. 15; Friend & Kinny 2001; Park 2005). They display a similar range of Meso- to
570 Neoarchaean protolith and metamorphic ages and both were strongly reworked during the
571 Palaeoproterozoic. In SE Greenland, the Nagssugtoqidian mobile belt is limited to the north
572 by Archaean rocks of the Central Greenland-Rae Craton (Fig. 15; Nutman et al. 2008; Kolb
573 2014) which was a stable crustal block during the Palaeoproterozoic. Detrital zircons in
574 Albian and Eocene sandstones from the Kangerlussuaq region of the Rae Craton indicate
575 three Archaean tectonothermal events (ca 2700–2750 Ma, 2960–3020 Ma and 3180–3200
576 Ma), and no evidence for subsequent thermal reworking (Whitham et al. 2004). The
577 absence of evidence for Palaeoproterozoic reworking of the basement west of Shetland
578 suggests that the eastern continuation of the northern limit of Nagssugtoqidian deformation
579 must run generally WNW-ESE close to the northern coastline of mainland Scotland (Fig. 15).
580 The basement rocks forming the small islands of Sula Sgeir, North Rona, Sule Skerry and
581 Stack Skerry (Walker 1931; Nisbet, 1961) all lie close to the projected terrane boundary.
582 New work to determine the compositions, ages and affinities of these gneisses will help to
583 better constrain the possible location and nature of this important crustal boundary.

584 *Another Lewisian terrane?*

585 The traditional view of the Lewisian Complex (following Sutton & Watson 1951) is of a single
586 crustal block that underwent early Scourian high-grade tectonothermal events which were
587 later divided into Badcallian and Inverian. These rocks were then intruded by
588 Palaeoproterozoic mafic dykes (Scourie dykes) and were then heterogeneously reworked
589 during a lower-grade Laxfordian event. A different interpretation was put forward by Friend
590 & Kinny (2001) and Kinny et al. (2005) who subdivided the complex into many discrete
591 terranes, characterised by different geochronological signatures that were thought to have
592 been amalgamated during the Proterozoic. This prompted a resurgence of interest in the
593 Lewisian Complex, although many workers have subsequently concluded that the number
594 of terranes may in fact be relatively small (e.g. Park 2005; Mason 2012, 2015).

595 In many ways, the debate illustrates the problems in applying “upper crustal” concepts such
596 as terranes to deep crustal rocks. To what extent do variations in protolith ages and/or
597 timing and grade of metamorphic events reflect dissection and telescoping of
598 heterogeneous crust as opposed to genuine accretion of terranes in the original Cordilleran
599 sense? Notwithstanding this, the Lewisian Complex does incorporate Palaeoproterozoic
600 volcanic arc material, accreted oceanic material, and preserves evidence for high-P
601 metamorphism, all of which are indicative of the presence of at least one suture (e.g. Baba
602 1998; Park et al. 2001; Mason et al. 2004). Furthermore, the northernmost mainland
603 terrane of Kinny et al. (2005), the Rhiconich Terrane (Fig. 13), is still regarded as being
604 sufficiently different from the Lewisian rocks to the south of the bounding Laxford Shear

605 Zone to constitute a separate terrane (Goodenough et al. 2010). Thus, a terrane approach to
606 the analysis of the Lewisian Complex is still justified.

607 There is at present insufficient geochemical and isotopic data to support a detailed
608 comparison of the Faroe-Shetland basement with the Rhiconich Terrane. Clearly the main
609 difference lies in the lack of significant Palaeoproterozoic reworking of the former crustal
610 block. Any Nagssugtoqidian suture likely lies further south within the Lewisian Complex (Fig.
611 15; see Mason 2015 for details). As a working hypothesis, however, we suggest that the
612 Faroe-Shetland basement should have formal terrane status, but without the implication
613 that the boundary with the Rhiconich Terrane is necessarily an additional suture zone. We
614 suggest that the “Faroe-Shetland Terrane” represents the eastwards continuation of the
615 foreland to the Nagssugtoqidian orogen, in much the same way that the Hebridean Terrane
616 (incorporating the Lewisian Complex) represents the foreland to the much younger
617 Caledonian orogen east of the Moine Thrust Zone (Bluck et al. 1992).

618 **Acknowledgements**

619 We are grateful to BP and Sindri for supporting the U-Pb geochronological studies of basement and
620 Triassic-Cretaceous sandstones in the Faroe-Shetland Basin, and to BGS for access to samples. Clair
621 JVG also supported the analysis of the basement cores and we would like to particularly
622 acknowledge the extensive help of Catherine Witt, Farkhad Sadikhov and Andrew Robertson (BP),
623 Caroline Gill (Shell), and Andy Conway (formerly ConocoPhillips). Ian Chaplin is thanked for his
624 excellent thin sectioning skills. Lydia-Marie Joubert and Madelaine Frazenburg (CAF, Stellenbosch
625 University) are thanked for their help with CL imaging. Editor Randy Parrish and reviewers Ian Millar
626 and Anonymous are thanked for their very positive and constructive comments.

627 Supplementary data files are provided at the end of this article or can be obtained from r.e.holdsworth@durham.ac.uk

628 **REFERENCES**

- 629 Baba, S. 1998. Proterozoic anticlockwise P-T path of the Lewisian Complex of South Harris, Outer
630 Hebrides, NW Scotland. *Journal of Metamorphic Geology*, 16, 819-41.
- 631 Bluck, B.J., Gibbons, W. and Ingham, J.K. 1992. Terranes. In: Cope, J.C.W. Ingham, J.K. and Rawson,
632 P.F. (eds), *Atlas of palaeogeography and lithofacies*. Memoir of the Geological Society, London, 13, 1-
633 4.
- 634 Bouvier, A., Vervoort, J. and Patchett, P. 2008. The Lu-Hf and Sm-Nd isotopic composition of CHUR:
635 constraints from unequilibrated chondrites and implications for the bulk composition of terrestrial
636 planets. *Earth and Planetary Science Letters*, 273, 48-57.
- 637 Chambers, L., Darbyshire, F., Noble, S. and Ritchie, D. 2005. NW UK continental margin: chronology
638 and isotope geochemistry. *British Geological Survey Commissioned Report*, CR/05/095.
- 639 Chauvel, C., Lewin, E., Carpentier, M., Arndt, N. T. and Marini, J. 2008. Role of recycled oceanic basalt
640 and sediment in generating the Hf-Nd mantle array. *Nature Geoscience*, 1, 64-67.

- 641 Corfu, F., Heaman L.M. and Rogers, G. 1994. Polymetamorphic evolution of the Lewisian complex,
642 NW Scotland, as recorded by U-Pb isotopic compositions of zircon, titanite and rutile. Contributions
643 to Mineralogy and Petrology, 117, 215-228.
- 644 Crowley, Q.C., Key, R. and Noble, S.R. 2015. High-precision U-Pb dating of complex zircon from the
645 Lewisian Gneiss Complex of Scotland using an incremental CA-ID-TIMS approach. Gondwana
646 Research, 27, 1381-1391.
- 647 Davies, J.H.F.L. and Heaman, L.M. 2014. New U-Pb baddeleyite and zircon ages for the Scourie dyke
648 swarm: a long-lived large igneous province with implications for the Palaeoproterozoic evolution of
649 NW Scotland. Precambrian Research, 249, 180-198.
- 650 Dyck, B., Reno, B.L. and Kokfelt, T.F. 2015. The Majorqaq Belt: A record of Neoarchaean orogenesis
651 during final assembly of the North Atlantic Craton, southern West Greenland. Lithos, 220, 253-271.
- 652 Flinn, D. 1985. The Caledonides of Shetland. In: Gee, D.G. and Sturt, B.A. (eds), The Caledonide
653 Orogen: Scandinavia and Related Areas. Wiley & Sons, New York, 1159-1172.
- 654 Flinn, D. 1988. The Moine rocks of Shetland. In: Winchester, J.A. (ed.), Later Proterozoic Stratigraphy
655 of the Northern Atlantic Regions. Blackie, Glasgow, 74-85.
- 656 Flinn, D. 2009. Uyea to North Roe Coast. Lewisian, Torridonian and Moine Rocks of Scotland.
657 Geological Conservation Review Series, 34, Joint Nature Conservation Committee, Peterborough,
658 628-634.
- 659 Flinn, D., Frank, P.L., Brook, M. and Pringle, I.R. 1979. Basement-cover relations in Shetland. In:
660 Harris, A.L., Holland, C.H. and Leake, B.E. (eds) The Caledonides of the British Isles - Reviewed.
661 Geological Society, London, Special Publications, 8, 109-115.
- 662 Frei, D. and Gerdes, A. 2009. Precise and accurate in-situ U-Pb dating of zircon with high sample
663 throughput by automated LA-SF-ICP-MS. Chemical Geology, 261, 261-270.
- 664 Friend, C.R.L. and Kinny, P.D. 2001. A reappraisal of the Lewisian Gneiss Complex: geochronological
665 evidence for its tectonic assembly from disparate terranes in the Proterozoic. Contributions to
666 Mineralogy and Petrology, 142, 198-218.
- 667 Friend, C.R.L., Strachan, R.A. and Kinny, P.D. 2008. U-Pb zircon dating of basement inliers within the
668 Moine Supergroup, Scottish Caledonides: implications of Archaean protolith ages. Journal of the
669 Geological Society, London, 165, 807-815.
- 670 Garde, A.A., Friend, C.R.L., Nutman, A.P. and Marker, M. 2000. Rapid maturation and stabilisation of
671 middle Archaean continental crust: the Akia terrane, southern West Greenland. Bulletin of the
672 Geological Society of Denmark, 47, 1-27.
- 673 Gerdes, A. and Zeh, A. 2006. Combined U-Pb and Hf isotope LA-(MC-)ICP-MS analyses of detrital
674 zircons: Comparison with SHRIMP and new constraints for the provenance and age of an Armorican
675 metasediment in Central Germany. Earth and Planetary Science Letters, 249, 47-61.

- 676 Gerdes, A. and Zeh, A. 2009. Zircon formation versus zircon alteration - new insights from combined
677 U-Pb and Lu-Hf in-situ LA-ICP-MS analyses, and consequences for the interpretation of Archean
678 zircon from the Central Zone of the Limpopo Belt. *Chemical Geology*, 261, 230-243.
- 679 Goodenough, K.M., Park, R.G., Krabbendam, M., Myers, J.S., Wheeler, J., Loughlin, S.C., Crowley,
680 Q.G., Friend, C.R.L., Beach, A., Kinny, P.D. and Graham, R.H. 2010. The Laxford Shear Zone: an end-
681 Archaean terrane boundary? In: Law, R.D., Butler, R.W.H., Holdsworth, R.E., Krabbendam, M.,
682 Strachan, R.A. (Eds.), *Continental Tectonics and Mountain Building : The Legacy of Peach and Horne*,
683 Geological Society, London, Special Publications, 335, 103-120.
- 684 Goodenough, K.M., Crowley, Q.C., Krabbendam, M. and Parry, S.F. 2013. New U-Pb age constraints
685 for the Laxford Shear Zone, NW Scotland: evidence for tectonomagmatic processes associated with
686 the formation of a Palaeoproterozoic supercontinent. *Precambrian Research*, 233, 1-19.
- 687 Jackson, S., Pearson, N.J., Griffin, W.L. and Belousova, E.A. 2004. The application of laser ablation –
688 inductively coupled plasma – mass spectrometry to in situ U-Pb zircon geochronology. *Chemical
689 Geology*, 211, 47-69.
- 690 Kalsbeek, F., Austrheim, H., Bridgwater, D., Hansen, B.T., Pedersen, S., Taylor, P.N. 1993.
691 Geochronology of Archaean and Proterozoic events in the Ammassalik area, South-East Greenland,
692 and comparisons with the Lewisian of Scotland and the Nagssugtoqidian of West Greenland.
693 *Precambrian Research* 62, 239–270.
- 694 Kinny, P.D. and Friend, C.R.L. 1997. U-Pb isotopic evidence for the accretion of different crustal
695 blocks to form the Lewisian Complex of northwest Scotland. *Contributions to Mineralogy and
696 Petrology*, 129, 326-340.
- 697 Kinny, P.D., Friend, C.R.L. and Love, G.J. 2005. Proposal for a terrane-based nomenclature for the
698 Lewisian Gneiss Complex of NW Scotland. *Journal of the Geological Society, London*, 162, 175-186.
- 699 Kolb, J. 2014. Structure of the Palaeoproterozoic Nagssugtoqidian Orogen, South-East Greenland:
700 model for the tectonic evolution. *Precambrian Research* 255, 809-822.
- 701 Ludwig, K. 2003. Isoplot/Ex version 3: a Geochronological toolkit for Microsoft Excel. *Geochronology
702 Center*, Berkeley, USA.
- 703 Mason, A.J. 2012. Major early thrusting as a control on the Palaeoproterozoic evolution of the
704 Lewisian Complex: evidence from the Outer Hebrides, NW Scotland. *Journal of the Geological
705 Society, London*, 169, 201-212.
- 706 Mason, A.J. 2015. The Palaeoproterozoic anatomy of the Lewisian Complex, NW Scotland: evidence
707 for two ‘Laxfordian’ tectono-thermal cycles. *Journal of the Geological Society*, 173, 153-169,
708 <https://doi.org/10.1144/jgs2015-026>
- 709 Mason, A.J., Temperley, S. and Parrish, R.R. 2004. New light on the construction, evolution and
710 correlation of the Langavat Belt (Lewisian Complex), Outer Hebrides, Scotland: field, petrographic
711 and geochronological evidence for an early Proterozoic imbricate zone. *Journal of the Geological
712 Society, London*, 161, 837-848.

- 713 Mattinson, J.M. 2010. Analysis of the relative decay constants of ^{235}U and ^{238}U by multi-step CA-TIMS
714 measurements of closed-system natural zircon samples. *Chemical Geology*, 275, 186-198.
- 715 Morton, A., Ellis, D., Fanning, M., Jolley, D. and Whitham, A. 2012. Heavy mineral constraints on
716 Paleocene sand transport routes in the Faroe-Shetland Basin. In: Varming, T. and Ziska, H. (eds),
717 Faroe Islands Exploration Conference: Proceedings of the 3rd Conference. *Annales Societatis
718 Scientiarum Faeroensis*, 56, 59-83.
- 719 Nasdala, L., Hofmeister, W., Norberg, N., Mattinson, J.M., Corfu, F., Dörr, W., Kamo, S.L., Kennedy,
720 A.K., Kronz, A., Reiners, P.W., Frei, D., Košler, J., Wan, Y., Götze, J., Häger, T., Kröner, A. and Valley,
721 J.W. 2008. Zircon M257 – a homogeneous natural reference material for the ion microprobe U-Pb
722 analysis of zircon. *Geostandards and Geoanalytical Research*, 32, 247-265.
- 723 Nisbet, H. C. 1961. The geology of North Rona. *Transactions of the Geological Society of Glasgow*,
724 24, 169-189.
- 725 Nutman, A.P., Kalsbeek, F. and Friend, C.R.L. 2008. The Nagssugtoqidian orogen in South-West
726 Greenland: evidence for Palaeoproterozoic collision and plate assembly. *American Journal of
727 Science*, 308, 529-572.
- 728 Nutman, A.P., Friend, C.R.L. and Heiss, J. 2010. Setting of the c. 2560 Qôrquq Granite complex in the
729 Archaean crustal evolution of southern West Greenland. *American Journal of Science*, 310, 1081-
730 1114.
- 731 Park, R.G. 2005. The Lewisian terrane model: a review. *Scottish Journal of Geology*, 41, 105-118.
- 732 Park, R.G., Tarney, J. and Connelly, J.N. 2001. The Loch Maree Group: Palaeoproterozoic subduction-
733 accretion complex in the Lewisian of NW Scotland. *Precambrian Research*, 105, 205-226.
- 734 Passchier, C.W. and Trouw, R.A.J. 2005. *Microtectonics* (Second edition) Springer, Berlin.
- 735 Pringle, I.R. 1970. The structural geology of the North Roe area of Shetland. *Geological Journal*. 7,
736 147-170.
- 737 Ritchie, J.D., Noble, D., Derbyshire, F., Millar, I. and Chambers, L., 2011. Pre-Devonian. In: Ritchie,
738 J.D., Ziska, H., Johnson, H. and Evans, D. (eds), *Geology of the Faroe-Shetland Basin and adjacent
739 areas*. BGS Research Report RR/11/01, 71-78.
- 740 Simpson, C. 1985. Deformation of granitic rocks across the brittle-ductile transition. *Journal of
741 Structural Geology*. 7, 503-11.
- 742 Sláma, J., Košler, J., Condon, D.J., Crowley, J.L., Gerdes, A., Hanchar, J.M., Horstwood, M.S.A., Morris,
743 G.A., Nasdala, L., Norberg, N., Schaltegger, U., Schoene, B., Tubrett, M.N. and Whitehouse, M.J.
744 2008. Plešovice zircon - a new natural reference material for U-Pb and Hf isotopic microanalysis.
745 *Chemical Geology*, 249, 1-35.
- 746 Stacey, J.S. and Kramers, J.D. 1975. Approximation of terrestrial lead isotope evolution by a two-
747 stage model. *Earth and Planetary Science Letters*, 26, 207-221.

- 748 Stoker, M., Holford, S.P. and Hillis, R.R. 2018. A rift-to-drift record of vertical crustal motions in the
749 Faroe–Shetland Basin, NW European margin: establishing constraints on NE Atlantic evolution.
750 *Journal of the Geological Society*, 175, <http://dx.doi.org/10.1144/jgs2017-076>
- 751 Sutton J. and Watson J. 1951. The pre-Torridonian metamorphic history of the Loch Torridon and
752 Scourie areas in the north-west Highlands, and its bearing on the chronological classification of the
753 Lewisian. *Quarterly Journal of the Geological Society*, London, 106, 241-307.
- 754 Tappe, S., Smart, K.A., Pearson, D.G., Steenfelt, A. and Simonetti, A. 2011. Craton formation in Late
755 Archaean subduction zones revealed by first Greenland eclogites. *Geology*, 39, 1103-1106.
- 756 Walker, F. 1931. The Geology of Skerryvore, Dubh Artach, and Sule Skerry. *Geological Magazine*, 68,
757 315-323.
- 758 Walker, S., Thirlwall, M.F., Strachan, R.A. and Bird, A.F. 2016. Evidence from Rb-Sr mineral ages for
759 multiple orogenic events in Caledonides of the Shetland Islands, Scotland. *Journal of the Geological
760 Society*, London, 173, 489-503.
- 761 Wheeler, J., Park, R.G., Rollinson, H.R. and Beach, A. 2010. The Lewisian Complex: insights into deep
762 crustal evolution. In: Law, R.D., Butler, R.W.H., Holdsworth, R.E., Krabbendam, M. and Strachan, R.A.
763 (eds), *Continental Tectonics and Mountain Building: The Legacy of Peach and Horne*. Geological
764 Society, London, Special Publications, 335, 51-79.
- 765 Whitehouse, M.J. 1989. Sm-Nd evidence for diachronous crustal accretion in the Lewisian Complex
766 of Northwest Scotland. In: Ashwal, L.D. (ed.), *Growth of the Continental Crust*. *Tectonophysics*, 161,
767 245-256.
- 768 Whitehouse, M.J. 1993. Age of the Corodale gneisses, South Uist. *Scottish Journal of Geology*, 29, 1-
769 7.
- 770 Whitehouse, M.J. and Bridgewater, D. 2001. Geochronological constraints on Palaeoproterozoic
771 crustal evolution and regional correlations of the northern Outer Hebridean Lewisian complex.
772 *Precambrian Research*, 105, 227-245.
- 773 Whitham, A.G., Morton, A.C. and Fanning, C.M. 2004. Insights into Cretaceous–Palaeogene sediment
774 transport paths and basin evolution in the North Atlantic from a heavy mineral study of sandstones
775 from southern East Greenland. *Petroleum Geoscience*, 10, 61-72.
- 776 Verstralen, I., Hartley, A. and Hurst, A. 1995. The sedimentological record of a late Jurassic
777 transgression: Rona Member (Kimmeridge Clay Formation equivalent), West Shetland Basin, UKCS.
778 In: Hartley, A. J. and Prosser, D. J. (eds), *Characterization of Deep Marine Clastic Systems*. Geological
779 Society, Special Publications, 94, 155-176.

781 **Tables**

782 **Table I)** Basement samples from offshore west of Shetland included in the current U-Pb
 783 isotopic analysis study. Locations are shown in Fig. 1.

Sample number	Site	Long deg	Long min	Lat deg	Lat min	Company	Site type	Sample Depth (m)	Lithology
SULA SGEIR-ORKNEY									
HM11705	88/02	59	12.54	6	18.10	BGS	Shallow bh	13.00	Granitic gneiss
	59-								
HM11709	04/85DM	59	37.68	3	21.84	BGS	Seabed core		Granodioritic gneiss
	59-								
HM11711	04/186DM	59	42.30	3	30.04	BGS	Seabed core		Granite
LANCASTER									
Granodioritic-tonalitic									
HM11686	204/25-1	60	10.42	4	2.17	Hess	Expl well	2870.43	gneiss
HM11687	204/26-1A	60	9.29	4	53.25	Hess	Expl well	2648.68	Granodioritic gneiss
HM11688	204/27-1	60	9.54	4	39.17	BP	Expl well	2136.20	Granite
HM11689	204/28-1	60	9.49	4	32.01	BP	Expl well	1941.55	Granodioritic gneiss
GREATER CLAIR									
HM11691	205/20-1	60	27.39	3	7.01	Total	Expl well	2017.50	Granitic gneiss
HM11692	206/7a-2	60	41.16	2	36.43	Total	Expl well	2141.40	Granodioritic gneiss
HM11694	206/7a-2	60	41.16	2	36.43	Total	Expl well	2593.30	Granodioritic gneiss
HM22702	206/12-1	60	59.77	2	76.72	Shell	Expl well	1716.63	Granodioritic gneiss
VICTORY									
HM11698	208/23-1	61	10.14	1	30.55	Lasmo	Expl well	2071.26	Granitic gneiss
HM11699	208/26-1	61	7.05	1	49.15	BP	Expl well	3741.31	Granodioritic gneiss
HM11700	208/27-2	61	8.04	1	38.50	BP	Expl well	1357.11	Mafic-granitic gneiss

784

785

786

787

788

789

790

791

792

793

794

Table II) LA-SF-ICP-MS U-Th-Pb dating methodology at CAF, Stellenbosch University

Laboratory & Sample Preparation	
Laboratory name	Central Analytical Facility, Stellenbosch University
Sample type / mineral	Magmatic and detrital zircons
Sample preparation	Conventional mineral separation, 1 inch resin mount, 1 µm polish to finish
Imaging	CL, LEO 1430 VP, 10 nA, 15 mm working distance
Laser ablation system	
Make, Model & type	ESI/New Wave Research, UP213, Nd:YAG
Ablation cell & volume	Custom build low volume cell, volume ca.3 cm ³
Laser wavelength	213 nm
Pulse width	3 ns
Fluence	2.5 J/cm ⁻²
Repetition rate	10 Hz
Spot size	30 µm
Sampling mode / pattern	30 µm single spot analyses
Carrier gas	100% He, Ar make-up gas combined using a T-connector close to sample cell
Pre-ablation laser warm-up (background collection)	40 seconds
Ablation duration	20 seconds
Wash-out delay	30 seconds
Cell carrier gas flow	0.3 l/min He
ICP-MS Instrument	
Make, Model & type	Thermo Finnigan Element2 single collector HR-SF-ICP-MS
Sample introduction	Via conventional tubing
RF power	1100 W
Make-up gas flow	1.0 l/min Ar
Detection system	Single collector secondary electron multiplier
Masses measured	202, 204, 206, 207, 208, 232, 233, 235, 238
Integration time per peak	4 ms
Total integration time per reading	Approx. 1 sec
Sensitivity	20000 cps/ppm Pb
Dead time	16 ns
Data Processing	
Gas blank	40 second on-peak
Calibration strategy	GJ-1 used as primary reference material, Plešovice and M127 used as secondary reference material (Quality Control)
Reference Material info	M127 (Nasdala et al. 2008; Mattinson 2010); Plešovice (Slama et al. 2008); GJ-1 (Jackson et al. 2004)
Data processing package used / Correction for LIEF	In-house spreadsheet data processing using intercept method for laser induced elemental fractionation (LIEF) correction
Mass discrimination	Standard-sample bracketing with ²⁰⁷ Pb/ ²⁰⁶ Pb and ²⁰⁶ Pb/ ²³⁸ U normalised to reference material GJ-1
Common-Pb correction, composition and uncertainty	204-method, Stacey and Kramers (1975) composition at the projected age of the mineral, 5% uncertainty assigned
Uncertainty level & propagation	Ages are quoted at 2 sigma absolute, propagation is by quadratic addition. Reproducibility and age uncertainty of reference material and common-Pb composition uncertainty are propagated.
Quality control / Validation	Plešovice: Wtd ave ²⁰⁶ Pb/ ²³⁸ U age = 337 ± 4 (2SD, MSWD = 0.2) M127: Wtd ave ²⁰⁶ Pb/ ²³⁸ U age = 520 ± 5 (2SD, MSWD = 0.8)
Other information	
Detailed method description reported by Frei and Gerdes (2009)	

799 **Table III) U-Pb ages of crystalline basement samples from the Hebridean margin.**

800 ¹ Upper intercept U-Pb zircon age, this study. ² Concordia U-Pb zircon age, this study. ³
 801 Inferred U-Pb zircon age, this study. ⁴ Upper intercept U-Pb zircon age from Chambers et al.
 802 (2005) and Ritchie et al. (2011), obtained by ID-TIMS.

Sample number	Site	Lithology	U-Pb age (Ma)
'SULA SGEIR-ORKNEY'			
HM11705	88/02, 13.00 m	Granitic gneiss	2754 ± 22 ¹
HM11709	59-04/85DM	Granodioritic gneiss	2747 ± 7 ²
HM11711	59-04/186DM	Granite	2826 ± 5 ²
'LANCASTER'			
	202/2-1, 1219.8 m	Quartzofeldspathic gneiss	2829 ± 46 ⁴
HM11686	204/25-1, 2870.43 m	Granodioritic-tonalitic gneiss	2729 ± 12 ¹
HM11687	204/26-1A, 2648.68 m	Granodioritic gneiss	2733 ± 14 ¹ , 2744 ± 16 ²
HM11688	204/27-1, 2136.20 m	Granite	2745 ± 15 ¹ , 2739 ± 8 ²
HM11689	204/28-1, 1941.55 m	Granodioritic gneiss	2762 ± 13 ¹ , 2793 ± 10 ²
	205/22-1, 3225.5 m	Dioritic gneiss	2700 ± 13 ⁴
'GREATER CLAIR'			
HM11691	205/20-1, 2017.50 m	Granitic gneiss	2736 ± 12 ¹
HM11692	206/7a-2, 2141.40 m	Granodioritic gneiss	2806 ± 8 ²
HM11694	206/7a-2, 2593.30 m	Granodioritic gneiss	2753 ± 14 ¹
HM22702	206/12-1, 1716.63 m	Granodioritic gneiss	2748 ± 6 ¹
	206/8-1A, 2310.9 m	Dioritic gneiss	2801.7 + 5.1/-4.6 ⁴
'VICTORY'			
HM11698	208/23-1, 2071.26 m	Granitic gneiss	2776 ± 12 ¹
HM11699	208/26-1, 3741.31 m	Granodioritic gneiss	ca 2720-2760, ca 2800-2860 ³
HM11700	208/27-2, 1357.11 m	Mafic-granitic gneiss	2789 ± 8 ²

805
 806
 807
 808
 809
 810
 811
 812
 813
 814
 815

817 **Figures**

818 **Figure 1)** Map showing basement distribution at seabed, structural elements (grey lines) and drilled
819 occurrences of basement (red dots, with well numbers) and cover sedimentary rocks (yellow dots)
820 offshore that are referred to in the current paper; a combined red/yellow dot means that both
821 basement and cover were studied. Boxes show location of sub-areas whilst inset map shows map of
822 main structural features. WBF=Walls Boundary Fault; MTZ = Moine Thrust Zone, NRU = North
823 Roe/Uyea area, Shetland, SSK = Sule Skerry, SST = Sule Stack, NR = North Rona, SSG = Sula Sgeir

824 **Figure 2)** Location and lithologies of borehole cores from the Clair Ridge. a) location map and
825 interpreted seismic reflection profile through the basement ridge showing location of the sub-
826 horizontal 206/7a-2 well and core sections (numbered). b) Logs of basement cores showing
827 lithologies, contact relationships, locations of main cross-cutting faults and radiometrically dated
828 samples (blue dots).

829 **Figure 3)** Location and lithologies of borehole cores from other key borehole cores. a) location map
830 showing locations of borehole cores shown here. b) Logs of basement cores – and in 3 cases
831 overlying cover rocks - showing lithologies, contact relationships and locations of early fault rock
832 types.

833 **Figure 4)** Representative core specimens of typical basement lithologies. A) granodioritic gneiss; b)
834 granitic gneiss; c) porphyritic granite; d) fold in gneisses cut by shear zone (SZ) that host a porphyritic
835 granite sheet (see Fig 2b, Core 6); e) foliated dioritic gneiss enclave hosted in granitic gneiss; f)
836 metre-scale folding of gneisses. Core and depths shown in all cases. Note that the prevalence of
837 samples from 206/8-8 is due to this core having been slabbed and polished.

838 **Figure 5)** Typical mineralogy and textures seen in basement cores, with core and depths shown for
839 each sample. a) Cross-polars view of typical granodioritic gneiss with cuspatelobate quartz-feldspar
840 contacts and irregular undulose extinction in quartz. b) PPL view of typical cuspatelobate mafics-
841 feldspar contacts, with late alteration of mafics (?originally pyroxene) to fine grained amphibole and
842 chlorite, and feldspars to sericite. c) Higher power PPL view of plagioclase grain (outlined) seeded
843 with numerous small clinzoisite/epidote grains reflecting static greenschist facies retrogression. d)
844 PPL view of intergrown aggregates of fine grained colourless amphibole, quartz, chlorite and calcite
845 (all after pyroxene – location of relict grain outlined) with rim of yellow epidote. e) PPL view of fine
846 quartz-epidote veins (labelled) overprinted by white mica-chlorite phyllonitic fabric (highlighted in
847 yellow), with feldspar clasts showing fibrous pressure shadows. f) Hand specimen sample of gneiss
848 and quartz-epidote veins (labelled) in basal Devonian Clair Group.

849 **Figure 6)** Selected minerals and microstructures from the samples analysed using U-Pb zircon
850 geochronology. a) PPL view of sheared granitic gneiss with brown foliation-parallel pseudotachylite
851 with tensile offshoot suggesting top to the left sense of shear (from BGS thin section collection). b)
852 Cross polar view of granodioritic-dioritic gneiss showing intergrown altered plagioclase, pyroxene,
853 amphibole and secondary blue birefringent chlorite (dated sample HM11686). c) Cross polar view of
854 marginal myrmekite (myrm) development in granitic gneiss, with weak subgrain development in
855 quartz (dated sample HM11691). d) Cross polar view of granodioritic gneiss showing localised
856 retrogression and breakdown of plagioclase to fine grained aligned aggregates of white mica and
857 epidote, marginal subgrain rotation recrystallization in quartz and fibrous quartz-white mica tails

(labelled) around feldspars (dated sample HM11692). e) PPL view of granodioritic gneiss showing fine aggregates of green amphibole, biotite and epidote, possibly after orthopyroxene (relict grain outlined) intergrown with plagioclase, quartz and a dark relict grain of altered clinopyroxene (CPx) (dated sample HM11699). f) PPL view of more mafic granitic gneiss showing intergrown plagioclase and brown partially altered pyroxene with prominent ore-rich alteration rims (dated sample HM11700).

Figure 7) Selected CL images of zircons from basement gneisses from the Sula Sgeir-Orkney, Lancaster, Greater Clair and Victory sub-areas. Spot size is 30 µm. A) HM11705: BGS borehole 88/02, analysis 106. B) HM11705: BGS borehole 88/02, analysis 107. C) HM11686: well 204/25-1, analysis 094. D) HM11688: well 204/27-1, analyses 022 and 023. E) HM11691: well 205/20-1, analyses 050 and 051. F) HM11691: well 205/20-1, analyses 063 and 064. G) HM22702: well 206/12-1, analysis 277. H) HM11698: well 208/23-1, analyses 012 and 013. I) HM11699: well 208/26-1, analysis 064. J) HM11699: well 208/26-1, analysis 050 and 051.

Figure 8) U-Pb isotopic compositions of zircons from the Sula Sgeir-Orkney sub-area displayed on Wetherill concordia diagrams, together with best estimates for zircon crystallisation ages. All data-point error ellipses are 2σ . A) Granitic gneiss, HM11705, BGS borehole 88/02, 13.00 m (all data); B) Granodioritic gneiss, HM11709, BGS shallow borehole 59-04/85DM (all data); C) Granodioritic gneiss, HM11709, BGS shallow borehole 59-04/85DM (showing zircons used for concordia age determination); D) Granite, HM11711, BGS shallow borehole 59-04/186DM (all data); E) Granite, HM11711, BGS shallow borehole 59-04/186DM (showing zircons used for concordia age determination).

Figure 9) U-Pb isotopic compositions of zircons from the Lancaster sub-area displayed on Wetherill concordia diagrams, together with best estimates for zircon crystallisation ages. All data-point error ellipses are 2σ . A) Granodioritic-tonalitic gneiss, HM11686, well 204/25-1, 2870.43 m (all data); B) Granodioritic-tonalitic gneiss, HM11686, well 204/25-1, 2870.43 m (showing data used for upper intercept age determination); C) Granodioritic gneiss, HM11687, 204/26-1A, well 2648.68 m (all data); D) Granodioritic gneiss, HM11687, 204/26-1A, well 2648.68 m (showing data used for upper intercept age determination); E) Granodioritic gneiss, HM11687, 204/26-1A, well 2648.68 m (showing data used for concordia age determination); F) HM11688, well 204/27-1, 2136.20 m (all data); G) HM11688, well 204/27-1, 2136.20 m (showing data used for upper intercept age determination); H) Granite, HM11688, well 204/27-1, 2136.20 m (showing data used for concordia age determination); I) Granodioritic gneiss, HM11689, well 204/28-1, 1941.55 m (showing all data and determination of upper intercept age); J) Granodioritic gneiss, HM11689, well 204/28-1, 1941.55 m (showing data used for concordia age determination).

Figure 10) U-Pb isotopic compositions of zircons from the Greater Clair and Victory sub-areas displayed on Wetherill concordia diagrams, together with best estimates for zircon crystallisation ages. All data-point error ellipses are 2σ .

Greater Clair: A) Granitic gneiss, HM11691, 205/20-1, 2017.50 m (showing all data and determination of upper intercept age); B) Granodioritic gneiss, HM11692, 206/7a-2, 2141.40 m (all data); C) Granodioritic gneiss, HM11692, 206/7a-2, 2141.40 m (showing data used for concordia age determination); D) Granodioritic gneiss, HM11694, 206/7a-2, 2593.30 m (all data); E) Granodioritic

899 gneiss, HM11694, 206/7a-2, 2593.30 m (showing data used for upper intercept age determination);
900 F) Granodioritic gneiss, HM22702, 206/12-1, 1716.63 m (showing all data and determination of
901 upper intercept age).

902 Victory: G) Granitic gneiss, HM11698, 208/23-1, 2071.26 m (showing all data and determination of
903 upper intercept age); H) Granodioritic gneiss, HM11699, 208/26-1, 3741.31 m (all data); I) Mafic-
904 granitic gneiss, HM11700, 208/27-2, 1357.11 m (all data); J) Mafic-granitic gneiss, HM11700, 208/27-
905 2, 1357.11 m (showing data used for concordia age determination).

906 **Figure 11)** Probability – density plots for selected samples of basement and cover sequences. Dark
907 grey areas are zircons with <10% discordance, pale grey areas are zircons with >10% discordance. n =
908 number of zircons with <10% discordance in total zircon data set. See Figure 1 for location of wells
909 unless indicated otherwise. A) Granodioritic basement gneiss sample HM11699, Victory sub-area
910 (208/26-1, 3741.31 m), 23 zircons with 99-101% concordance; B) Upper Jurassic Rona Member
911 sandstone sample HM12189, Lancaster sub-area (204/27-1, 2094.65 m), n = 89/106. No zircons
912 <2500 Ma detected. C) Upper Jurassic Rona Member sandstone sample HM12194, Lancaster sub-
913 area (202/3-1A, 1642.50 m), n = 55/89. Spectrum also includes six younger zircons with <10%
914 discordance at 494 Ma, 1014 Ma, 1353 Ma, 1551 Ma, 1960 Ma and 2127 Ma. D) Lower Cretaceous
915 Royal Sovereign Formation sample HM12357, Greater Clair sub-area (206/4-1, 4115 m), n=84/99.
916 Spectrum also includes one younger zircon with <10% discordance at 1692 Ma. E) Triassic sandstone
917 sample HM12172, Victory sub-area (213/23-1, 3598.36 m), n=54/107. Spectrum also includes two
918 younger zircons with <10% discordance at 1096 Ma and 1751 Ma. F) Lower Cretaceous (Albian)
919 sample W4629, Kangerlussuaq, East Greenland, n=34/53. See Figure 15 for location. Data from
920 Whitham et al. (2004), acquired by SHRIMP.

921 **Figure 12)** Hf isotope data displayed in the $\epsilon\text{Hf}(t)$ versus U-Pb age diagram. Symbols represent
922 analyses of individual growth domains of zircon from the different samples. The depleted mantle
923 (Chauvel et al. 2008) and the fields of the Neoarchaean to Palaeoarchaean crust, assuming a crustal
924 $^{176}\text{Lu}/^{177}\text{Hf}$ of 0.0113, are shown for comparison.

925 **Figure 13)** Map based on Fig. 1 showing geographic distribution of U-Pb zircon and Hf T_{DM} ages from
926 the basement gneisses, offshore west of Shetland (current study) and from Ritchie et al. (2011).

927 **Figure 14)** Probability – density plot of all zircon ages with <5% discordance from crystalline
928 basement west of Shetland (n=313), showing the dominance of crystallisation ages between ca 2720
929 Ma and 2750 Ma, with a subordinate older group between ca 2790 Ma and 2840 Ma.

930 **Figure 15)** Simplified map showing the major age provinces within the British Isles, Ireland and
931 Greenland, showing suggested location and extent of FST and its approximate southern boundary.
932 MTZ = Moine Thrust Zone; WBF = Walls Boundary Fault; GGFZ = Great Glen Fault Zone; Nag =
933 Nagssugtoqidian; CGC = Central Greenland (Rae) Craton; KB = Kangerlussuaq Basin; EGC = East
934 Greenland Caledonides. RT = Rhiconich Terrane of Lewisian Gneiss Complex

935

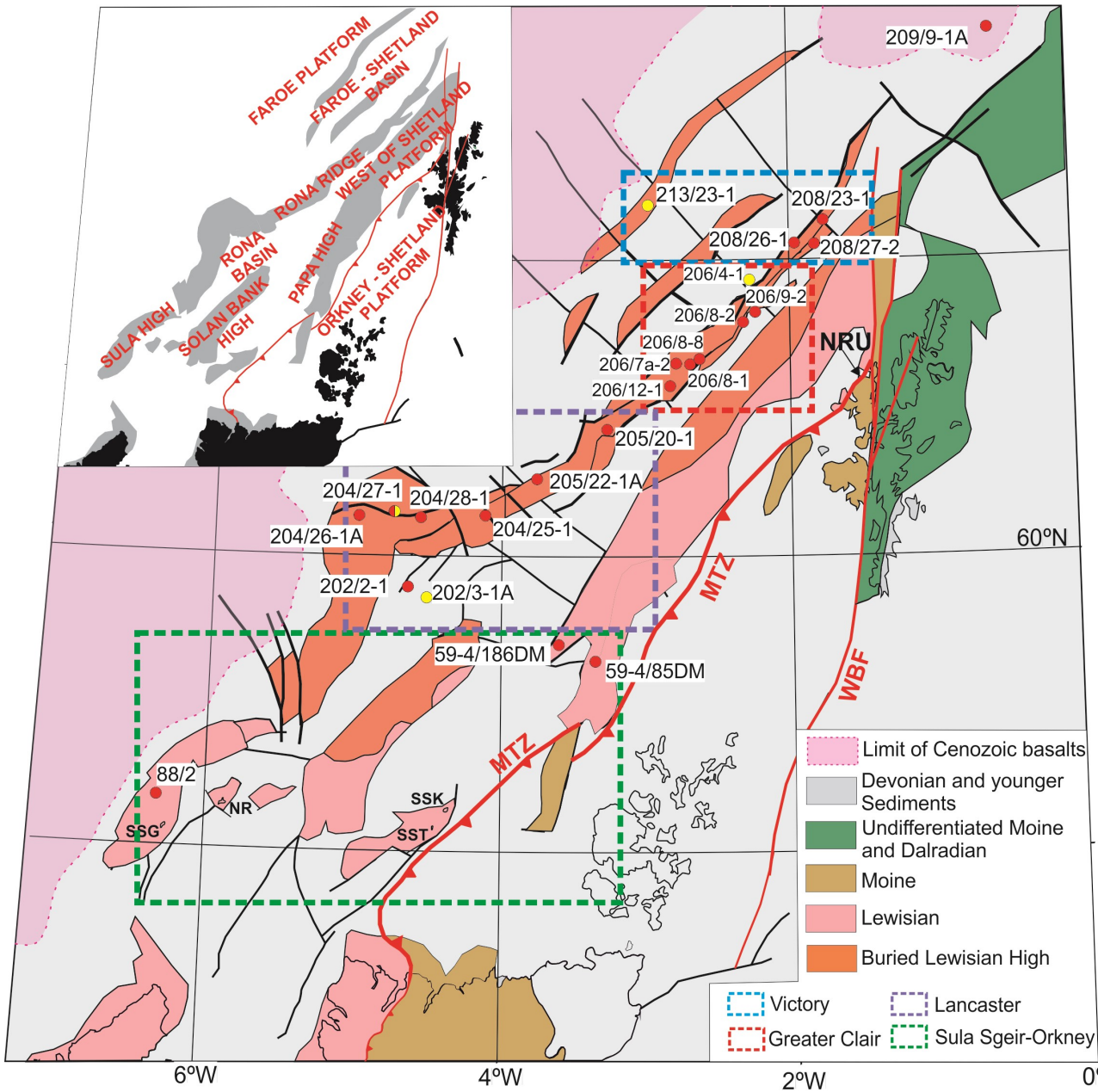


Figure 1

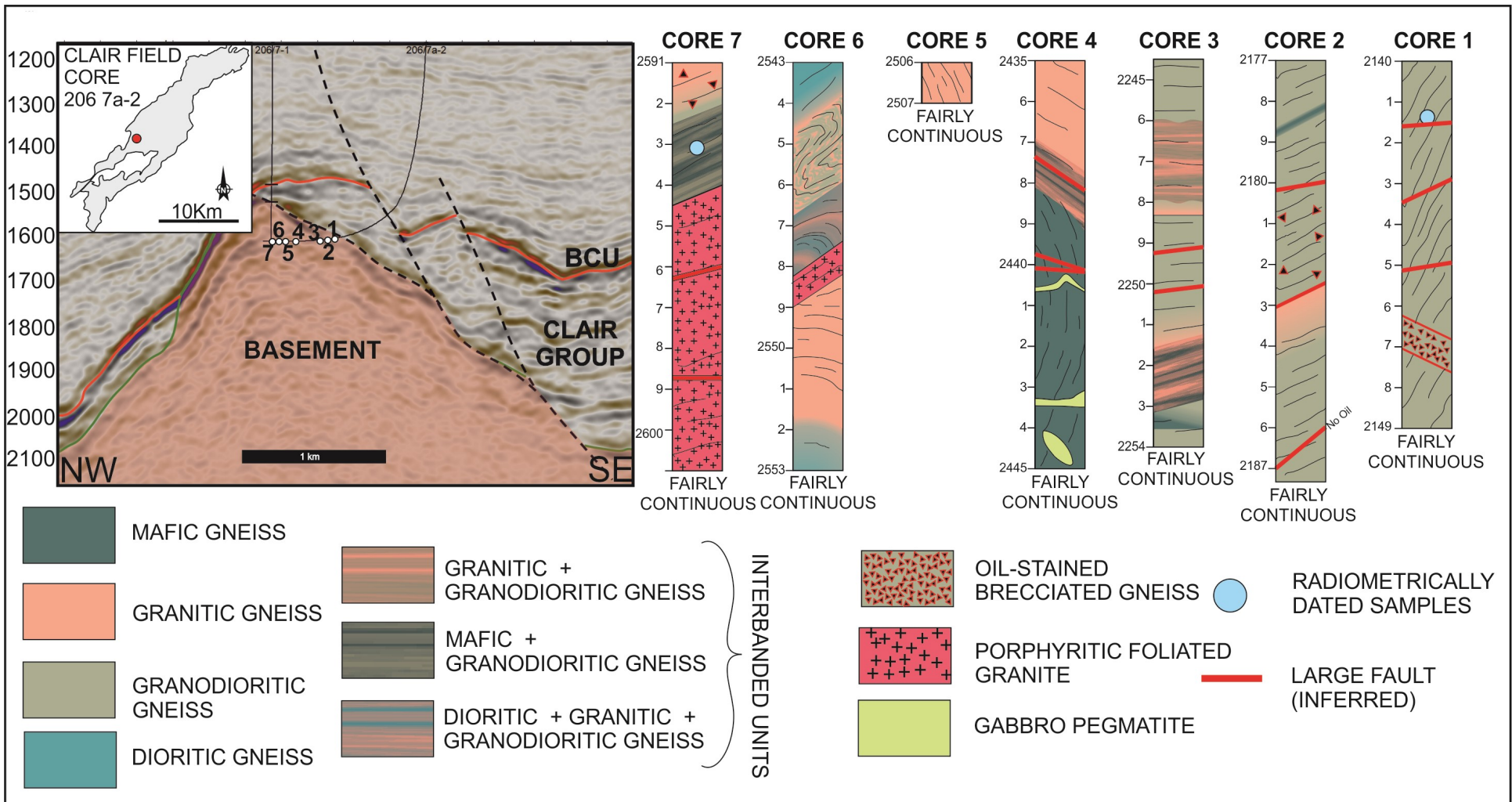


Figure 2

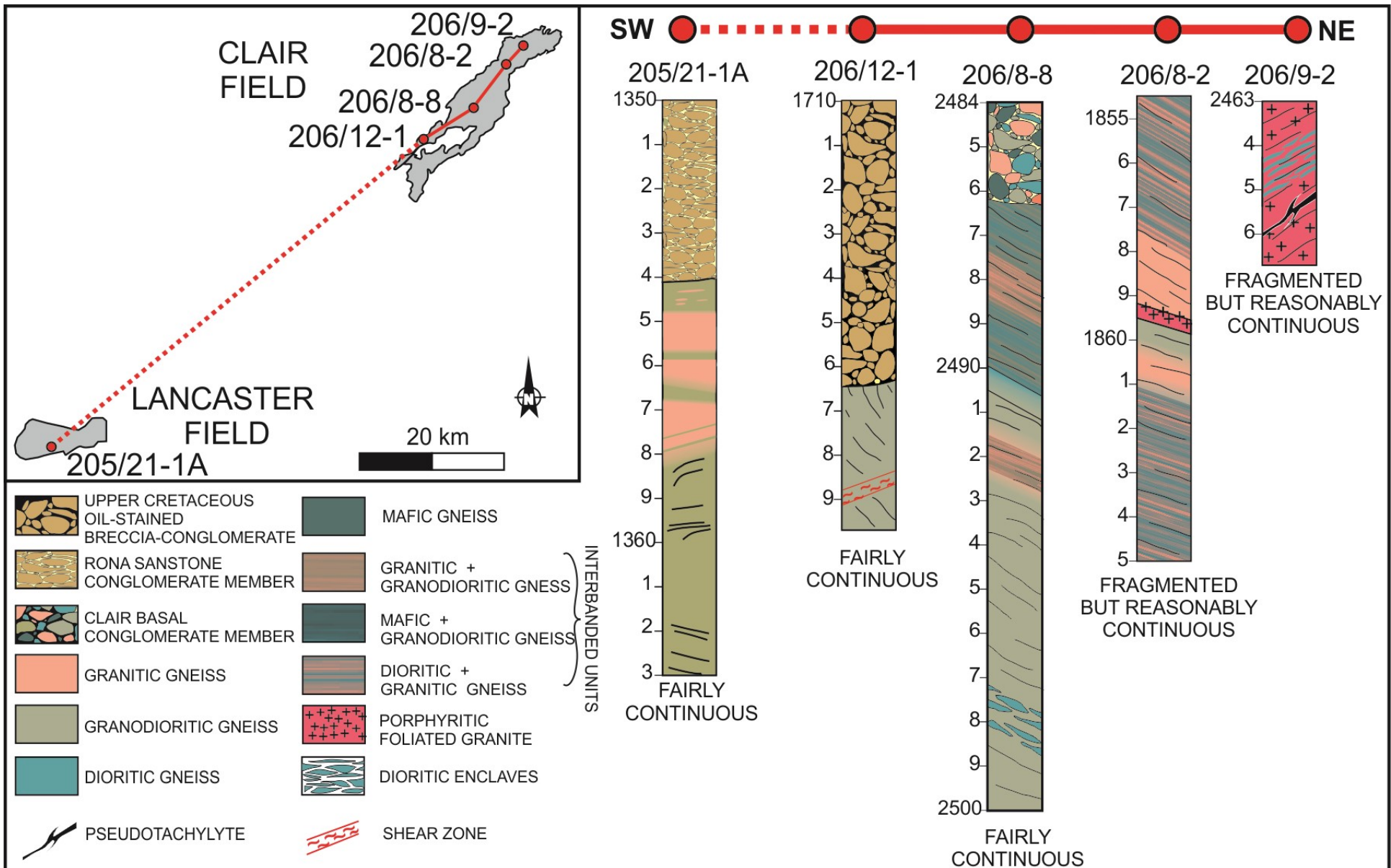
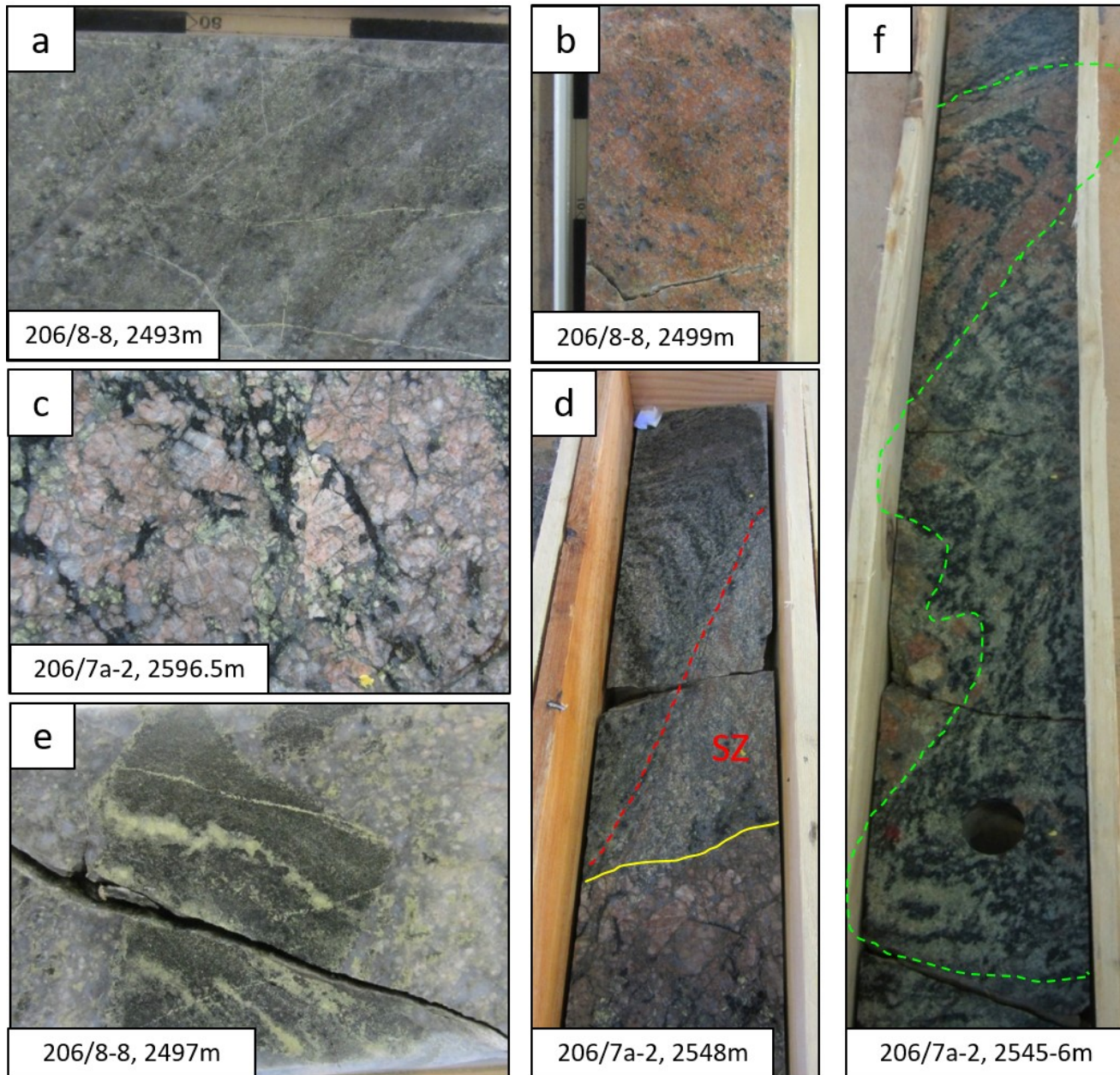


Figure 3

Figure 4



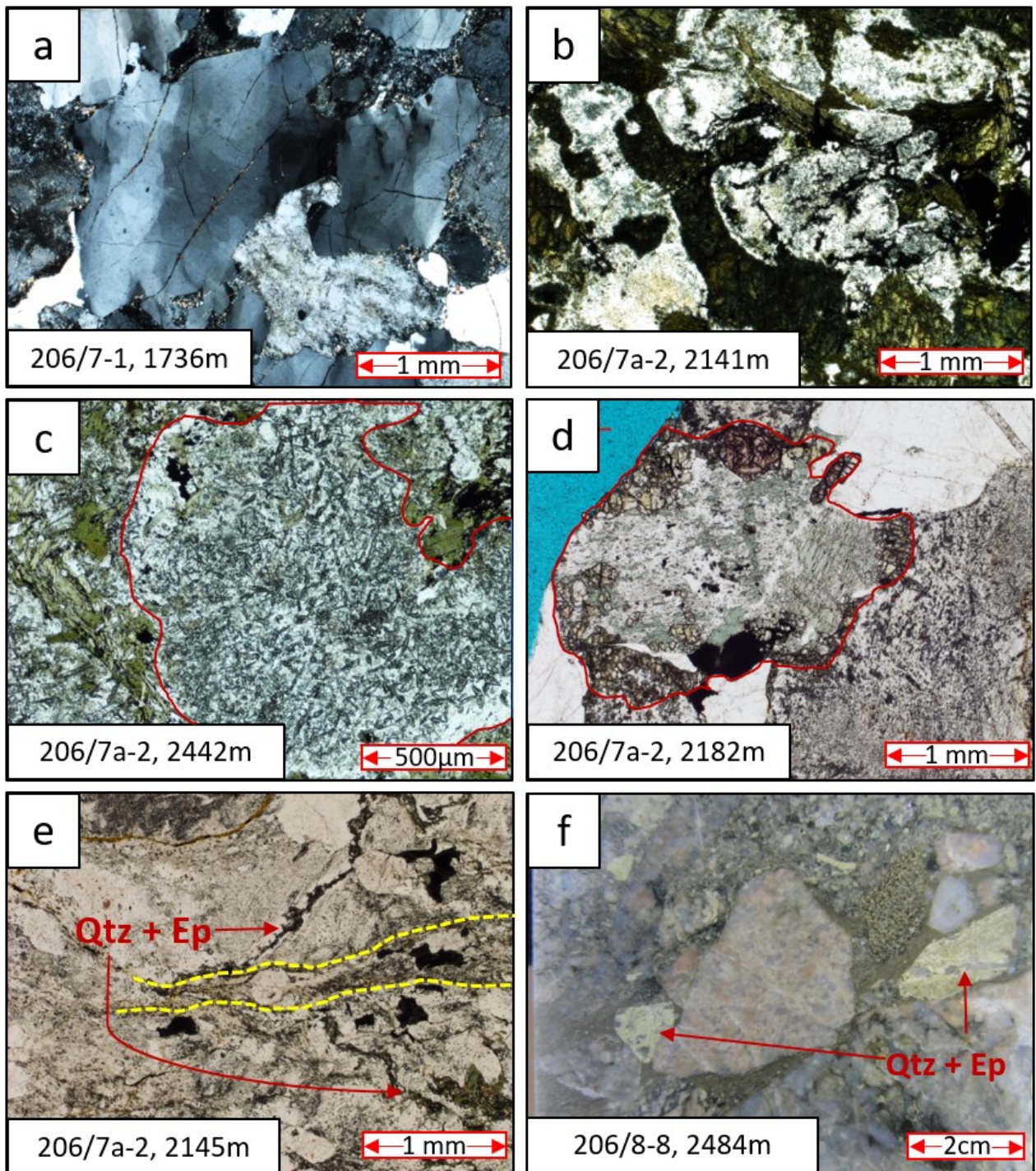


Figure 5

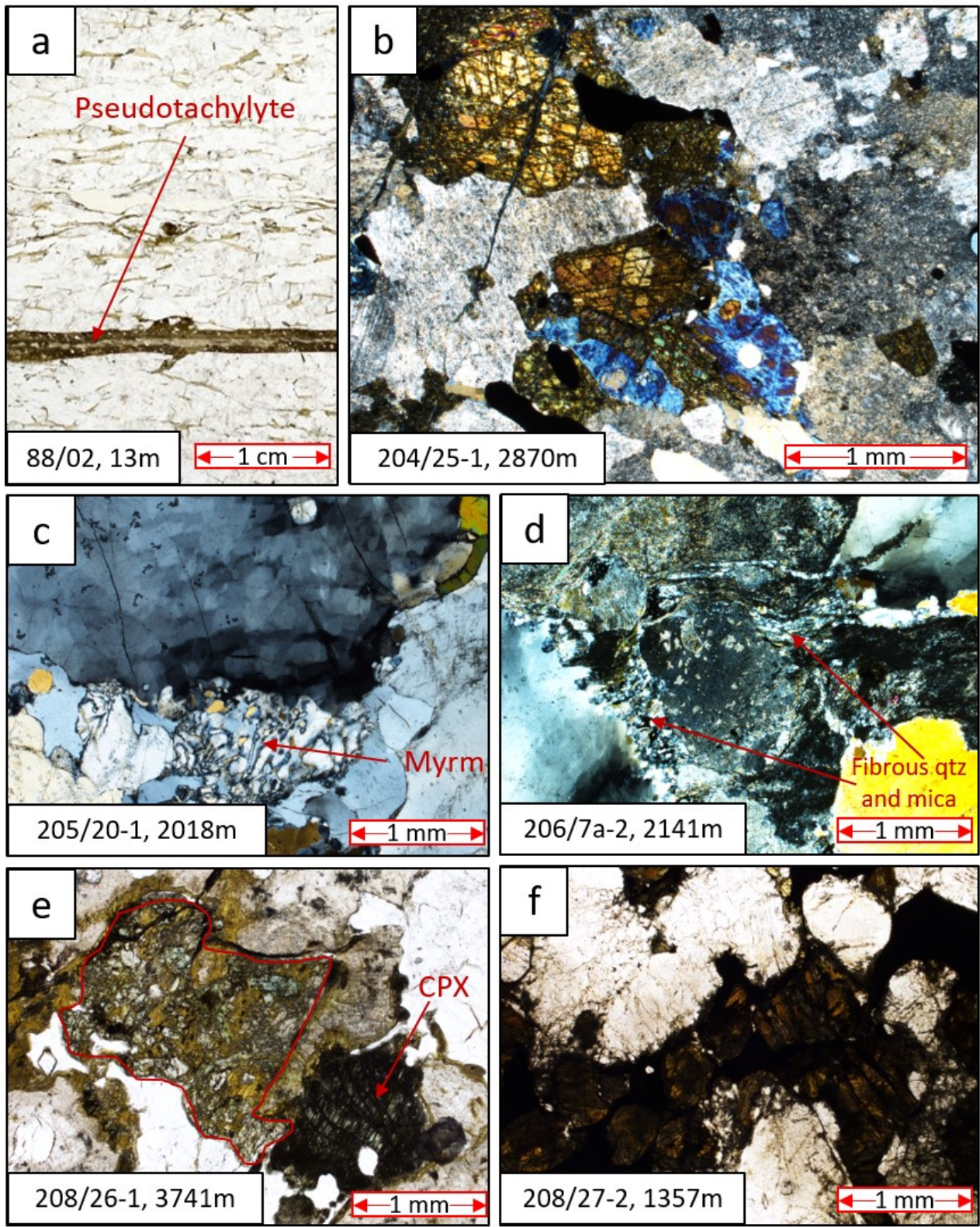


Figure 6

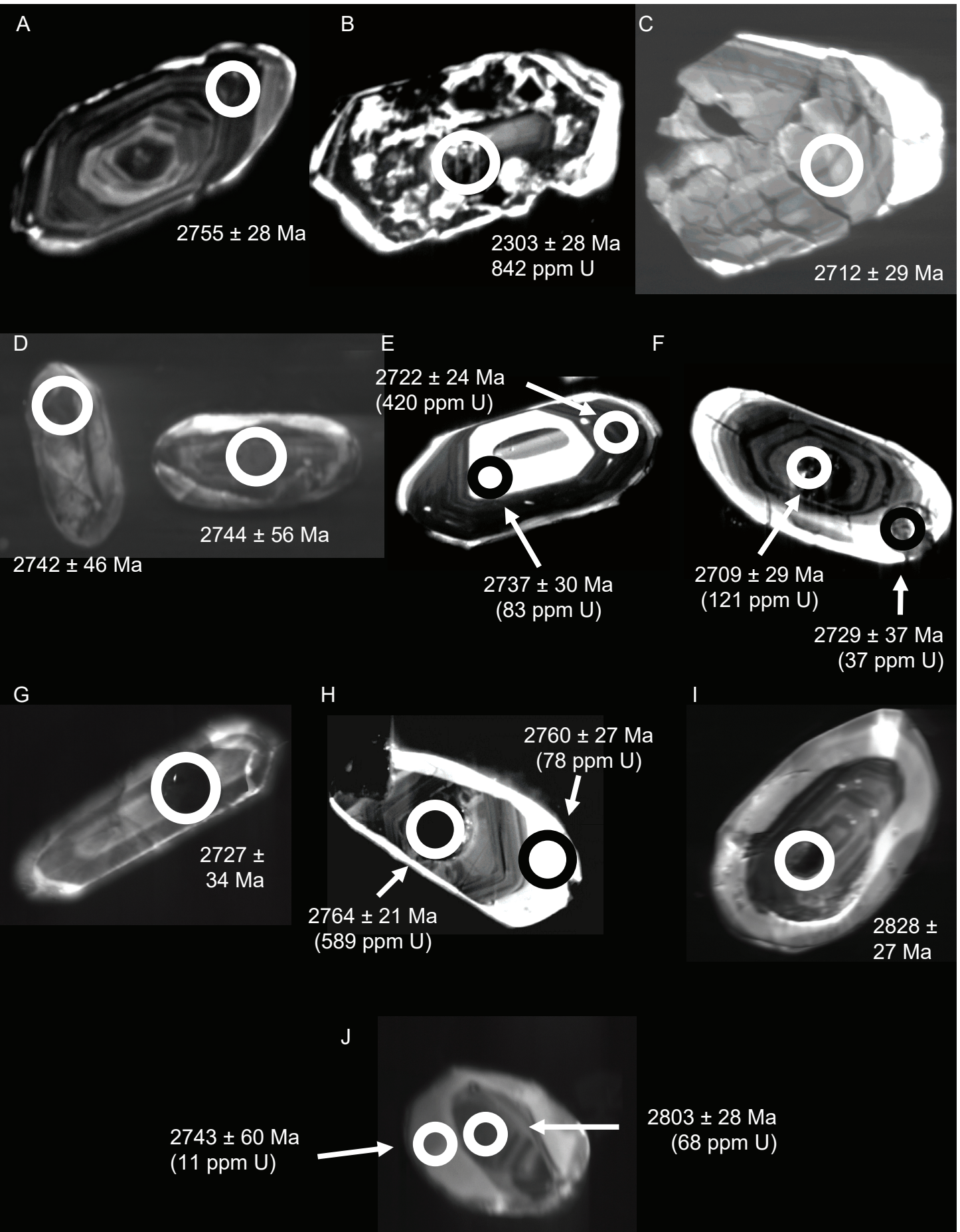


Figure 7

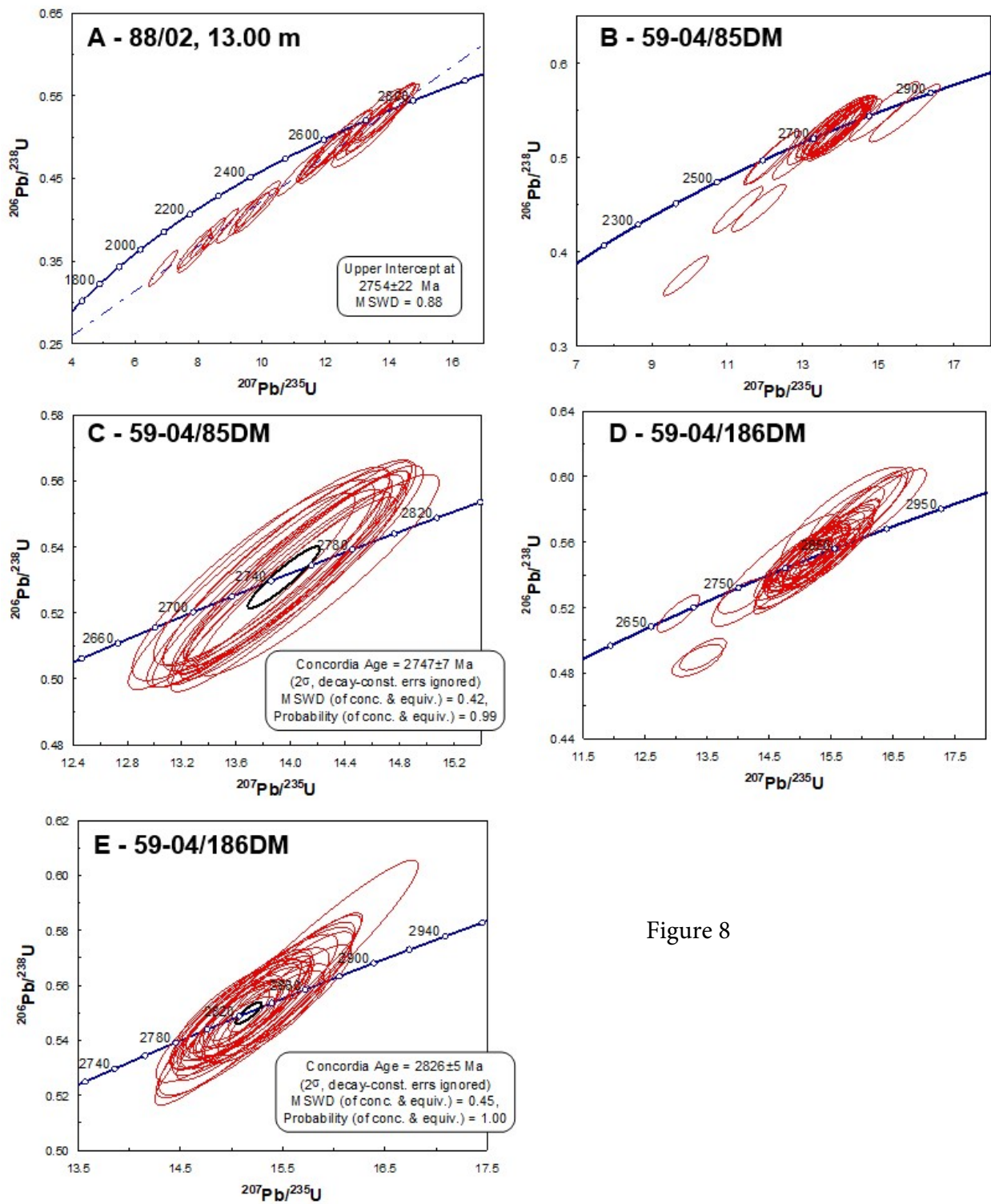


Figure 8

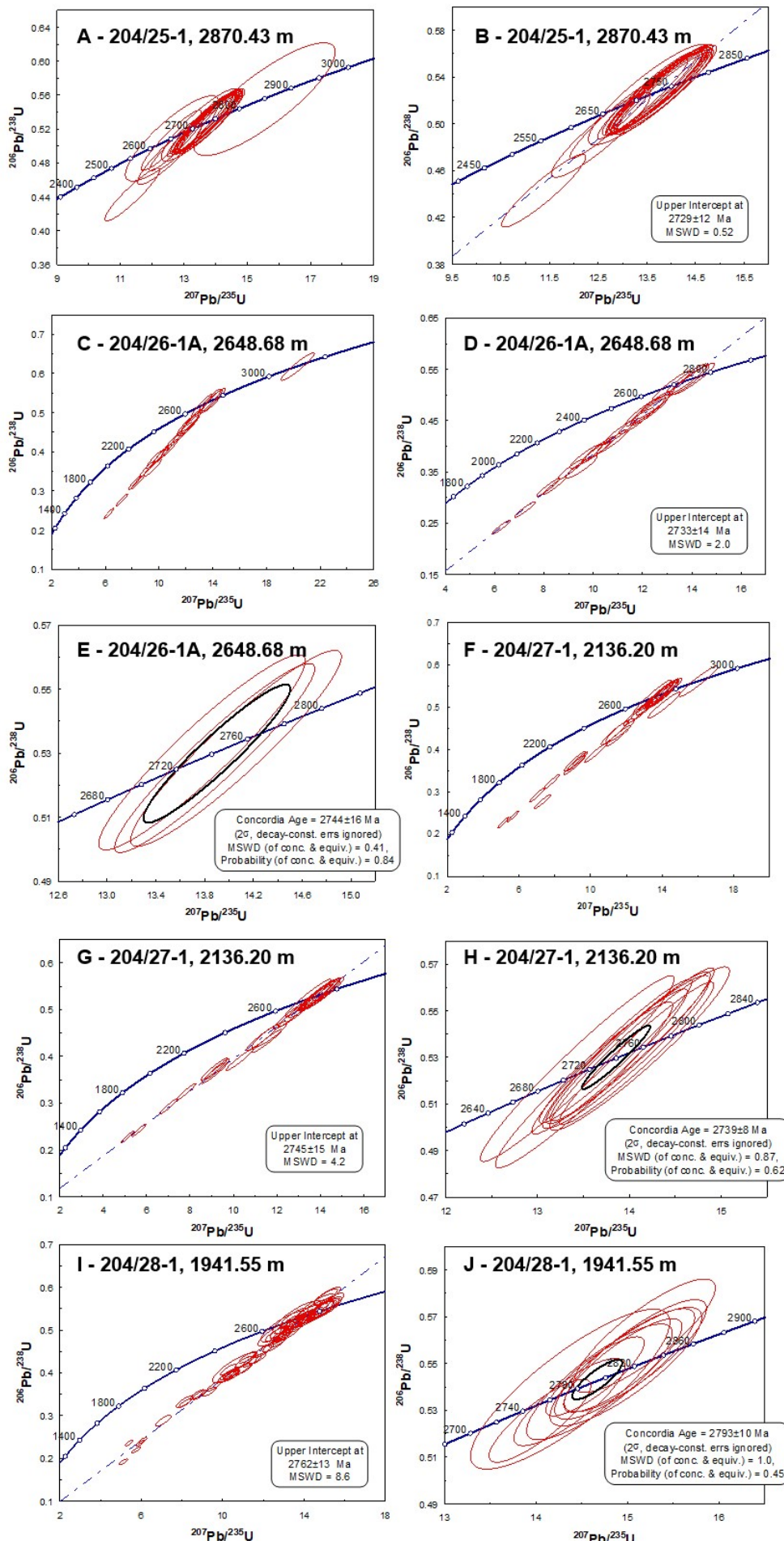


Figure 9

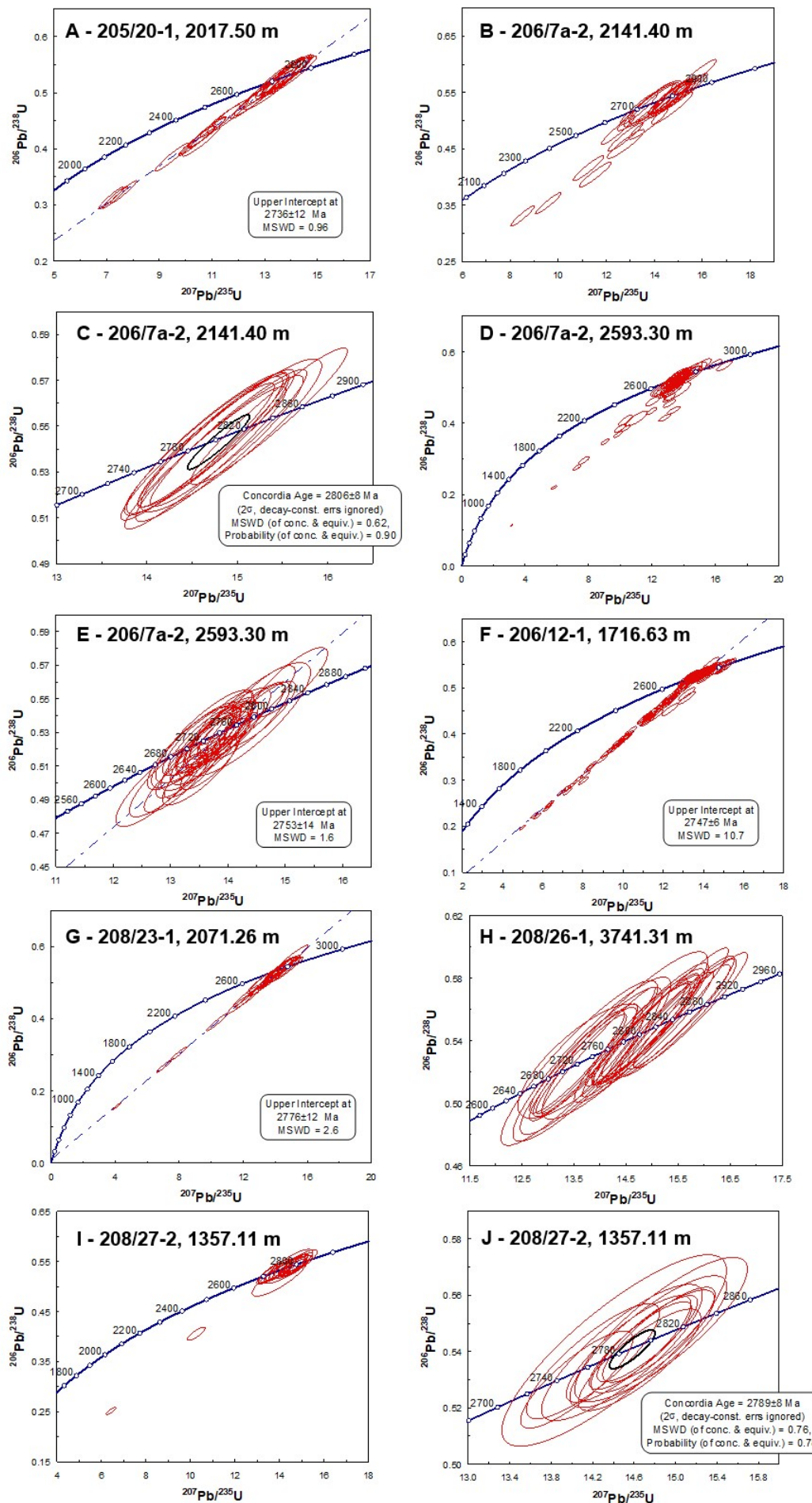


Figure 10

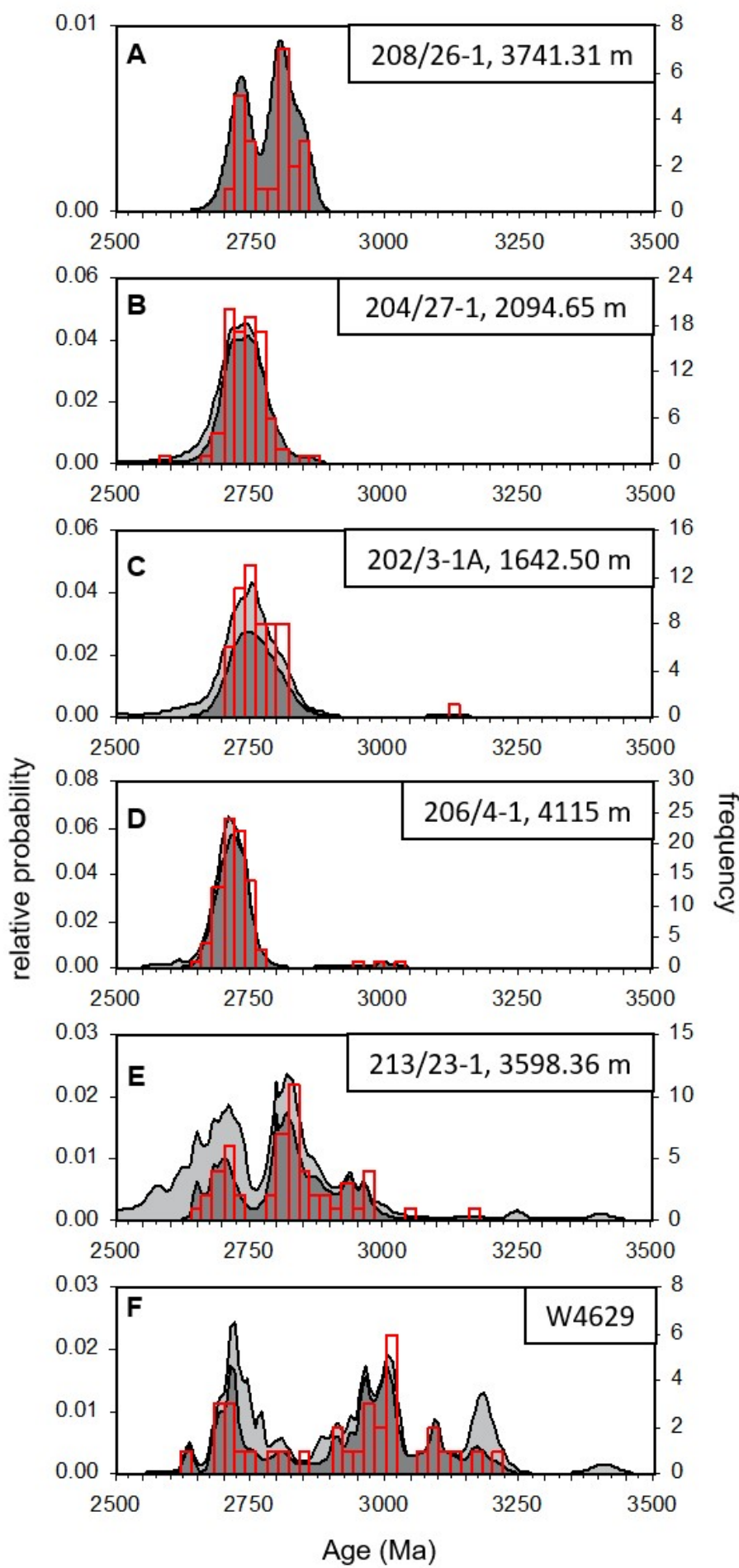


Figure 11

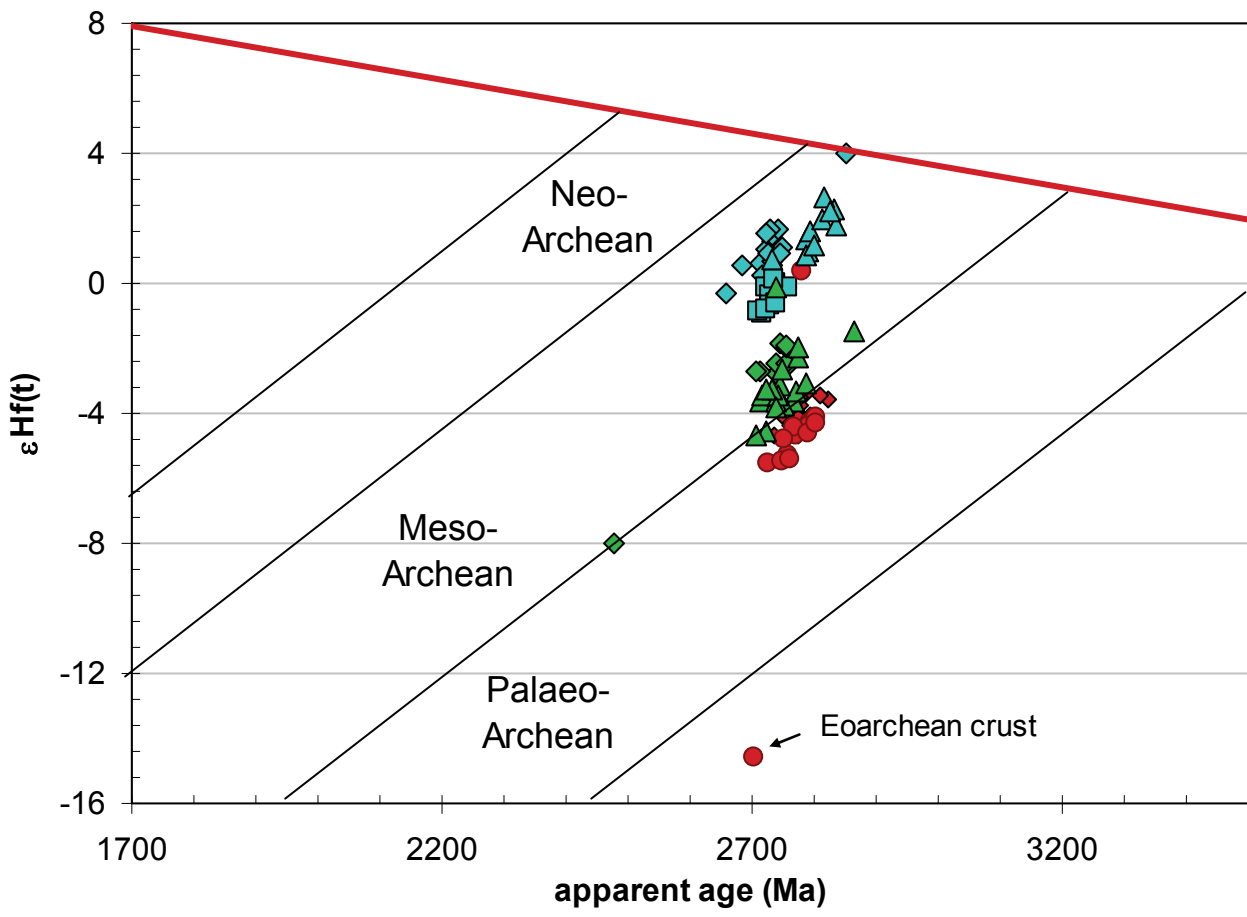
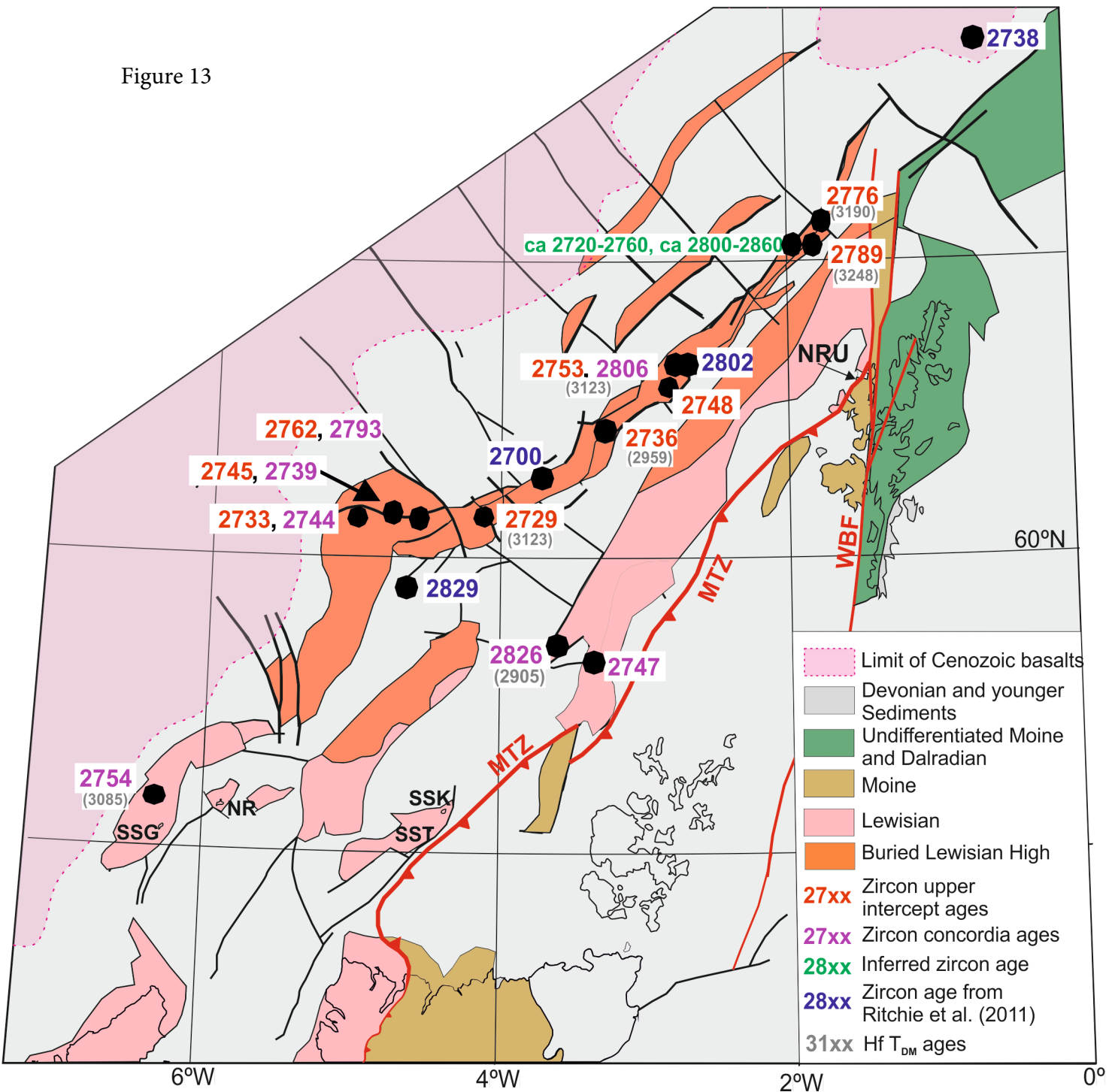


Figure 12

Figure 13



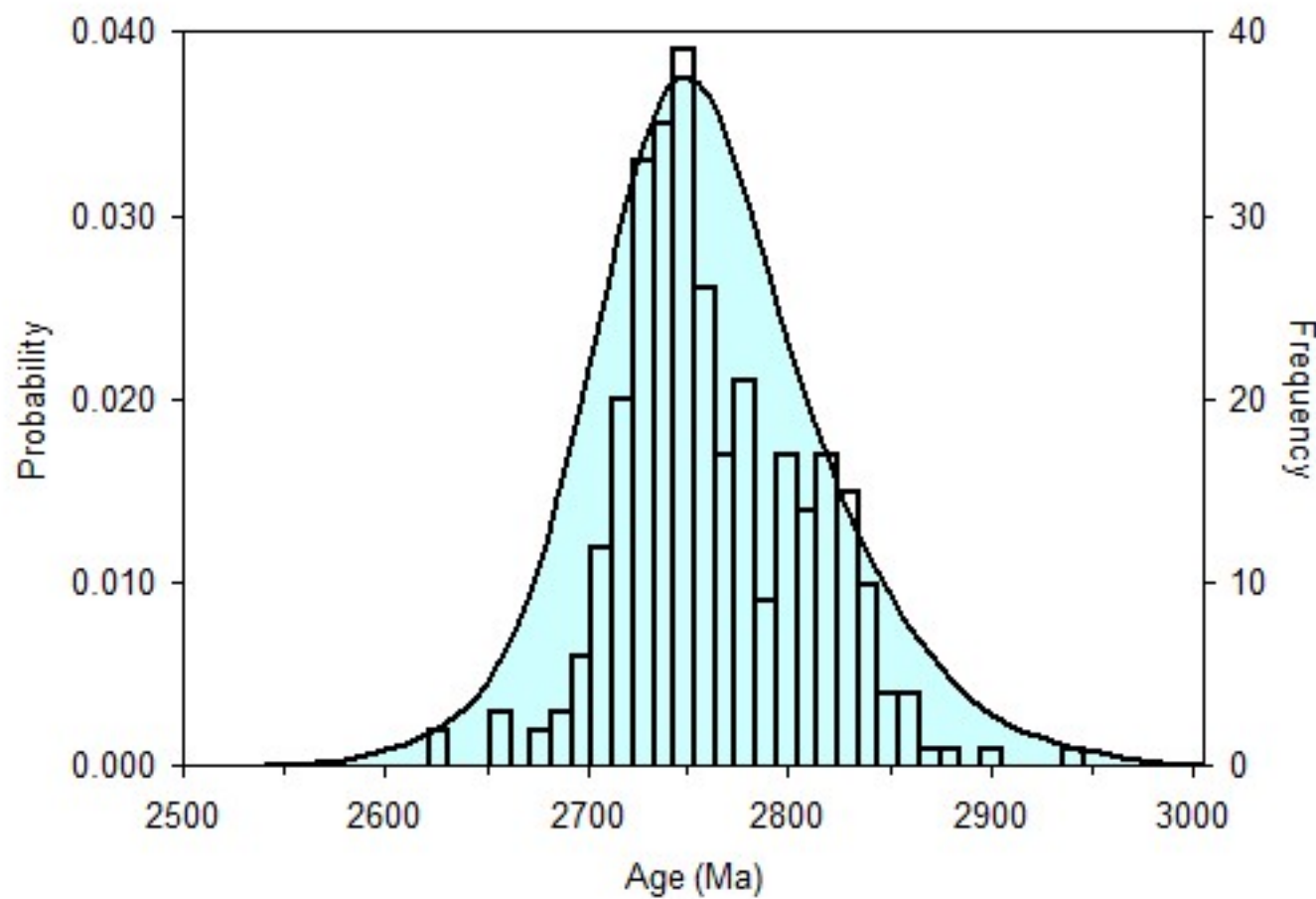


Figure 14

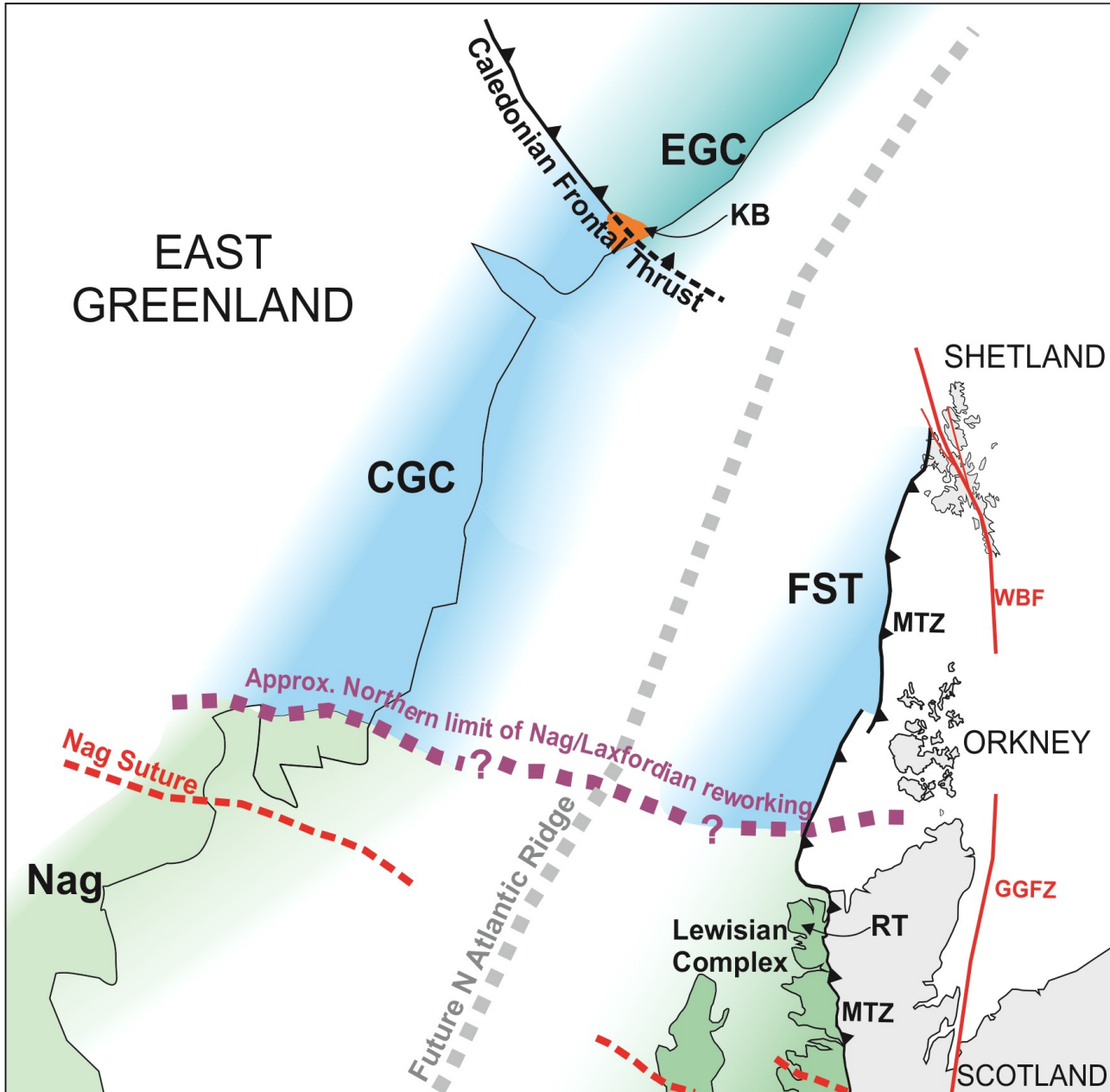


Figure 15

Sample	Analysis	U [ppm] ^a	Pb [ppm] ^a	Th/U ^a	RATIOS						AGES [Ma]						Conc.	use for UI age	
					$^{207}\text{Pb}/^{235}\text{U}$ ^b	$2\sigma^d$	$^{206}\text{Pb}/^{238}\text{U}$ ^b	$2\sigma^d$	ρ_{ho}^c	$^{207}\text{Pb}/^{206}\text{Pb}$ ^e	$2\sigma^d$	$^{207}\text{Pb}/^{235}\text{U}$	2σ	$^{206}\text{Pb}/^{238}\text{U}$	2σ	$^{207}\text{Pb}/^{206}\text{Pb}$	2σ		
204/25-1, 2870.43 m	Zircon_Sample_085	111	56	0.45	12.78	0.70	0.503	0.026	0.95	0.184	0.003	2664	146	2626	113	2693	27	98	x
204/25-1, 2870.43 m	Zircon_Sample_086	70	37	0.75	13.86	0.79	0.530	0.029	0.94	0.190	0.004	2740	157	2743	120	2739	31	100	x
204/25-1, 2870.43 m	Zircon_Sample_087	40	22	0.59	13.83	0.83	0.531	0.030	0.93	0.189	0.004	2738	165	2747	125	2732	36	101	x
204/25-1, 2870.43 m	Zircon_Sample_088	45	24	0.84	13.54	1.02	0.525	0.035	0.89	0.187	0.006	2718	204	2720	148	2717	55	100	x
204/25-1, 2870.43 m	Zircon_Sample_089	112	59	0.97	13.71	0.77	0.527	0.028	0.95	0.189	0.003	2730	153	2728	119	2731	29	100	x
204/25-1, 2870.43 m	Zircon_Sample_090	108	57	0.75	13.84	0.80	0.526	0.029	0.94	0.191	0.004	2739	158	2726	121	2749	31	99	x
204/25-1, 2870.43 m	Zircon_Sample_091	7	3	0.11	12.64	1.20	0.509	0.041	0.85	0.180	0.009	2653	252	2652	176	2654	81	100	x
204/25-1, 2870.43 m	Zircon_Sample_092	82	44	0.54	13.81	0.81	0.531	0.029	0.94	0.189	0.004	2737	160	2744	123	2732	32	100	x
204/25-1, 2870.43 m	Zircon_Sample_093	96	50	0.69	13.63	0.77	0.526	0.028	0.95	0.188	0.003	2725	153	2727	119	2723	28	100	x
204/25-1, 2870.43 m	Zircon_Sample_094	154	80	0.74	13.41	0.76	0.522	0.028	0.95	0.187	0.003	2709	153	2706	118	2712	29	100	x
204/25-1, 2870.43 m	Zircon_Sample_098	76	40	0.67	13.91	0.84	0.531	0.030	0.94	0.190	0.004	2744	165	2744	126	2743	35	100	x
204/25-1, 2870.43 m	Zircon_Sample_099	42	18	0.57	11.38	0.70	0.443	0.025	0.93	0.186	0.004	2555	158	2364	114	2710	38	87	x
204/25-1, 2870.43 m	Zircon_Sample_100	202	106	0.42	13.71	0.76	0.527	0.028	0.96	0.189	0.003	2730	152	2727	118	2731	27	100	x
204/25-1, 2870.43 m	Zircon_Sample_101	75	40	0.57	13.74	0.81	0.527	0.029	0.94	0.189	0.004	2732	161	2730	123	2733	32	100	x
204/25-1, 2870.43 m	Zircon_Sample_102	4	2	0.21	15.55	1.82	0.555	0.054	0.84	0.203	0.013	2850	334	2847	225	2852	101	100	
204/25-1, 2870.43 m	Zircon_Sample_103	48	25	0.68	13.72	0.84	0.528	0.030	0.93	0.189	0.004	2731	167	2732	127	2730	36	100	x
204/25-1, 2870.43 m	Zircon_Sample_104	82	44	0.80	13.73	0.82	0.529	0.030	0.94	0.188	0.004	2731	163	2738	125	2726	33	100	x
204/25-1, 2870.43 m	Zircon_Sample_106	77	40	0.56	13.56	0.80	0.526	0.029	0.94	0.187	0.004	2719	160	2725	123	2715	32	100	x
204/25-1, 2870.43 m	Zircon_Sample_107	88	44	0.71	12.61	0.77	0.507	0.029	0.93	0.181	0.004	2651	162	2642	124	2658	36	99	x
204/25-1, 2870.43 m	Zircon_Sample_111	102	54	0.59	13.64	0.81	0.526	0.029	0.94	0.188	0.004	2725	162	2724	124	2726	33	100	x
204/25-1, 2870.43 m	Zircon_Sample_113	79	42	0.63	13.85	0.83	0.527	0.030	0.94	0.190	0.004	2739	165	2731	126	2746	34	99	x
204/25-1, 2870.43 m	Zircon_Sample_114	51	25	0.64	12.56	0.83	0.491	0.030	0.92	0.186	0.005	2647	174	2573	128	2704	43	95	x
204/25-1, 2870.43 m	Zircon_Sample_115	92	49	0.54	13.68	0.83	0.528	0.030	0.94	0.188	0.004	2728	165	2732	126	2724	34	100	x

^aU and Pb concentrations and Th/U ratios are calculated relative to GJ-1 reference zircon^bCorrected for background and within-run Pb/U fractionation and normalised to reference zircon GJ-1 (ID-TIMS values/measured value); $^{207}\text{Pb}/^{235}\text{U}$ calculated using $(^{207}\text{Pb}/^{206}\text{Pb})/(^{238}\text{U}/^{206}\text{Pb} * 1/137.88)$ ^cRho is the error correlation defined as the quotient of the propagated errors of the $^{206}\text{Pb}/^{238}\text{U}$ and the $^{207}/^{235}\text{U}$ ratio^dQuadratic addition of within-run errors (2 SD) and daily reproducibility of GJ-1 (2 SD)^eCorrected for mass-bias by normalising to GJ-1 reference zircon (~0.6 per atomic mass unit) and common Pb using the model Pb composition of Stacey & Kramers (1975)

Sample	Analysis	U [ppm] ^a	Pb [ppm] ^a	Th/U ^a	RATIOS						AGES [Ma]						Conc.		use for UI age	use for conc age
					$^{207}\text{Pb}/^{235}\text{U}$ ^b	$2\sigma^d$	$^{206}\text{Pb}/^{238}\text{U}$ ^b	$2\sigma^d$	ρho^c	$^{207}\text{Pb}/^{206}\text{Pb}$ ^e	$2\sigma^d$	$^{207}\text{Pb}/^{235}\text{U}$	2σ	$^{206}\text{Pb}/^{238}\text{U}$	2σ	$^{207}\text{Pb}/^{206}\text{Pb}$	2σ	%		
204/26-1A, 2648.68 m	Zircon_Sample_008	1520	491	0.01	8.43	0.38	0.323	0.014	0.96	0.189	0.002	2278	104	1806	69	2734	21	66	x	
204/26-1A, 2648.68 m	Zircon_Sample_009	865	307	0.01	9.09	0.44	0.355	0.016	0.94	0.186	0.003	2347	113	1959	77	2704	26	72	x	
204/26-1A, 2648.68 m	Zircon_Sample_010	945	303	0.25	8.18	0.38	0.320	0.014	0.95	0.185	0.003	2251	104	1791	69	2700	23	66	x	
204/26-1A, 2648.68 m	Zircon_Sample_011	131	63	0.33	12.46	0.62	0.481	0.022	0.94	0.188	0.003	2640	131	2531	98	2724	28	93	x	
204/26-1A, 2648.68 m	Zircon_Sample_013	318	136	0.51	11.07	0.53	0.428	0.019	0.95	0.188	0.003	2529	121	2297	87	2721	25	84	x	
204/26-1A, 2648.68 m	Zircon_Sample_014	257	136	0.54	13.88	0.67	0.528	0.024	0.95	0.191	0.003	2742	132	2735	102	2747	26	100	x	x
204/26-1A, 2648.68 m	Zircon_Sample_015	989	274	0.41	7.23	0.34	0.277	0.012	0.95	0.189	0.003	2140	101	1576	63	2737	24	58	x	
204/26-1A, 2648.68 m	Zircon_Sample_016	982	238	0.14	6.26	0.30	0.243	0.011	0.95	0.187	0.003	2014	95	1400	57	2719	24	51	x	
204/26-1A, 2648.68 m	Zircon_Sample_020	254	132	0.02	13.18	0.63	0.518	0.023	0.95	0.184	0.003	2692	128	2692	99	2693	24	100	x	
204/26-1A, 2648.68 m	Zircon_Sample_021	159	98	0.37	20.33	1.01	0.618	0.029	0.94	0.239	0.004	3107	154	3101	115	3111	26	100		
204/26-1A, 2648.68 m	Zircon_Sample_023	131	61	0.25	12.12	0.66	0.469	0.023	0.92	0.188	0.004	2614	142	2478	103	2721	35	91	x	
204/26-1A, 2648.68 m	Zircon_Sample_024	436	170	0.09	10.12	0.48	0.390	0.018	0.95	0.188	0.003	2446	116	2121	82	2728	24	78	x	
204/26-1A, 2648.68 m	Zircon_Sample_025	299	108	0.14	9.53	0.52	0.360	0.018	0.92	0.192	0.004	2390	130	1982	85	2759	35	72	x	
204/26-1A, 2648.68 m	Zircon_Sample_027	674	268	0.13	10.29	0.51	0.397	0.018	0.94	0.188	0.003	2461	121	2154	85	2725	27	79	x	
204/26-1A, 2648.68 m	Zircon_Sample_028	150	80	0.19	14.06	0.71	0.532	0.025	0.94	0.192	0.003	2754	138	2748	105	2758	29	100	x	x
204/26-1A, 2648.68 m	Zircon_Sample_029	446	183	0.14	10.78	0.52	0.410	0.019	0.95	0.191	0.003	2505	120	2214	85	2750	25	80	x	
204/26-1A, 2648.68 m	Zircon_Sample_033	217	83	0.29	9.71	0.53	0.380	0.019	0.92	0.185	0.004	2407	131	2078	89	2699	35	77	x	
204/26-1A, 2648.68 m	Zircon_Sample_034	262	118	0.07	11.75	0.58	0.449	0.021	0.94	0.190	0.003	2585	128	2392	93	2740	28	87	x	
204/26-1A, 2648.68 m	Zircon_Sample_035	161	75	0.25	12.25	0.61	0.467	0.022	0.94	0.190	0.003	2624	131	2472	96	2743	29	90	x	
204/26-1A, 2648.68 m	Zircon_Sample_036	329	156	0.03	12.31	0.61	0.473	0.022	0.94	0.189	0.003	2628	131	2495	97	2733	28	91	x	
204/26-1A, 2648.68 m	Zircon_Sample_037	247	131	0.38	13.78	0.69	0.530	0.025	0.94	0.188	0.003	2735	137	2743	105	2729	29	100	x	x

^aU and Pb concentrations and Th/U ratios are calculated relative to GJ-1 reference zircon

^bCorrected for background and within-run Pb/U fractionation and normalised to reference zircon GJ-1 (ID-TIMS values/measured value); $^{207}\text{Pb}/^{235}\text{U}$ calculated using $(^{207}\text{Pb}/^{206}\text{Pb})/(^{238}\text{U}/^{206}\text{Pb} * 1/137.88)$

^cRho is the error correlation defined as the quotient of the propagated errors of the $^{206}\text{Pb}/^{238}\text{U}$ and the $^{207}/^{235}\text{U}$ ratio

^dQuadratic addition of within-run errors (2 SD) and daily reproducibility of GJ-1 (2 SD)

^eCorrected for mass-bias by normalising to GJ-1 reference zircon (~0.6 per atomic mass unit) and common Pb using the model Pb composition of Stacey & Kramers (1975)

Sample	Analysis	U [ppm] ^a	Pb [ppm] ^a	Th/U ^a	RATIOS						AGES [Ma]						Conc.	use for UI age	use for conc age	
					$^{207}\text{Pb}/^{235}\text{U}$ ^b	$2\sigma^d$	$^{206}\text{Pb}/^{238}\text{U}$ ^b	$2\sigma^d$	ρho^c	$^{207}\text{Pb}/^{206}\text{Pb}$ ^e	$2\sigma^d$	$^{207}\text{Pb}/^{235}\text{U}$ ^b	2σ	$^{206}\text{Pb}/^{238}\text{U}$ ^b	2σ	$^{207}\text{Pb}/^{206}\text{Pb}$ ^e	2σ			
204/27-1, 2136.20 m	Zircon_Sample_007	843	273	0.02	7.82	0.37	0.324	0.015	0.96	0.175	0.004	2210	104	1811	72	2605	42	70	x	
204/27-1, 2136.20 m	Zircon_Sample_008	381	203	0.24	13.85	0.68	0.533	0.025	0.96	0.189	0.005	2740	134	2753	106	2730	42	101	x	x
204/27-1, 2136.20 m	Zircon_Sample_009	1773	429	0.01	5.65	0.27	0.242	0.011	0.97	0.169	0.004	1923	91	1397	57	2550	41	55	x	
204/27-1, 2136.20 m	Zircon_Sample_010	171	90	0.53	13.79	0.69	0.528	0.025	0.96	0.189	0.005	2735	137	2734	107	2736	46	100	x	x
204/27-1, 2136.20 m	Zircon_Sample_011	596	258	0.07	11.54	0.55	0.433	0.020	0.96	0.193	0.005	2568	123	2320	90	2771	42	84	x	
204/27-1, 2136.20 m	Zircon_Sample_012	291	155	0.45	14.08	0.69	0.532	0.025	0.96	0.192	0.005	2755	135	2749	105	2760	44	100	x	x
204/27-1, 2136.20 m	Zircon_Sample_013	1760	400	0.02	5.11	0.25	0.227	0.011	0.96	0.163	0.004	1837	89	1321	56	2486	43	53	x	
204/27-1, 2136.20 m	Zircon_Sample_014	1012	297	0.36	7.02	0.34	0.293	0.014	0.96	0.174	0.004	2114	103	1658	68	2592	43	64	x	
204/27-1, 2136.20 m	Zircon_Sample_015	219	108	0.42	12.89	0.64	0.493	0.023	0.96	0.190	0.005	2672	132	2584	101	2739	46	94	x	
204/27-1, 2136.20 m	Zircon_Sample_016	564	222	0.20	10.28	0.50	0.393	0.019	0.96	0.190	0.005	2461	121	2136	86	2741	44	78	x	
204/27-1, 2136.20 m	Zircon_Sample_020	917	342	0.35	9.26	0.46	0.373	0.018	0.96	0.180	0.005	2364	118	2044	84	2653	44	77	x	
204/27-1, 2136.20 m	Zircon_Sample_021	48	22	0.22	11.66	0.66	0.446	0.023	0.90	0.189	0.009	2577	145	2380	101	2737	78	87	x	
204/27-1, 2136.20 m	Zircon_Sample_022	394	211	0.90	14.03	0.73	0.536	0.027	0.96	0.190	0.005	2752	143	2765	113	2742	46	101	x	x
204/27-1, 2136.20 m	Zircon_Sample_023	84	45	0.29	13.96	0.74	0.532	0.027	0.95	0.190	0.007	2747	146	2751	113	2744	56	100	x	x
204/27-1, 2136.20 m	Zircon_Sample_024	134	70	0.23	13.43	0.86	0.525	0.033	0.97	0.186	0.006	2711	174	2721	138	2703	54	101	x	x
204/27-1, 2136.20 m	Zircon_Sample_025	127	66	0.35	13.51	0.79	0.518	0.029	0.96	0.189	0.006	2716	159	2692	123	2734	53	98	x	x
204/27-1, 2136.20 m	Zircon_Sample_026	206	110	0.43	13.99	0.73	0.534	0.027	0.96	0.190	0.006	2749	143	2759	112	2742	50	101	x	x
204/27-1, 2136.20 m	Zircon_Sample_027	215	105	0.46	12.65	0.66	0.488	0.024	0.96	0.188	0.006	2654	139	2561	106	2725	51	94	x	
204/27-1, 2136.20 m	Zircon_Sample_028	2006	556	0.16	7.30	0.38	0.277	0.014	0.96	0.191	0.006	2149	111	1578	69	2751	47	57		
204/27-1, 2136.20 m	Zircon_Sample_029	482	244	0.34	14.10	0.74	0.505	0.025	0.96	0.202	0.006	2756	144	2637	108	2845	48	93		
204/27-1, 2136.20 m	Zircon_Sample_033	232	86	0.13	9.12	0.49	0.373	0.019	0.95	0.178	0.006	2350	127	2042	90	2630	55	78	x	
204/27-1, 2136.20 m	Zircon_Sample_034	355	156	0.66	11.34	0.61	0.440	0.023	0.95	0.187	0.006	2551	137	2351	101	2715	53	87	x	
204/27-1, 2136.20 m	Zircon_Sample_035	739	269	0.07	9.12	0.49	0.365	0.019	0.96	0.181	0.006	2350	126	2004	89	2665	52	75	x	
204/27-1, 2136.20 m	Zircon_Sample_036	367	206	0.26	16.02	0.88	0.562	0.030	0.96	0.207	0.007	2878	158	2877	122	2879	52	100		
204/27-1, 2136.20 m	Zircon_Sample_037	128	68	0.19	14.11	0.80	0.534	0.029	0.95	0.192	0.007	2757	156	2758	121	2757	58	100	x	x

^aU and Pb concentrations and Th/U ratios are calculated relative to GJ-1 reference zircon^bCorrected for background and within-run Pb/U fractionation and normalised to reference zircon GJ-1 (ID-TIMS values/measured value); $^{207}\text{Pb}/^{235}\text{U}$ calculated using $(^{207}\text{Pb}/^{206}\text{Pb})/(^{238}\text{U}/^{206}\text{Pb} * 1/137.88)$ ^cRho is the error correlation defined as the quotient of the propagated errors of the $^{206}\text{Pb}/^{238}\text{U}$ and the $^{207}/^{235}\text{U}$ ratio^dQuadratic addition of within-run errors (2 SD) and daily reproducibility of GJ-1 (2 SD)^eCorrected for mass-bias by normalising to GJ-1 reference zircon (~0.6 per atomic mass unit) and common Pb using the model Pb composition of Stacey & Kramers (1975)

Sample	Analysis	U [ppm] ^a	Pb [ppm] ^a	Th/U ^a	RATIOS						AGES [Ma]						Conc.			use for UI age	use for conc age
					²⁰⁷ Pb/ ²³⁵ U ^b	2 σ ^d	²⁰⁶ Pb/ ²³⁸ U ^b	2 σ ^d	ρho ^c	²⁰⁷ Pb/ ²⁰⁶ Pb ^e	2 σ ^d	²⁰⁷ Pb/ ²³⁵ U	2 σ	²⁰⁶ Pb/ ²³⁸ U	2 σ	²⁰⁷ Pb/ ²⁰⁶ Pb	2 σ	%			
204/28-1, 1941.55 m	Zircon_Sample_007	15	8	0.85	13.66	0.98	0.530	0.032	0.83	0.187	0.007	2727	195	2741	133	2716	64	101	x	x	
204/28-1, 1941.55 m	Zircon_Sample_008	116	65	0.49	15.19	0.63	0.562	0.020	0.84	0.196	0.004	2827	118	2874	82	2793	36	103	x		
204/28-1, 1941.55 m	Zircon_Sample_009	14	7	0.53	12.99	0.90	0.508	0.029	0.83	0.185	0.007	2679	185	2649	125	2701	62	98	x		
204/28-1, 1941.55 m	Zircon_Sample_010	80	42	0.21	14.04	0.45	0.526	0.014	0.85	0.194	0.003	2753	89	2723	61	2775	28	98	x		
204/28-1, 1941.55 m	Zircon_Sample_011	110	53	0.11	12.95	0.39	0.487	0.013	0.85	0.193	0.003	2676	81	2557	55	2767	26	92	x		
204/28-1, 1941.55 m	Zircon_Sample_012	266	58	0.13	5.75	0.17	0.220	0.005	0.85	0.190	0.003	1939	57	1280	29	2741	25	47	x		
204/28-1, 1941.55 m	Zircon_Sample_013	188	90	0.11	12.86	0.36	0.482	0.012	0.86	0.194	0.003	2669	75	2534	50	2774	24	91	x		
204/28-1, 1941.55 m	Zircon_Sample_015	67	31	0.45	12.51	0.44	0.465	0.014	0.85	0.195	0.004	2644	92	2463	60	2785	30	88	x		
204/28-1, 1941.55 m	Zircon_Sample_020	82	47	0.02	15.12	0.55	0.579	0.018	0.85	0.190	0.004	2823	102	2944	72	2738	31	108	x		
204/28-1, 1941.55 m	Zircon_Sample_021	56	16	0.18	7.09	0.31	0.288	0.011	0.83	0.178	0.004	2122	94	1632	53	2638	41	62	x		
204/28-1, 1941.55 m	Zircon_Sample_022	22	12	0.66	14.37	0.89	0.539	0.028	0.84	0.193	0.007	2775	172	2779	117	2771	54	100	x	x	
204/28-1, 1941.55 m	Zircon_Sample_023	132	52	0.31	10.26	0.31	0.396	0.010	0.85	0.188	0.003	2459	75	2152	47	2723	26	79	x		
204/28-1, 1941.55 m	Zircon_Sample_024	84	45	0.25	14.20	0.47	0.533	0.015	0.85	0.193	0.003	2763	92	2754	63	2770	28	99	x		
204/28-1, 1941.55 m	Zircon_Sample_025	110	58	0.17	13.52	0.55	0.529	0.018	0.84	0.185	0.004	2717	110	2738	76	2701	36	101	x	x	
204/28-1, 1941.55 m	Zircon_Sample_026	158	53	0.10	8.13	0.33	0.332	0.011	0.83	0.177	0.004	2245	92	1849	55	2629	38	70	x		
204/28-1, 1941.55 m	Zircon_Sample_027	91	53	0.16	15.07	0.47	0.578	0.015	0.85	0.189	0.003	2820	88	2939	63	2736	27	107	x		
204/28-1, 1941.55 m	Zircon_Sample_033	19	10	0.25	13.66	0.70	0.516	0.022	0.84	0.192	0.005	2726	139	2681	94	2761	45	97	x		
204/28-1, 1941.55 m	Zircon_Sample_034	381	126	0.14	8.16	0.24	0.329	0.008	0.85	0.180	0.003	2249	66	1836	40	2649	25	69	x		
204/28-1, 1941.55 m	Zircon_Sample_035	186	99	0.14	14.08	0.40	0.533	0.013	0.85	0.192	0.003	2755	78	2753	54	2757	24	100	x	x	
204/28-1, 1941.55 m	Zircon_Sample_036	323	113	0.11	8.87	0.28	0.349	0.009	0.85	0.184	0.003	2324	72	1929	44	2692	27	72	x		
204/28-1, 1941.55 m	Zircon_Sample_037	46	25	0.32	14.69	0.65	0.542	0.020	0.84	0.197	0.005	2796	124	2792	85	2798	39	100	x	x	
204/28-1, 1941.55 m	Zircon_Sample_038	151	72	0.12	12.75	0.38	0.474	0.012	0.85	0.195	0.003	2662	79	2500	52	2787	25	90	x		
204/28-1, 1941.55 m	Zircon_Sample_039	119	66	0.13	15.09	0.63	0.553	0.020	0.84	0.198	0.004	2821	119	2839	81	2808	37	101	x	x	
204/28-1, 1941.55 m	Zircon_Sample_041	147	64	0.13	11.22	0.34	0.436	0.011	0.85	0.187	0.003	2542	76	2335	50	2712	26	86	x		
204/28-1, 1941.55 m	Zircon_Sample_042	107	54	0.43	13.37	0.41	0.505	0.013	0.85	0.192	0.003	2706	83	2637	56	2758	26	96	x		
204/28-1, 1941.55 m	Zircon_Sample_046	184	64	0.12	8.75	0.28	0.349	0.009	0.84	0.182	0.003	2312	74	1930	45	2669	28	72	x		
204/28-1, 1941.55 m	Zircon_Sample_049	179	89	0.16	12.79	0.38	0.496	0.012	0.85	0.187	0.003	2665	79	2597	53	2716	25	96	x		
204/28-1, 1941.55 m	Zircon_Sample_050	137	53	0.10	10.16	0.32	0.390	0.010	0.84	0.189	0.003	2449	77	2124	48	2731	28	78	x		
204/28-1, 1941.55 m	Zircon_Sample_051	190	70	0.21	9.58	0.28	0.369	0.009	0.85	0.188	0.003	2395	71	2023	43	2729	26	74	x		
204/28-1, 1941.55 m	Zircon_Sample_055	144	78	0.11	14.65	0.44	0.545	0.014	0.85	0.195	0.003	2792	84	2802	58	2785	26	101	x	x	
204/28-1, 1941.55 m	Zircon_Sample_059	161	64	0.21	10.40	0.32	0.397	0.010	0.84	0.190	0.003	2471	76	2157	48	2741	27	79	x		
204/28-1, 1941.55 m	Zircon_Sample_060	73	40	0.23	14.97	0.63	0.550	0.019	0.84	0.197	0.004	2813	118	2824	80	2805	37	101	x	x	
204/28-1, 1941.55 m	Zircon_Sample_061	178	70	0.08	10.43	0.32	0.396	0.010	0.84	0.191	0.003	2474	75	2151	47	2751	26	78	x		
204/28-1, 1941.55 m	Zircon_Sample_062	105	45	0.07	11.45	0.37	0.428	0.012	0.84	0.194	0.003	2560	84	2298	53						

Sample	Analysis	U [ppm] ^a	Pb [ppm] ^a	Th/U ^a	RATIOS						AGES [Ma]						Conc.	use for UI age	
					$^{207}\text{Pb}/^{235}\text{U}$ ^b	$2\sigma^d$	$^{206}\text{Pb}/^{238}\text{U}$ ^b	$2\sigma^d$	ρho^c	$^{207}\text{Pb}/^{206}\text{Pb}$ ^e	$2\sigma^d$	$^{207}\text{Pb}/^{235}\text{U}$	2σ	$^{206}\text{Pb}/^{238}\text{U}$	2σ	$^{207}\text{Pb}/^{206}\text{Pb}$	2σ		
205/20-1, 2017.50 m	Zircon_Sample_046	771	249	0.74	7.64	0.41	0.323	0.017	0.97	0.172	0.002	2190	117	1803	81	2574	22	70	x
205/20-1, 2017.50 m	Zircon_Sample_048	191	102	0.80	13.93	0.76	0.533	0.028	0.96	0.189	0.003	2745	149	2754	117	2738	24	101	x
205/20-1, 2017.50 m	Zircon_Sample_049	512	220	0.70	10.82	0.58	0.429	0.022	0.97	0.183	0.002	2508	134	2300	100	2680	22	86	x
205/20-1, 2017.50 m	Zircon_Sample_050	83	44	0.89	13.81	0.79	0.529	0.029	0.95	0.189	0.003	2737	157	2737	121	2737	30	100	x
205/20-1, 2017.50 m	Zircon_Sample_051	420	203	0.53	12.54	0.68	0.484	0.025	0.96	0.188	0.003	2645	144	2547	110	2722	24	94	x
205/20-1, 2017.50 m	Zircon_Sample_052	611	255	0.55	10.48	0.56	0.417	0.022	0.97	0.182	0.002	2478	133	2245	98	2675	22	84	x
205/20-1, 2017.50 m	Zircon_Sample_053	589	244	0.53	10.42	0.56	0.414	0.021	0.97	0.182	0.003	2472	133	2235	98	2674	23	84	x
205/20-1, 2017.50 m	Zircon_Sample_054	348	175	0.31	12.91	0.69	0.503	0.026	0.96	0.186	0.003	2673	144	2625	112	2709	23	97	x
205/20-1, 2017.50 m	Zircon_Sample_055	198	102	0.61	13.30	0.76	0.515	0.028	0.95	0.187	0.003	2701	154	2680	119	2717	30	99	x
205/20-1, 2017.50 m	Zircon_Sample_059	153	81	0.73	14.03	0.77	0.531	0.028	0.96	0.192	0.003	2752	151	2745	118	2757	26	100	x
205/20-1, 2017.50 m	Zircon_Sample_060	116	62	0.59	13.85	0.77	0.533	0.028	0.96	0.188	0.003	2739	152	2755	119	2728	27	101	x
205/20-1, 2017.50 m	Zircon_Sample_061	345	155	0.51	11.31	0.62	0.450	0.024	0.96	0.182	0.003	2549	139	2394	104	2676	25	89	x
205/20-1, 2017.50 m	Zircon_Sample_062	137	72	0.44	13.62	0.75	0.528	0.028	0.96	0.187	0.003	2724	150	2734	118	2716	26	101	x
205/20-1, 2017.50 m	Zircon_Sample_063	37	20	2.00	13.67	0.84	0.526	0.030	0.93	0.189	0.004	2727	167	2724	127	2729	37	100	x
205/20-1, 2017.50 m	Zircon_Sample_064	121	64	0.67	13.57	0.77	0.529	0.028	0.95	0.186	0.003	2720	154	2735	120	2709	29	101	x
205/20-1, 2017.50 m	Zircon_Sample_065	518	223	0.50	10.81	0.58	0.430	0.022	0.96	0.182	0.003	2507	136	2306	101	2674	25	86	x
205/20-1, 2017.50 m	Zircon_Sample_066	210	103	0.40	12.70	0.70	0.490	0.026	0.96	0.188	0.003	2658	146	2573	111	2723	26	94	x
205/20-1, 2017.50 m	Zircon_Sample_067	874	274	0.27	7.31	0.40	0.314	0.016	0.96	0.169	0.003	2150	116	1759	80	2549	25	69	x
205/20-1, 2017.50 m	Zircon_Sample_068	771	241	0.38	7.16	0.39	0.312	0.016	0.96	0.166	0.003	2132	116	1752	80	2521	26	69	x
205/20-1, 2017.50 m	Zircon_Sample_072	256	135	1.09	13.82	0.76	0.529	0.028	0.95	0.190	0.003	2738	151	2737	117	2738	27	100	x
205/20-1, 2017.50 m	Zircon_Sample_073	41	21	1.47	13.16	0.79	0.504	0.028	0.93	0.189	0.004	2691	162	2633	121	2735	36	96	x
205/20-1, 2017.50 m	Zircon_Sample_074	624	240	1.07	9.48	0.52	0.385	0.020	0.95	0.179	0.003	2385	130	2099	93	2639	27	80	x
205/20-1, 2017.50 m	Zircon_Sample_075	159	73	0.68	11.60	0.65	0.457	0.024	0.95	0.184	0.003	2573	144	2428	107	2688	29	90	x
205/20-1, 2017.50 m	Zircon_Sample_076	493	204	0.51	10.59	0.58	0.413	0.022	0.95	0.186	0.003	2488	137	2229	99	2706	27	82	x

^aU and Pb concentrations and Th/U ratios are calculated relative to GJ-1 reference zircon^bCorrected for background and within-run Pb/U fractionation and normalised to reference zircon GJ-1 (ID-TIMS values/measured value); $^{207}\text{Pb}/^{235}\text{U}$ calculated using $(^{207}\text{Pb}/^{206}\text{Pb})/(^{238}\text{U}/^{206}\text{Pb} * 1/137.88)$ ^cRho is the error correlation defined as the quotient of the propagated errors of the $^{206}\text{Pb}/^{238}\text{U}$ and the $^{207}/^{235}\text{U}$ ratio^dQuadratic addition of within-run errors (2 SD) and daily reproducibility of GJ-1 (2 SD)^eCorrected for mass-bias by normalising to GJ-1 reference zircon (~0.6 per atomic mass unit) and common Pb using the model Pb composition of Stacey & Kramers (1975)

Sample	Analysis	U [ppm] ^a	Pb [ppm] ^a	Th/U ^a	RATIOS						AGES [Ma]						Conc. ^c	use for conc age	
					$^{207}\text{Pb}/^{235}\text{U}$ ^b	$2\sigma^d$	$^{206}\text{Pb}/^{238}\text{U}$ ^b	$2\sigma^d$	ρho^c	$^{207}\text{Pb}/^{206}\text{Pb}$ ^e	$2\sigma^d$	$^{207}\text{Pb}/^{235}\text{U}$	2σ	$^{206}\text{Pb}/^{238}\text{U}$	2σ	$^{207}\text{Pb}/^{206}\text{Pb}$	2σ		
206/7a-2, 2141.40 m	Zircon_Sample_046	646	373	0.05	15.71	0.72	0.578	0.025	0.95	0.197	0.005	2859	131	2940	103	2803	45	105	
206/7a-2, 2141.40 m	Zircon_Sample_047	431	208	0.08	12.49	0.57	0.483	0.021	0.95	0.187	0.005	2642	121	2542	92	2720	46	93	x
206/7a-2, 2141.40 m	Zircon_Sample_048	40	22	1.26	14.93	0.82	0.546	0.027	0.91	0.198	0.009	2811	154	2808	114	2813	72	100	
206/7a-2, 2141.40 m	Zircon_Sample_049	791	280	0.06	9.58	0.44	0.354	0.016	0.95	0.197	0.006	2396	110	1952	74	2798	46	70	
206/7a-2, 2141.40 m	Zircon_Sample_050	528	249	0.06	12.80	0.59	0.471	0.021	0.95	0.197	0.006	2665	123	2489	90	2801	47	89	
206/7a-2, 2141.40 m	Zircon_Sample_051	533	290	0.05	14.73	0.68	0.544	0.024	0.95	0.196	0.006	2798	129	2799	99	2797	46	100	x
206/7a-2, 2141.40 m	Zircon_Sample_052	44	23	1.31	13.64	0.96	0.525	0.035	0.96	0.188	0.008	2725	192	2722	149	2728	67	100	
206/7a-2, 2141.40 m	Zircon_Sample_053	124	64	0.18	13.35	0.64	0.521	0.024	0.94	0.186	0.006	2705	130	2706	100	2705	53	100	
206/7a-2, 2141.40 m	Zircon_Sample_054	693	384	0.08	15.35	0.71	0.554	0.024	0.95	0.201	0.006	2837	131	2843	101	2833	45	100	x
206/7a-2, 2141.40 m	Zircon_Sample_055	999	415	0.10	11.26	0.52	0.416	0.018	0.95	0.196	0.006	2545	118	2242	83	2796	49	80	
206/7a-2, 2141.40 m	Zircon_Sample_059	18	10	2.39	13.93	0.97	0.530	0.034	0.91	0.191	0.011	2745	191	2742	142	2747	93	100	
206/7a-2, 2141.40 m	Zircon_Sample_060	947	313	0.05	8.51	0.40	0.331	0.015	0.94	0.187	0.006	2287	107	1843	71	2712	50	68	
206/7a-2, 2141.40 m	Zircon_Sample_061	773	417	0.05	14.56	0.69	0.539	0.024	0.95	0.196	0.006	2787	133	2779	102	2793	48	99	x
206/7a-2, 2141.40 m	Zircon_Sample_062	416	223	0.07	14.65	0.73	0.536	0.025	0.95	0.198	0.006	2793	139	2767	106	2811	49	98	x
206/7a-2, 2141.40 m	Zircon_Sample_063	441	240	0.04	14.90	0.71	0.545	0.024	0.94	0.198	0.006	2809	133	2804	102	2813	51	100	x
206/7a-2, 2141.40 m	Zircon_Sample_064	476	192	0.10	11.53	0.54	0.404	0.018	0.94	0.207	0.006	2567	121	2189	83	2881	50	76	
206/7a-2, 2141.40 m	Zircon_Sample_065	70	37	0.55	13.94	0.80	0.530	0.029	0.94	0.191	0.007	2746	158	2741	121	2750	63	100	
206/7a-2, 2141.40 m	Zircon_Sample_066	379	207	0.03	14.77	0.71	0.545	0.024	0.94	0.197	0.006	2801	134	2803	102	2798	53	100	x
206/7a-2, 2141.40 m	Zircon_Sample_067	399	208	0.12	14.74	0.70	0.523	0.023	0.94	0.204	0.007	2798	133	2710	99	2862	52	95	
206/7a-2, 2141.40 m	Zircon_Sample_068	312	154	0.13	13.74	0.66	0.494	0.022	0.94	0.202	0.007	2732	131	2589	96	2840	54	91	
206/7a-2, 2141.40 m	Zircon_Sample_072	23	12	1.63	14.00	0.87	0.531	0.029	0.89	0.191	0.011	2750	170	2747	123	2752	91	100	
206/7a-2, 2141.40 m	Zircon_Sample_073	350	190	0.06	14.67	0.73	0.543	0.025	0.93	0.196	0.007	2794	140	2795	105	2794	61	100	x
206/7a-2, 2141.40 m	Zircon_Sample_074	513	277	0.06	14.80	0.76	0.540	0.026	0.94	0.199	0.007	2803	144	2784	109	2816	56	99	x
206/7a-2, 2141.40 m	Zircon_Sample_075	424	230	0.06	14.63	0.72	0.541	0.025	0.93	0.196	0.007	2791	137	2789	104	2793	57	100	x
206/7a-2, 2141.40 m	Zircon_Sample_076	351	161	0.22	12.81	0.63	0.459	0.021	0.93	0.203	0.007	2666	131	2434	92	2847	58	85	

^aU and Pb concentrations and Th/U ratios are calculated relative to GJ-1 reference zircon^bCorrected for background and within-run Pb/U fractionation and normalised to reference zircon GJ-1 (ID-TIMS values/measured value); $^{207}\text{Pb}/^{235}\text{U}$ calculated using $(^{207}\text{Pb}/^{206}\text{Pb})/(^{238}\text{U}/^{206}\text{Pb} * 1/137.88)$ ^cRho is the error correlation defined as the quotient of the propagated errors of the $^{206}\text{Pb}/^{238}\text{U}$ and the $^{207}/^{235}\text{U}$ ratio^dQuadratic addition of within-run errors (2 SD) and daily reproducibility of GJ-1 (2 SD)^eCorrected for mass-bias by normalising to GJ-1 reference zircon (~0.6 per atomic mass unit) and common Pb using the model Pb composition of Stacey & Kramers (1975)

Sample	Analysis	U [ppm] ^a	Pb [ppm] ^a	Th/U ^a	RATIOS						AGES [Ma]						Conc. use for UI age	
					$^{207}\text{Pb}/^{235}\text{U}$ ^b	$2\sigma^d$	$^{206}\text{Pb}/^{238}\text{U}$ ^b	$2\sigma^d$	ρho^c	$^{207}\text{Pb}/^{206}\text{Pb}$ ^e	$2\sigma^d$	$^{207}\text{Pb}/^{235}\text{U}$	2σ	$^{206}\text{Pb}/^{238}\text{U}$	2σ	$^{207}\text{Pb}/^{206}\text{Pb}$	2σ	
HM11694	Zircon_Sample_007	28	14	1.06	13.22	0.54	0.497	0.017	0.84	0.193	0.004	2695	111	2600	73	2767	36	94
HM11694	Zircon_Sample_008	254	133	0.59	13.98	0.33	0.526	0.011	0.84	0.193	0.002	2748	66	2723	45	2767	21	98
HM11694	Zircon_Sample_009	860	317	0.12	9.85	0.22	0.368	0.007	0.84	0.194	0.002	2421	55	2020	33	2778	20	73
HM11694	Zircon_Sample_012	672	292	0.26	11.98	0.27	0.434	0.008	0.85	0.200	0.002	2603	59	2324	37	2828	20	82
HM11694	Zircon_Sample_014	462	248	0.16	14.24	0.32	0.535	0.010	0.85	0.193	0.002	2766	63	2764	43	2767	20	100
HM11694	Zircon_Sample_016	642	248	0.24	10.33	0.23	0.386	0.007	0.85	0.194	0.002	2465	56	2102	34	2780	20	76
HM11694	Zircon_Sample_020	91	49	1.17	13.93	0.40	0.538	0.013	0.84	0.188	0.003	2745	78	2777	54	2722	25	102
HM11694	Zircon_Sample_022	55	16	1.00	7.70	0.29	0.295	0.009	0.83	0.189	0.004	2197	82	1669	45	2735	34	61
HM11694	Zircon_Sample_024	79	42	1.05	14.00	0.43	0.531	0.014	0.84	0.191	0.003	2750	85	2748	58	2751	27	100
HM11694	Zircon_Sample_025	26	14	1.37	14.34	0.60	0.537	0.019	0.84	0.194	0.004	2773	116	2771	79	2774	37	100
HM11694	Zircon_Sample_026	92	50	1.28	14.46	0.43	0.542	0.014	0.84	0.193	0.003	2781	83	2793	57	2772	26	101
HM11694	Zircon_Sample_027	2693	305	0.12	3.15	0.07	0.113	0.002	0.84	0.202	0.002	1444	33	692	12	2839	20	24
HM11694	Zircon_Sample_028	548	310	0.20	15.96	0.36	0.565	0.011	0.85	0.205	0.002	2874	65	2889	45	2865	20	101
HM11694	Zircon_Sample_029	76	40	1.48	13.59	0.41	0.525	0.013	0.84	0.188	0.003	2722	82	2722	56	2722	27	100
HM11694	Zircon_Sample_036	117	57	1.02	12.56	0.36	0.487	0.012	0.84	0.187	0.003	2647	76	2559	51	2716	25	94
HM11694	Zircon_Sample_037	19	10	1.47	13.45	0.64	0.522	0.021	0.83	0.187	0.005	2712	129	2709	88	2714	43	100
HM11694	Zircon_Sample_038	54	29	1.27	14.56	0.51	0.541	0.016	0.84	0.195	0.004	2787	97	2787	66	2786	31	100
HM11694	Zircon_Sample_039	185	98	0.44	13.92	0.37	0.531	0.012	0.84	0.190	0.003	2744	73	2744	50	2745	24	100
HM11694	Zircon_Sample_040	533	282	0.19	14.13	0.33	0.529	0.010	0.84	0.194	0.002	2758	64	2738	44	2773	20	99
HM11694	Zircon_Sample_042	434	209	0.23	12.75	0.30	0.481	0.010	0.84	0.192	0.002	2661	63	2532	42	2761	21	92
HM11694	Zircon_Sample_046	45	24	1.65	13.83	0.49	0.530	0.016	0.84	0.189	0.004	2738	96	2740	66	2737	31	100
HM11694	Zircon_Sample_047	26	13	1.06	12.97	0.56	0.502	0.018	0.83	0.187	0.004	2677	116	2622	78	2720	39	96
HM11694	Zircon_Sample_048	825	287	0.16	9.04	0.21	0.348	0.007	0.84	0.188	0.002	2342	55	1925	33	2729	21	71
HM11694	Zircon_Sample_049	355	183	0.23	13.55	0.33	0.516	0.011	0.84	0.190	0.002	2719	66	2684	45	2745	21	98
HM11694	Zircon_Sample_050	60	32	1.36	13.91	0.47	0.532	0.015	0.84	0.189	0.003	2744	92	2752	63	2738	30	101
HM11694	Zircon_Sample_051	33	17	1.23	13.35	0.62	0.520	0.020	0.83	0.186	0.005	2705	126	2701	85	2708	42	100
HM11694	Zircon_Sample_052	33	16	1.35	12.79	0.61	0.498	0.020	0.83	0.186	0.005	2664	126	2605	85	2710	43	96
HM11694	Zircon_Sample_053	28	15	1.41	13.60	0.70	0.528	0.023	0.83	0.187	0.005	2722	140	2731	95	2715	46	101
HM11694	Zircon_Sample_054	49	26	1.44	14.00	0.61	0.533	0.019	0.83	0.191	0.005	2750	119	2753	81	2747	39	100
HM11694	Zircon_Sample_055	618	303	0.16	12.86	0.30	0.490	0.010	0.84	0.190	0.002	2669	63	2570	42	2746	21	94
HM11694	Zircon_Sample_059	47	25	2.02	13.59	0.48	0.533	0.016	0.83	0.185	0.004	2721	95	2752	65	2699	32	102
HM11694	Zircon_Sample_060	41	23	1.71	15.07	0.54	0.560	0.017	0.84	0.195	0.004	2820	102	2866	70	2787	32	103
HM11694	Zircon_Sample_061	209	58	0.59	7.27	0.21	0.276	0.007	0.83	0.191	0.003	2145	61	1571	33	2751	26	57
HM11694	Zircon_Sample_062	732	344	0.12	13.08	0.31	0.471	0.009	0.84	0.202	0.003	2686	64	2487	41	2839	21	88
HM11694	Zircon_Sample_063	44	23	3.02	13.83	0.50	0.528	0.016	0.83	0.190	0.004	2738	98	2734	67	2741	32	100
HM11694	Zircon_Sample_064	59	24	0.64	10.34	0.36	0.408	0.012	0.83	0.184	0.004	2465	85	2206	54	2686	32	82
HM11694	Zircon_Sample_065	817	339	0.07	12.80	0.31	0.415	0.008	0.84	0.224	0.003	2665	64	2238	38	3008	21	74
HM11694	Zircon_Sample_066	32	17	1.83	13.51	0.53	0.525	0.017	0.83	0.187	0.004	2716	107	2721</td				

Sample	Analysis	U [ppm] ^a	Pb [ppm] ^a	Th/U ^a	RATIOS						AGES [Ma]						Conc.	use for UI age	
					$^{207}\text{Pb}/^{235}\text{U}$ ^b	$2\sigma^d$	$^{206}\text{Pb}/^{238}\text{U}$ ^b	$2\sigma^d$	rho^c	$^{207}\text{Pb}/^{206}\text{Pb}$ ^e	$2\sigma^d$	$^{207}\text{Pb}/^{235}\text{U}$	2σ	$^{206}\text{Pb}/^{238}\text{U}$	2σ	$^{207}\text{Pb}/^{206}\text{Pb}$	2σ		
208/23-1, 2071.26 m	Zircon_Sample_007	435	222	0.39	13.80	0.73	0.510	0.026	0.97	0.196	0.003	2736	145	2658	111	2795	22	95	x
208/23-1, 2071.26 m	Zircon_Sample_008	238	118	0.68	13.26	0.71	0.495	0.025	0.97	0.194	0.003	2699	144	2591	110	2780	23	93	x
208/23-1, 2071.26 m	Zircon_Sample_009	1292	203	0.57	4.08	0.22	0.157	0.008	0.97	0.189	0.003	1651	87	939	45	2732	22	34	x
208/23-1, 2071.26 m	Zircon_Sample_010	536	246	0.81	12.34	0.65	0.458	0.023	0.97	0.195	0.003	2630	138	2431	103	2787	21	87	x
208/23-1, 2071.26 m	Zircon_Sample_011	634	192	1.16	7.97	0.42	0.303	0.016	0.97	0.191	0.003	2228	118	1708	77	2748	22	62	x
208/23-1, 2071.26 m	Zircon_Sample_012	589	230	1.37	10.37	0.55	0.391	0.020	0.97	0.192	0.003	2468	130	2126	92	2764	21	77	x
208/23-1, 2071.26 m	Zircon_Sample_013	78	45	1.64	15.02	0.83	0.567	0.030	0.96	0.192	0.003	2816	155	2896	123	2760	26	105	x
208/23-1, 2071.26 m	Zircon_Sample_014	497	267	0.14	14.80	0.78	0.538	0.027	0.97	0.199	0.003	2802	148	2775	115	2822	21	98	x
208/23-1, 2071.26 m	Zircon_Sample_015	661	177	1.18	7.04	0.37	0.268	0.014	0.97	0.191	0.003	2117	112	1531	70	2747	22	56	x
208/23-1, 2071.26 m	Zircon_Sample_016	115	58	1.23	13.10	0.71	0.502	0.026	0.96	0.189	0.003	2687	147	2622	113	2736	26	96	x
208/23-1, 2071.26 m	Zircon_Sample_020	587	315	0.34	14.66	0.77	0.537	0.027	0.97	0.198	0.003	2794	148	2772	115	2809	22	99	x
208/23-1, 2071.26 m	Zircon_Sample_021	459	247	0.35	14.40	0.77	0.537	0.028	0.96	0.194	0.003	2776	148	2773	116	2779	23	100	x
208/23-1, 2071.26 m	Zircon_Sample_022	183	98	0.87	14.18	0.78	0.534	0.028	0.96	0.193	0.003	2762	151	2760	118	2764	26	100	x
208/23-1, 2071.26 m	Zircon_Sample_023	363	168	1.24	12.17	0.65	0.463	0.024	0.96	0.191	0.003	2618	139	2454	105	2748	23	89	x
208/23-1, 2071.26 m	Zircon_Sample_025	60	30	2.28	13.31	0.76	0.506	0.027	0.94	0.191	0.004	2702	154	2641	117	2747	30	96	x
208/23-1, 2071.26 m	Zircon_Sample_026	326	173	0.16	14.12	0.76	0.532	0.027	0.96	0.192	0.003	2758	148	2751	115	2762	24	100	x
208/23-1, 2071.26 m	Zircon_Sample_027	429	222	0.23	13.81	0.74	0.518	0.027	0.96	0.193	0.003	2737	146	2693	113	2770	24	97	x
208/23-1, 2071.26 m	Zircon_Sample_028	244	125	1.08	13.73	0.74	0.514	0.027	0.96	0.194	0.003	2731	147	2674	113	2774	25	96	x
208/23-1, 2071.26 m	Zircon_Sample_029	129	69	0.78	14.21	0.78	0.536	0.028	0.95	0.192	0.003	2764	153	2767	118	2762	27	100	x
208/23-1, 2071.26 m	Zircon_Sample_033	467	252	0.14	14.56	0.79	0.541	0.028	0.96	0.195	0.003	2787	152	2788	118	2786	26	100	x
208/23-1, 2071.26 m	Zircon_Sample_034	169	91	0.70	14.40	0.79	0.538	0.028	0.95	0.194	0.003	2777	152	2776	118	2777	27	100	x
208/23-1, 2071.26 m	Zircon_Sample_035	219	117	0.75	14.29	0.80	0.535	0.028	0.95	0.194	0.003	2769	154	2764	119	2774	29	100	x
208/23-1, 2071.26 m	Zircon_Sample_036	495	254	0.17	13.72	0.74	0.514	0.027	0.96	0.194	0.003	2731	147	2673	113	2774	26	96	x
208/23-1, 2071.26 m	Zircon_Sample_037	400	177	0.32	11.79	0.64	0.442	0.023	0.95	0.193	0.003	2588	140	2360	102	2772	26	85	x

^aU and Pb concentrations and Th/U ratios are calculated relative to GJ-1 reference zircon^bCorrected for background and within-run Pb/U fractionation and normalised to reference zircon GJ-1 (ID-TIMS values/measured value); $^{207}\text{Pb}/^{235}\text{U}$ calculated using $(^{207}\text{Pb}/^{206}\text{Pb})/(^{238}\text{U}/^{206}\text{Pb} * 1/137.88)$ ^cRho is the error correlation defined as the quotient of the propagated errors of the $^{206}\text{Pb}/^{238}\text{U}$ and the $^{207}/^{235}\text{U}$ ratio^dQuadratic addition of within-run errors (2 SD) and daily reproducibility of GJ-1 (2 SD)^eCorrected for mass-bias by normalising to GJ-1 reference zircon (~0.6 per atomic mass unit) and common Pb using the model Pb composition of Stacey & Kramers (1975)

Sample	Analysis	U [ppm] ^a	Pb [ppm] ^a	Th/U ^a	RATIOS						AGES [Ma]						Conc.	
					$^{207}\text{Pb}/^{235}\text{U}$ ^b	$2\sigma^d$	$^{206}\text{Pb}/^{238}\text{U}$ ^b	$2\sigma^d$	ρ_{co} ^c	$^{207}\text{Pb}/^{206}\text{Pb}$ ^e	$2\sigma^d$	$^{207}\text{Pb}/^{235}\text{U}$	2σ	$^{206}\text{Pb}/^{238}\text{U}$	2σ	$^{207}\text{Pb}/^{206}\text{Pb}$	2σ	
208/26-1, 3741.31 m	Zircon_Sample_046	29	16	0.20	14.80	1.05	0.545	0.037	0.94	0.197	0.005	2802	199	2805	152	2801	38	100
208/26-1, 3741.31 m	Zircon_Sample_047	14	8	0.58	13.63	0.98	0.527	0.030	0.79	0.188	0.008	2724	196	2728	126	2721	71	100
208/26-1, 3741.31 m	Zircon_Sample_048	30	16	0.57	13.71	0.81	0.526	0.029	0.92	0.189	0.004	2730	161	2726	121	2733	38	100
208/26-1, 3741.31 m	Zircon_Sample_049	14	7	0.28	13.83	1.11	0.527	0.039	0.91	0.190	0.006	2738	220	2729	163	2745	53	99
208/26-1, 3741.31 m	Zircon_Sample_050	11	6	0.27	13.84	1.24	0.528	0.043	0.91	0.190	0.007	2739	245	2734	181	2743	60	100
208/26-1, 3741.31 m	Zircon_Sample_051	68	37	0.22	14.78	0.92	0.544	0.032	0.96	0.197	0.003	2801	174	2798	135	2803	28	100
208/26-1, 3741.31 m	Zircon_Sample_052	13	7	0.49	14.48	1.30	0.543	0.044	0.90	0.193	0.008	2782	249	2797	183	2770	63	101
208/26-1, 3741.31 m	Zircon_Sample_053	121	63	0.19	13.64	0.71	0.525	0.026	0.95	0.188	0.003	2725	142	2721	110	2728	27	100
208/26-1, 3741.31 m	Zircon_Sample_054	181	96	0.11	13.97	0.89	0.534	0.033	0.97	0.190	0.003	2748	176	2758	139	2740	25	101
208/26-1, 3741.31 m	Zircon_Sample_059	10	5	0.40	13.60	1.23	0.526	0.043	0.91	0.188	0.007	2722	245	2724	182	2722	60	100
208/26-1, 3741.31 m	Zircon_Sample_061	105	58	0.20	15.51	0.81	0.555	0.027	0.95	0.203	0.003	2847	148	2847	114	2847	27	100
208/26-1, 3741.31 m	Zircon_Sample_062	79	44	0.34	15.74	0.89	0.559	0.030	0.95	0.204	0.004	2861	163	2864	125	2859	29	100
208/26-1, 3741.31 m	Zircon_Sample_063	41	21	0.27	13.68	0.85	0.526	0.031	0.94	0.189	0.004	2728	169	2725	129	2730	35	100
208/26-1, 3741.31 m	Zircon_Sample_064	138	76	0.43	15.14	0.84	0.548	0.029	0.95	0.200	0.003	2824	157	2819	121	2828	27	100
208/26-1, 3741.31 m	Zircon_Sample_065	65	36	0.45	15.19	1.04	0.555	0.036	0.96	0.199	0.004	2828	193	2845	151	2815	30	101
208/26-1, 3741.31 m	Zircon_Sample_066	58	31	0.63	13.56	0.74	0.526	0.027	0.93	0.187	0.004	2720	149	2727	114	2715	33	100
208/26-1, 3741.31 m	Zircon_Sample_067	145	80	0.45	14.98	0.77	0.549	0.027	0.94	0.198	0.003	2814	145	2823	111	2807	28	101
208/26-1, 3741.31 m	Zircon_Sample_068	56	31	0.25	15.49	0.92	0.555	0.031	0.93	0.203	0.004	2846	169	2845	128	2847	34	100
208/26-1, 3741.31 m	Zircon_Sample_072	363	198	0.03	14.81	0.76	0.545	0.026	0.94	0.197	0.004	2803	143	2803	109	2803	29	100
208/26-1, 3741.31 m	Zircon_Sample_073	65	36	0.46	14.92	0.88	0.549	0.030	0.94	0.197	0.004	2810	166	2821	127	2803	33	101
208/26-1, 3741.31 m	Zircon_Sample_074	181	99	0.12	14.71	0.80	0.545	0.028	0.94	0.196	0.004	2796	152	2805	116	2790	30	101
208/26-1, 3741.31 m	Zircon_Sample_075	96	52	0.23	14.84	0.79	0.545	0.027	0.93	0.198	0.004	2805	150	2804	113	2806	31	100
208/26-1, 3741.31 m	Zircon_Sample_076	106	59	0.24	15.44	0.94	0.555	0.032	0.95	0.202	0.004	2843	172	2847	132	2840	31	100

^aU and Pb concentrations and Th/U ratios are calculated relative to GJ-1 reference zircon

^bCorrected for background and within-run Pb/U fractionation and normalised to reference zircon GJ-1 (ID-TIMS values/measured value); $^{207}\text{Pb}/^{235}\text{U}$ calculated using $(^{207}\text{Pb}/^{206}\text{Pb})/(^{238}\text{U}/^{206}\text{Pb} * 1/137.88)$

^cRho is the error correlation defined as the quotient of the propagated errors of the $^{206}\text{Pb}/^{238}\text{U}$ and the $^{207}/^{235}\text{U}$ ratio

^dQuadratic addition of within-run errors (2 SD) and daily reproducibility of GJ-1 (2 SD)

^eCorrected for mass-bias by normalising to GJ-1 reference zircon (~0.6 per atomic mass unit) and common Pb using the model Pb composition of Stacey & Kramers (1975)

Sample	Analysis	U [ppm] ^a	Pb [ppm] ^a	Th/U ^a	RATIOS						AGES [Ma]						Conc. use for conc age	
					$^{207}\text{Pb}/^{235}\text{U}$ ^b	$2\sigma^d$	$^{206}\text{Pb}/^{238}\text{U}$ ^b	$2\sigma^d$	ρho^c	$^{207}\text{Pb}/^{206}\text{Pb}$ ^e	$2\sigma^d$	$^{207}\text{Pb}/^{235}\text{U}$	2σ	$^{206}\text{Pb}/^{238}\text{U}$	2σ	$^{207}\text{Pb}/^{206}\text{Pb}$	2σ	
208/27-2, 1357.11 m	Zircon_Sample_007	64	34	0.35	14.20	0.52	0.537	0.017	0.84	0.192	0.004	2763	102	2769	70	2759	32	100
208/27-2, 1357.11 m	Zircon_Sample_008	47	25	0.30	13.64	0.53	0.526	0.017	0.84	0.188	0.004	2725	107	2723	73	2726	34	100
208/27-2, 1357.11 m	Zircon_Sample_009	366	198	0.33	14.66	0.40	0.542	0.013	0.86	0.196	0.003	2794	77	2792	53	2795	23	100
208/27-2, 1357.11 m	Zircon_Sample_010	62	33	0.22	13.92	0.50	0.530	0.016	0.84	0.191	0.004	2745	100	2740	68	2748	32	100
208/27-2, 1357.11 m	Zircon_Sample_011	440	240	0.29	14.73	0.40	0.545	0.013	0.86	0.196	0.003	2798	75	2802	52	2794	23	100
208/27-2, 1357.11 m	Zircon_Sample_012	105	57	0.35	14.55	0.49	0.541	0.015	0.85	0.195	0.004	2786	94	2787	65	2785	29	100
208/27-2, 1357.11 m	Zircon_Sample_013	13	7	0.13	14.41	0.89	0.540	0.028	0.84	0.193	0.006	2777	171	2785	116	2771	54	101
208/27-2, 1357.11 m	Zircon_Sample_014	162	87	0.39	14.30	0.44	0.538	0.014	0.85	0.193	0.003	2770	85	2775	59	2766	26	100
208/27-2, 1357.11 m	Zircon_Sample_015	65	35	0.41	14.04	0.54	0.533	0.017	0.84	0.191	0.004	2753	106	2754	73	2752	34	100
208/27-2, 1357.11 m	Zircon_Sample_020	41	22	0.41	14.48	0.63	0.540	0.020	0.84	0.195	0.005	2782	122	2782	83	2782	39	100
208/27-2, 1357.11 m	Zircon_Sample_021	1521	383	0.28	6.44	0.18	0.252	0.006	0.85	0.186	0.003	2037	57	1447	31	2703	24	54
208/27-2, 1357.11 m	Zircon_Sample_022	44	24	0.33	14.74	0.62	0.544	0.019	0.84	0.197	0.004	2798	118	2798	80	2799	37	100
208/27-2, 1357.11 m	Zircon_Sample_023	286	156	0.30	14.84	0.44	0.546	0.014	0.85	0.197	0.003	2805	84	2808	58	2803	26	100
208/27-2, 1357.11 m	Zircon_Sample_024	70	37	0.34	13.80	0.57	0.532	0.018	0.84	0.188	0.004	2736	112	2749	77	2726	37	101
208/27-2, 1357.11 m	Zircon_Sample_025	9	5	0.13	14.01	1.01	0.519	0.031	0.84	0.196	0.008	2751	199	2694	133	2792	64	97
208/27-2, 1357.11 m	Zircon_Sample_026	70	37	0.33	13.70	0.52	0.528	0.017	0.84	0.188	0.004	2729	104	2732	71	2727	34	100
208/27-2, 1357.11 m	Zircon_Sample_027	229	121	0.40	14.05	0.44	0.530	0.014	0.84	0.192	0.003	2753	87	2742	59	2761	28	99
208/27-2, 1357.11 m	Zircon_Sample_029	63	34	0.35	14.86	0.68	0.548	0.021	0.84	0.197	0.005	2806	128	2816	87	2799	41	101
208/27-2, 1357.11 m	Zircon_Sample_034	542	220	0.16	10.26	0.33	0.406	0.011	0.84	0.184	0.003	2459	78	2195	49	2685	29	82
208/27-2, 1357.11 m	Zircon_Sample_035	620	333	0.41	14.65	0.48	0.537	0.015	0.83	0.198	0.004	2793	92	2771	62	2809	29	99
208/27-2, 1357.11 m	Zircon_Sample_036	276	150	0.32	14.78	0.49	0.544	0.015	0.83	0.197	0.004	2801	92	2799	62	2803	29	100

^aU and Pb concentrations and Th/U ratios are calculated relative to GJ-1 reference zircon

^bCorrected for background and within-run Pb/U fractionation and normalised to reference zircon GJ-1 (ID-TIMS values/measured value); ^c $^{207}\text{Pb}/^{235}\text{U}$ calculated using $(^{207}\text{Pb}/^{206}\text{Pb})/(^{238}\text{U}/^{206}\text{Pb} * 1/137.88)$

^dRho is the error correlation defined as the quotient of the propagated errors of the $^{206}\text{Pb}/^{238}\text{U}$ and the $^{207}/^{235}\text{U}$ ratio

^eQuadratic addition of within-run errors (2 SD) and daily reproducibility of GJ-1 (2 SD)

^fCorrected for mass-bias by normalising to GJ-1 reference zircon (-0.6 per atomic mass unit) and common Pb using the model Pb composition of Stacey & Kramers (1975)

Sample	Analysis	U [ppm] ^a	Pb [ppm] ^a	Th/U ^a	RATIOS							AGES [Ma]							Conc.	use for UI age
					$^{207}\text{Pb}/^{235}\text{U}$ ^b	$2\sigma^d$	$^{206}\text{Pb}/^{238}\text{U}$ ^b	$2\sigma^d$	ρho^c	$^{207}\text{Pb}/^{206}\text{Pb}$ ^e	$2\sigma^d$	$^{207}\text{Pb}/^{235}\text{U}$	2σ	$^{206}\text{Pb}/^{238}\text{U}$	2σ	$^{207}\text{Pb}/^{206}\text{Pb}$	2σ	%		
88/02, 13.00 m	Zircon_Sample_085	90	45	0.84	13.23	0.85	0.500	0.030	0.92	0.192	0.005	2696	173	2613	127	2759	41	95	x	
88/02, 13.00 m	Zircon_Sample_086	305	145	0.67	11.98	0.65	0.474	0.025	0.96	0.183	0.003	2603	142	2502	108	2682	25	93	x	
88/02, 13.00 m	Zircon_Sample_087	112	57	0.24	13.22	0.73	0.505	0.027	0.96	0.190	0.003	2696	148	2636	114	2740	26	96	x	
88/02, 13.00 m	Zircon_Sample_088	299	143	0.80	11.95	0.64	0.478	0.025	0.96	0.181	0.003	2600	139	2519	108	2664	23	95	x	
88/02, 13.00 m	Zircon_Sample_089	82	44	0.73	13.87	0.78	0.530	0.028	0.95	0.190	0.003	2741	154	2743	120	2739	29	100	x	
88/02, 13.00 m	Zircon_Sample_090	406	207	0.56	13.11	0.70	0.509	0.026	0.97	0.187	0.003	2688	143	2654	112	2713	23	98	x	
88/02, 13.00 m	Zircon_Sample_091	414	197	0.52	11.84	0.63	0.476	0.025	0.96	0.180	0.003	2592	138	2509	107	2657	23	94	x	
88/02, 13.00 m	Zircon_Sample_092	789	307	0.42	8.69	0.46	0.389	0.020	0.97	0.162	0.002	2306	123	2118	93	2477	23	86	x	
88/02, 13.00 m	Zircon_Sample_093	202	106	0.63	13.43	0.77	0.524	0.028	0.95	0.186	0.003	2711	155	2715	120	2707	30	100	x	
88/02, 13.00 m	Zircon_Sample_094	77	40	0.58	13.56	0.76	0.514	0.027	0.95	0.191	0.003	2720	153	2673	117	2755	28	97	x	
88/02, 13.00 m	Zircon_Sample_098	50	26	0.42	13.85	0.81	0.528	0.029	0.94	0.190	0.004	2739	161	2733	123	2744	33	100	x	
88/02, 13.00 m	Zircon_Sample_099	157	78	0.76	12.52	0.75	0.497	0.028	0.93	0.183	0.004	2644	159	2600	120	2678	36	97	x	
88/02, 13.00 m	Zircon_Sample_100	331	139	0.63	9.87	0.57	0.419	0.023	0.94	0.171	0.003	2423	139	2255	103	2568	31	88	x	
88/02, 13.00 m	Zircon_Sample_101	227	93	0.48	9.60	0.53	0.407	0.021	0.96	0.171	0.003	2397	131	2202	98	2566	27	86	x	
88/02, 13.00 m	Zircon_Sample_102	138	69	0.56	12.57	0.74	0.499	0.028	0.94	0.183	0.004	2648	156	2610	118	2677	33	97	x	
88/02, 13.00 m	Zircon_Sample_103	439	201	0.42	11.22	0.61	0.458	0.024	0.96	0.178	0.003	2541	138	2431	105	2630	25	92	x	
88/02, 13.00 m	Zircon_Sample_104	464	169	0.70	7.86	0.44	0.364	0.019	0.95	0.157	0.003	2215	125	2002	92	2419	30	83	x	
88/02, 13.00 m	Zircon_Sample_105	522	197	0.51	8.29	0.45	0.378	0.020	0.96	0.159	0.003	2264	123	2068	92	2446	27	85	x	
88/02, 13.00 m	Zircon_Sample_106	172	91	0.52	14.00	0.78	0.530	0.028	0.95	0.192	0.003	2750	153	2742	118	2755	28	100	x	
88/02, 13.00 m	Zircon_Sample_107	842	287	0.43	6.88	0.38	0.341	0.018	0.95	0.146	0.002	2096	115	1892	86	2303	28	82	x	
88/02, 13.00 m	Zircon_Sample_111	302	108	0.19	7.90	0.45	0.359	0.019	0.94	0.159	0.003	2219	126	1979	91	2449	32	81	x	
88/02, 13.00 m	Zircon_Sample_112	142	73	0.23	13.64	0.78	0.517	0.028	0.94	0.191	0.004	2725	155	2686	118	2755	31	98	x	
88/02, 13.00 m	Zircon_Sample_113	344	167	0.43	12.06	0.67	0.485	0.026	0.95	0.180	0.003	2609	145	2548	111	2657	29	96	x	
88/02, 13.00 m	Zircon_Sample_114	337	134	0.46	9.21	0.53	0.398	0.022	0.94	0.168	0.003	2359	137	2159	100	2537	34	85	x	
88/02, 13.00 m	Zircon_Sample_115	465	191	0.64	9.81	0.56	0.411	0.022	0.94	0.173	0.003	2417	138	2219	101	2588	32	86	x	

^aU and Pb concentrations and Th/U ratios are calculated relative to GJ-1 reference zircon^bCorrected for background and within-run Pb/U fractionation and normalised to reference zircon GJ-1 (ID-TIMS values/measured value); $^{207}\text{Pb}/^{235}\text{U}$ calculated using $(^{207}\text{Pb}/^{206}\text{Pb})/(^{238}\text{U}/^{206}\text{Pb} * 1/137.88)$ ^cRho is the error correlation defined as the quotient of the propagated errors of the $^{206}\text{Pb}/^{238}\text{U}$ and the $^{207}/^{235}\text{U}$ ratio^dQuadratic addition of within-run errors (2 SD) and daily reproducibility of GJ-1 (2 SD)^eCorrected for mass-bias by normalising to GJ-1 reference zircon (-0.6 per atomic mass unit) and common Pb using the model Pb composition of Stacey & Kramers (1975)

Sample	Analysis	U [ppm] ^a	Pb [ppm] ^a	Th/U ^a	RATIOS						AGES [Ma]						Conc.	use for conc age
					$^{207}\text{Pb}/^{235}\text{U}$ ^b	$2\sigma^d$	$^{206}\text{Pb}/^{238}\text{U}$ ^b	$2\sigma^d$	ρho^c	$^{207}\text{Pb}/^{206}\text{Pb}$ ^e	$2\sigma^d$	$^{207}\text{Pb}/^{235}\text{U}$	2σ	$^{206}\text{Pb}/^{238}\text{U}$	2σ	$^{207}\text{Pb}/^{206}\text{Pb}$	2σ	
59-04/85DM	Zircon_Sample_046	623	277	0.07	11.28	0.54	0.444	0.020	0.94	0.184	0.003	2547	123	2371	90	2690	27	88
59-04/85DM	Zircon_Sample_047	411	205	0.21	12.16	0.59	0.499	0.023	0.95	0.177	0.003	2617	127	2610	99	2621	26	100
59-04/85DM	Zircon_Sample_048	113	61	0.61	13.90	0.68	0.534	0.024	0.93	0.189	0.003	2743	135	2756	102	2733	30	101
59-04/85DM	Zircon_Sample_049	167	88	0.27	13.95	0.68	0.526	0.024	0.94	0.192	0.003	2746	133	2723	102	2764	26	99
59-04/85DM	Zircon_Sample_050	125	66	0.05	13.64	0.68	0.527	0.024	0.93	0.188	0.004	2725	136	2727	103	2724	31	100
59-04/85DM	Zircon_Sample_051	143	76	0.27	14.02	0.70	0.532	0.025	0.94	0.191	0.003	2751	138	2751	106	2751	28	100
59-04/85DM	Zircon_Sample_052	520	275	0.23	14.02	0.68	0.529	0.024	0.94	0.192	0.003	2751	133	2739	102	2761	26	99
59-04/85DM	Zircon_Sample_053	177	95	0.35	14.05	0.69	0.536	0.025	0.94	0.190	0.003	2753	135	2765	104	2745	26	101
59-04/85DM	Zircon_Sample_054	415	222	0.32	14.04	0.67	0.533	0.024	0.95	0.191	0.003	2753	132	2756	102	2751	25	100
59-04/85DM	Zircon_Sample_055	617	325	0.15	13.92	0.67	0.527	0.024	0.95	0.191	0.003	2744	132	2731	101	2754	25	99
59-04/85DM	Zircon_Sample_059	177	66	0.21	9.90	0.49	0.375	0.017	0.93	0.192	0.003	2425	120	2051	81	2757	29	74
59-04/85DM	Zircon_Sample_060	173	77	0.12	11.83	0.59	0.446	0.021	0.93	0.192	0.004	2591	129	2379	92	2761	30	86
59-04/85DM	Zircon_Sample_061	122	65	0.28	13.86	0.71	0.534	0.025	0.90	0.188	0.004	2740	140	2759	103	2727	37	101
59-04/85DM	Zircon_Sample_062	547	288	0.15	13.83	0.69	0.527	0.025	0.93	0.190	0.004	2738	137	2731	104	2744	30	100
59-04/85DM	Zircon_Sample_063	195	107	0.19	15.15	0.75	0.549	0.026	0.94	0.200	0.004	2825	141	2821	106	2828	28	100
59-04/85DM	Zircon_Sample_064	176	94	0.46	13.98	0.69	0.532	0.025	0.93	0.191	0.003	2748	136	2749	104	2748	29	100
59-04/85DM	Zircon_Sample_065	245	124	0.73	12.97	0.64	0.505	0.023	0.94	0.186	0.003	2677	131	2636	100	2708	28	97
59-04/85DM	Zircon_Sample_066	265	132	0.42	12.23	0.60	0.500	0.023	0.94	0.177	0.003	2622	129	2614	99	2628	28	99
59-04/85DM	Zircon_Sample_067	158	84	0.35	13.85	0.74	0.529	0.026	0.92	0.190	0.004	2739	146	2738	110	2740	33	100
59-04/85DM	Zircon_Sample_068	516	282	0.51	15.71	0.77	0.547	0.025	0.94	0.208	0.004	2859	139	2813	104	2892	27	97
59-04/85DM	Zircon_Sample_072	53	29	0.55	13.99	0.76	0.534	0.026	0.90	0.190	0.004	2749	149	2760	110	2742	38	101
59-04/85DM	Zircon_Sample_073	70	37	0.70	13.73	0.73	0.530	0.025	0.88	0.188	0.005	2731	145	2741	105	2724	40	101
59-04/85DM	Zircon_Sample_074	261	136	0.11	13.43	0.69	0.522	0.024	0.91	0.186	0.004	2710	138	2709	103	2711	35	100
59-04/85DM	Zircon_Sample_075	680	363	0.05	14.11	0.71	0.534	0.025	0.92	0.191	0.004	2757	139	2760	104	2755	32	100
59-04/85DM	Zircon_Sample_076	563	299	0.17	14.20	0.73	0.531	0.025	0.92	0.194	0.004	2763	141	2748	105	2775	33	99

^aU and Pb concentrations and Th/U ratios are calculated relative to GJ-1 reference zircon

^bCorrected for background and within-run Pb/U fractionation and normalised to reference zircon GJ-1 (ID-TIMS values/measured value); $^{207}\text{Pb}/^{235}\text{U}$ calculated using $(^{207}\text{Pb}/^{206}\text{Pb})/(^{238}\text{U}/^{206}\text{Pb} * 1/137.88)$

^cRho is the error correlation defined as the quotient of the propagated errors of the $^{206}\text{Pb}/^{238}\text{U}$ and the $^{207}/^{235}\text{U}$ ratio

^dQuadratic addition of within-run errors (2 SD) and daily reproducibility of GJ-1 (2 SD)

^eCorrected for mass-bias by normalising to GJ-1 reference zircon (-0.6 per atomic mass unit) and common Pb using the model Pb composition of Stacey & Kramers (1975)

Sample	Analysis	U [ppm] ^a	Pb [ppm] ^a	Th/U ^a	RATIOS						AGES [Ma]						Conc.	use for conc age	
					$^{207}\text{Pb}/^{235}\text{U}$ ^b	$2\sigma^d$	$^{206}\text{Pb}/^{238}\text{U}$ ^b	$2\sigma^d$	ρ_{ho}^c	$^{207}\text{Pb}/^{206}\text{Pb}$ ^e	$2\sigma^d$	$^{207}\text{Pb}/^{235}\text{U}$ ^b	2σ	$^{206}\text{Pb}/^{238}\text{U}$ ^b	2σ	$^{207}\text{Pb}/^{206}\text{Pb}$ ^e	2σ		
59-04/186DM	Zircon_Sample_007	47	26	0.27	15.06	0.44	0.548	0.012	0.75	0.199	0.008	2819	82	2815	49	2822	61	100	x
59-04/186DM	Zircon_Sample_008	167	92	0.22	15.20	0.30	0.549	0.009	0.83	0.201	0.004	2828	57	2820	38	2833	36	100	x
59-04/186DM	Zircon_Sample_009	108	57	0.19	14.07	0.32	0.527	0.009	0.72	0.194	0.006	2754	63	2729	36	2773	51	98	
59-04/186DM	Zircon_Sample_010	85	41	0.49	13.34	0.33	0.488	0.008	0.66	0.198	0.007	2704	67	2561	35	2814	60	91	
59-04/186DM	Zircon_Sample_011	77	43	0.19	15.23	0.47	0.552	0.015	0.88	0.200	0.006	2830	88	2835	63	2826	48	100	x
59-04/186DM	Zircon_Sample_012	194	107	0.06	15.13	0.29	0.551	0.009	0.81	0.199	0.004	2823	55	2828	36	2820	36	100	x
59-04/186DM	Zircon_Sample_013	201	110	0.09	15.07	0.31	0.549	0.009	0.80	0.199	0.005	2820	58	2821	38	2819	40	100	x
59-04/186DM	Zircon_Sample_014	165	90	0.12	15.07	0.30	0.545	0.009	0.82	0.200	0.005	2819	55	2805	36	2830	37	99	x
59-04/186DM	Zircon_Sample_015	196	107	0.22	15.00	0.31	0.547	0.009	0.84	0.199	0.004	2815	58	2814	39	2816	36	100	x
59-04/186DM	Zircon_Sample_016	175	86	0.11	13.43	0.30	0.491	0.008	0.71	0.198	0.006	2711	61	2577	34	2812	51	92	
59-04/186DM	Zircon_Sample_020	63	35	0.19	15.58	0.49	0.556	0.015	0.86	0.203	0.006	2851	89	2851	62	2851	50	100	x
59-04/186DM	Zircon_Sample_024	61	35	0.35	15.79	0.69	0.574	0.024	0.94	0.199	0.006	2864	126	2926	97	2821	50	104	
59-04/186DM	Zircon_Sample_025	42	23	0.27	15.37	0.74	0.556	0.025	0.92	0.201	0.007	2838	136	2848	102	2831	59	101	x
59-04/186DM	Zircon_Sample_028	41	24	0.25	16.24	0.65	0.580	0.020	0.88	0.203	0.008	2891	115	2947	83	2852	60	103	
59-04/186DM	Zircon_Sample_033	56	32	0.33	15.89	0.67	0.574	0.022	0.90	0.201	0.007	2870	120	2926	88	2831	59	103	
59-04/186DM	Zircon_Sample_034	39	21	0.30	15.03	0.52	0.549	0.016	0.83	0.199	0.008	2817	98	2819	66	2816	61	100	x
59-04/186DM	Zircon_Sample_035	113	62	0.38	15.39	0.42	0.550	0.013	0.83	0.203	0.006	2839	78	2825	52	2849	50	99	x
59-04/186DM	Zircon_Sample_036	42	23	0.35	15.35	0.50	0.550	0.015	0.82	0.202	0.008	2837	93	2824	62	2846	59	99	x
59-04/186DM	Zircon_Sample_037	84	46	0.26	15.03	0.38	0.550	0.012	0.82	0.198	0.006	2817	72	2823	48	2812	46	100	x
59-04/186DM	Zircon_Sample_038	60	33	0.24	15.12	0.53	0.551	0.017	0.88	0.199	0.007	2823	99	2830	71	2818	54	100	x
59-04/186DM	Zircon_Sample_039	184	95	0.02	13.04	0.28	0.516	0.009	0.83	0.183	0.004	2682	58	2684	39	2681	39	100	
59-04/186DM	Zircon_Sample_040	129	70	0.20	15.05	0.38	0.547	0.012	0.86	0.199	0.005	2819	72	2815	50	2821	41	100	x
59-04/186DM	Zircon_Sample_041	93	51	0.43	15.22	0.41	0.552	0.012	0.81	0.200	0.006	2829	76	2833	50	2826	50	100	x
59-04/186DM	Zircon_Sample_042	46	25	0.26	15.21	0.48	0.551	0.014	0.84	0.200	0.007	2828	88	2830	60	2827	55	100	x
59-04/186DM	Zircon_Sample_046	41	23	0.27	15.45	0.60	0.556	0.019	0.89	0.202	0.007	2843	111	2849	80	2839	56	100	x
59-04/186DM	Zircon_Sample_048	82	45	0.22	15.23	0.66	0.553	0.021	0.88	0.200	0.008	2830	123	2837	87	2824	67	100	x
59-04/186DM	Zircon_Sample_050	92	52	0.35	15.62	0.54	0.565	0.018	0.91	0.201	0.006	2854	98	2886	73	2832	45	102	
59-04/186DM	Zircon_Sample_052	30	17	0.37	15.54	1.05	0.561	0.036	0.96	0.201	0.008	2849	193	2871	150	2833	62	101	x
59-04/186DM	Zircon_Sample_053	44	24	0.28	15.10	0.53	0.551	0.015	0.77	0.199	0.009	2822	100	2829	63	2817	72	100	x
59-04/186DM	Zircon_Sample_054	33	18	0.39	15.23	0.59	0.552	0.018	0.83	0.200	0.009	2830	110	2832	74	2828	68	100	x
59-04/186DM	Zircon_Sample_064	45	25	0.28	15.10	0.56	0.551	0.018	0.87	0.199	0.007	2822	105	2831	74	2816	59	101	x
59-04/186DM	Zircon_Sample_065	17	9	0.25	14.60	0.84	0.543	0.028	0.89	0.195	0.010	2790	160	2795	116	2786	82	100	x
59-04/186DM	Zircon_Sample_072	75	43	0.10	15.75	0.49	0.576	0.015	0.81	0.198	0.007	2862	90	2932	60	2813	58	104	
59-04/186DM	Zircon_Sample_073	32	18	0.37	15.24	0.79	0.551	0.026	0.91	0.201	0.009	2830	147	2830	108	2830	69	100	x
59-04/186DM	Zircon_Sample_074	60	33	0.18	15.24	0.78	0.551	0.025	0.89	0.201	0.009	2830	145	2828	104	2832	75	100	x
59-04/186DM	Zircon_Sample_075	51	28	0.43	14.97	0.58	0.547	0.018	0.87	0.198	0.008</td								

Sample	Analysis	U [ppm] ^a	Pb [ppm] ^a	Th/U ^a	RATIOS						AGES [Ma]						Conc.	use for UI age	
					$^{207}\text{Pb}/^{235}\text{U}$ ^b	$2\sigma^d$	$^{206}\text{Pb}/^{238}\text{U}$ ^b	$2\sigma^d$	ρ_{ho}^c	$^{207}\text{Pb}/^{206}\text{Pb}$ ^e	$2\sigma^d$	$^{207}\text{Pb}/^{235}\text{U}$	2σ	$^{206}\text{Pb}/^{238}\text{U}$	2σ	$^{207}\text{Pb}/^{206}\text{Pb}$	2σ		
206/12-1, 1716.65 m	Zircon_Sample_276	218	115	0.40	13.86	0.35	0.527	0.012	0.91	0.191	0.004	2740	68	2730	51	2748	34	99	x
206/12-1, 1716.65 m	Zircon_Sample_277	227	120	0.36	13.76	0.34	0.530	0.012	0.91	0.188	0.004	2733	68	2742	51	2727	34	101	x
206/12-1, 1716.65 m	Zircon_Sample_278	255	104	0.36	10.36	0.26	0.406	0.009	0.91	0.185	0.004	2468	62	2195	42	2701	34	81	x
206/12-1, 1716.65 m	Zircon_Sample_279	401	199	0.62	12.76	0.32	0.496	0.011	0.91	0.187	0.004	2662	66	2595	49	2714	34	96	x
206/12-1, 1716.65 m	Zircon_Sample_280	260	103	0.53	10.19	0.25	0.396	0.009	0.91	0.187	0.004	2452	61	2148	42	2714	34	79	x
206/12-1, 1716.65 m	Zircon_Sample_281	387	143	0.50	9.49	0.24	0.370	0.008	0.91	0.186	0.004	2387	60	2029	40	2708	33	75	x
206/12-1, 1716.65 m	Zircon_Sample_282	229	117	0.90	13.11	0.33	0.510	0.012	0.91	0.187	0.004	2688	67	2656	50	2712	34	98	x
206/12-1, 1716.65 m	Zircon_Sample_283	525	118	0.54	5.58	0.14	0.224	0.005	0.91	0.181	0.004	1914	48	1304	27	2658	34	49	x
206/12-1, 1716.65 m	Zircon_Sample_284	440	166	0.52	9.74	0.24	0.378	0.009	0.91	0.187	0.004	2410	60	2065	40	2717	33	76	x
206/12-1, 1716.65 m	Zircon_Sample_285	306	120	0.55	10.13	0.25	0.392	0.009	0.91	0.188	0.004	2447	61	2130	41	2721	33	78	x
206/12-1, 1716.65 m	Zircon_Sample_286	333	100	0.33	8.03	0.20	0.299	0.007	0.91	0.195	0.004	2235	56	1686	34	2784	34	61	x
206/12-1, 1716.65 m	Zircon_Sample_287	297	158	0.65	13.88	0.35	0.530	0.012	0.91	0.190	0.004	2742	69	2741	51	2742	33	100	x
206/12-1, 1716.65 m	Zircon_Sample_288	58	31	0.68	13.90	0.35	0.529	0.012	0.91	0.191	0.004	2743	69	2738	51	2747	34	100	x
206/12-1, 1716.65 m	Zircon_Sample_289	20	11	0.71	13.76	0.36	0.528	0.012	0.90	0.189	0.004	2733	71	2734	52	2733	38	100	x
206/12-1, 1716.65 m	Zircon_Sample_290	59	31	1.50	13.68	0.35	0.525	0.012	0.91	0.189	0.004	2728	69	2719	51	2735	35	99	x
206/12-1, 1716.65 m	Zircon_Sample_293	155	81	0.26	13.75	0.34	0.524	0.012	0.91	0.190	0.004	2732	69	2718	51	2743	34	99	x
206/12-1, 1716.65 m	Zircon_Sample_294	166	90	0.67	14.25	0.36	0.539	0.012	0.91	0.192	0.004	2766	69	2781	52	2756	34	101	x
206/12-1, 1716.65 m	Zircon_Sample_295	121	64	1.49	13.78	0.35	0.527	0.012	0.91	0.190	0.004	2735	69	2728	51	2740	34	100	x
206/12-1, 1716.65 m	Zircon_Sample_296	407	175	0.71	11.24	0.28	0.429	0.010	0.91	0.190	0.004	2543	64	2301	44	2743	33	84	x
206/12-1, 1716.65 m	Zircon_Sample_297	263	115	0.58	11.30	0.28	0.437	0.010	0.91	0.188	0.004	2548	64	2336	45	2721	33	86	x
206/12-1, 1716.65 m	Zircon_Sample_298	211	93	0.53	11.64	0.29	0.440	0.010	0.91	0.192	0.004	2576	65	2352	45	2758	33	85	x
206/12-1, 1716.65 m	Zircon_Sample_299	267	141	1.07	14.00	0.35	0.530	0.012	0.91	0.192	0.004	2749	69	2741	51	2756	33	99	x
206/12-1, 1716.65 m	Zircon_Sample_300	48	25	1.35	13.24	0.34	0.511	0.012	0.91	0.188	0.004	2697	68	2663	50	2723	35	98	x
206/12-1, 1716.65 m	Zircon_Sample_301	211	112	0.61	14.04	0.35	0.530	0.012	0.91	0.192	0.004	2752	69	2742	51	2760	34	99	x
206/12-1, 1716.65 m	Zircon_Sample_302	170	75	0.63	11.49	0.29	0.442	0.010	0.91	0.189	0.004	2564	64	2359	45	2731	34	86	x
206/12-1, 1716.65 m	Zircon_Sample_303	517	171	0.67	8.42	0.21	0.331	0.008	0.91	0.184	0.004	2277	57	1846	37	2691	34	69	x
206/12-1, 1716.65 m	Zircon_Sample_304	18	10	1.76	14.86	0.39	0.546	0.013	0.90	0.197	0.004	2806	73	2808	53	2805	37	100	x
206/12-1, 1716.65 m	Zircon_Sample_305	24	13	2.97	15.08	0.39	0.546	0.013	0.90	0.200	0.004	2820	73	2809	53	2828	36	99	x
206/12-1, 1716.65 m	Zircon_Sample_306	249	132	0.44	13.89	0.35	0.531	0.012	0.91	0.190	0.004	2742	69	2745	51	2740	33	100	x
206/12-1, 1716.65 m	Zircon_Sample_307	371	173	0.38	12.01	0.30	0.466	0.011	0.91	0.187	0.004	2605	66	2468	47	2713	33	91	x
206/12-1, 1716.65 m	Zircon_Sample_310	139	73	0.34	13.74	0.35	0.526	0.012	0.91	0.189	0.004	2732	69	2726	51	2736	34	100	x
206/12-1, 1716.65 m	Zircon_Sample_311	343	112	0.30	8.33	0.21	0.326	0.008	0.91	0.185	0.004	2268	57	1818	36	2702	34	67	x
206/12-1, 1716.65 m	Zircon_Sample_312	174	87	0.42	13.09	0.33	0.502	0.012	0.91	0.189	0.004	2686	68	2622	50	2735	34	96	x
206/12-1, 1716.65 m	Zircon_Sample_313	244	90	0.50	9.53	0.24	0.368	0.008	0.91	0.188	0.004	2391	60	2021	40	2722	34	74	x
206/12-1, 1716.65 m	Zircon_Sample_314	820	162	0.58															

^aCorrected for mass-bias by normalising to GJ-1 reference zircon (~0.6 per atomic mass unit) and common Pb using the model Pb composition of Stacey & Kramers (1975)

Supplementary files #2- Cover Sequences Detrital Zircon Data

Sample	Analysis	U [ppm] ^a	Pb [ppm] ^a	Th/U ^a	RATIOS						AGES [Ma]						Conc.	
					$^{207}\text{Pb}/^{235}\text{U}$ ^b	$2\sigma^d$	$^{206}\text{Pb}/^{238}\text{U}$ ^b	$2\sigma^d$	ρ_{ho}^c	$^{207}\text{Pb}/^{206}\text{Pb}$ ^e	$2\sigma^d$	$^{207}\text{Pb}/^{235}\text{U}$ ^b	2σ	$^{206}\text{Pb}/^{238}\text{U}$ ^b	2σ	$^{207}\text{Pb}/^{206}\text{Pb}$ ^e	2σ	
213/23-1, 3598.36 m	Zircon_sample-007	88	49	1.54	16.62	0.40	0.563	0.013	0.93	0.214	0.002	2913	23	2880	52	2936	14	98
213/23-1, 3598.36 m	Zircon_sample-008	779	390	2.23	12.52	0.65	0.501	0.025	0.95	0.181	0.003	2644	49	2619	106	2663	28	98
213/23-1, 3598.36 m	Zircon_sample-009	422	107	0.58	6.32	0.47	0.254	0.017	0.90	0.180	0.006	2021	65	1460	87	2656	55	55
213/23-1, 3598.36 m	Zircon_sample-010	675	146	0.46	4.97	0.43	0.215	0.017	0.92	0.167	0.006	1814	73	1258	91	2530	57	50
213/23-1, 3598.36 m	Zircon_sample-011	165	91	1.71	15.16	0.87	0.552	0.015	0.47	0.199	0.010	2826	55	2831	61	2821	83	100
213/23-1, 3598.36 m	Zircon_sample-012	285	99	0.64	9.03	0.12	0.346	0.003	0.76	0.189	0.002	2341	12	1916	16	2735	14	70
213/23-1, 3598.36 m	Zircon_sample-014	190	104	0.37	15.08	1.18	0.547	0.020	0.47	0.200	0.014	2821	75	2812	84	2827	112	99
213/23-1, 3598.36 m	Zircon_sample-015	313	165	0.91	13.35	0.22	0.529	0.008	0.92	0.183	0.001	2704	15	2736	33	2681	11	102
213/23-1, 3598.36 m	Zircon_sample-016	1086	289	0.72	6.01	0.28	0.266	0.010	0.80	0.164	0.005	1978	40	1521	50	2496	46	61
213/23-1, 3598.36 m	Zircon_sample-020	700	246	0.92	8.58	0.50	0.351	0.020	0.95	0.177	0.003	2295	53	1941	94	2627	30	74
213/23-1, 3598.36 m	Zircon_sample-021	165	103	0.67	19.76	1.44	0.621	0.015	0.32	0.231	0.016	3080	70	3113	58	3058	110	102
213/23-1, 3598.36 m	Zircon_sample-022	290	161	1.53	15.12	0.57	0.555	0.020	0.94	0.198	0.002	2823	36	2844	81	2807	20	101
213/23-1, 3598.36 m	Zircon_sample-023	99	62	0.99	26.89	0.66	0.620	0.013	0.85	0.314	0.004	3379	24	3111	52	3543	20	88
213/23-1, 3598.36 m	Zircon_sample-024	259	115	1.14	11.41	0.20	0.442	0.006	0.77	0.187	0.002	2557	16	2362	26	2717	18	87
213/23-1, 3598.36 m	Zircon_sample-025	428	193	1.13	11.59	0.61	0.450	0.023	0.98	0.187	0.002	2572	49	2395	103	2715	17	88
213/23-1, 3598.36 m	Zircon_sample-026	195	62	0.41	8.44	0.60	0.318	0.019	0.86	0.192	0.007	2280	64	1782	95	2761	58	65
213/23-1, 3598.36 m	Zircon_sample-027	191	97	1.31	13.92	0.79	0.506	0.029	0.99	0.199	0.002	2744	54	2641	122	2820	15	94
213/23-1, 3598.36 m	Zircon_sample-028	219	115	0.95	14.28	0.38	0.526	0.014	0.99	0.197	0.001	2768	26	2725	59	2800	6	97
213/23-1, 3598.36 m	Zircon_sample-029	769	221	0.24	6.82	0.29	0.288	0.012	0.95	0.172	0.002	2088	38	1630	58	2576	21	63
213/23-1, 3598.36 m	Zircon_sample-033	302	169	2.09	15.72	0.72	0.560	0.018	0.68	0.204	0.007	2860	44	2866	73	2856	55	100
213/23-1, 3598.36 m	Zircon_sample-034	244	58	1.49	5.98	0.34	0.237	0.012	0.88	0.183	0.005	1972	49	1369	62	2682	44	51
213/23-1, 3598.36 m	Zircon_sample-035	121	49	0.47	10.65	0.22	0.407	0.006	0.71	0.190	0.003	2493	19	2203	27	2739	24	80
213/23-1, 3598.36 m	Zircon_sample-036	279	152	0.56	14.90	0.67	0.547	0.023	0.92	0.197	0.004	2809	43	2813	95	2805	29	100
213/23-1, 3598.36 m	Zircon_sample-037	636	320	0.31	12.55	0.88	0.503	0.035	0.98	0.181	0.003	2647	66	2627	149	2662	23	99
213/23-1, 3598.36 m	Zircon_sample-038	487	147	2.15	7.87	0.58	0.303	0.022	0.97	0.189	0.003	2216	67	1704	107	2730	30	62
213/23-1, 3598.36 m	Zircon_sample-039	1607	535	0.20	12.47	1.61	0.333	0.017	0.40	0.272	0.032	2640	122	1852	84	3316	186	56
213/23-1, 3598.36 m	Zircon_sample-040	202	110	1.18	16.48	0.62	0.547	0.016	0.77	0.218	0.005	2905	36	2813	66	2970	39	95
213/23-1, 3598.36 m	Zircon_sample-041	486	230	0.44	12.79	0.48	0.473	0.015	0.84	0.196	0.004	2664	36	2497	66	2794	34	89
213/23-1, 3598.36 m	Zircon_sample-042	356	186	0.32	13.55	0.61	0.524	0.017	0.72	0.187	0.006	2719	43	2717	72	2720	52	100
213/23-1, 3598.36 m	Zircon_sample-046	241	138	0.28	15.97	1.02	0.571	0.034	0.93	0.203	0.005	2875	61	2912	139	2849	37	102
213/23-1, 3598.36 m	Zircon_sample-047	598	269	0.15	12.42	0.50	0.449	0.014	0.80	0.200	0.005	2637	38	2392	64	2830	40	85
213/23-1, 3598.36 m	Zircon_sample-048	236	127	0.60	15.86	0.58	0.541	0.018	0.89	0.213	0.003	2869	35	2786	73	2927	26	95
213/23-1, 3598.36 m	Zircon_sample-049	210	65	0.26	4.60	0.18	0.312	0.008	0.69	0.107	0.003	1750	33	1750	41	1751	52	100
213/23-1, 3598.36 m	Zircon_sample-050	204	130	0.67	21.65	1.10	0.635	0.024	0.75	0.247	0.008	3168	49	3171	96	3166	53	100
213/23-1, 3598.36 m	Zircon_sample-051	284	149	1.11	13.48	1.05	0.524	0.031	0.75	0.187	0.010	2714	74	2717	130	2712	84	100
213/23-1, 3598																		

^aU and Pb concentrations and Th/U ratios are calculated relative to GJ-1 reference zircon

^bCorrected for background and within-run Pb/U fractionation and normalised to reference zircon GJ-1 (ID-TIMS values/measured value); $^{207}\text{Pb}/^{235}\text{U}$ calculated using $(^{207}\text{Pb}/^{206}\text{Pb})/(^{238}\text{U}/^{206}\text{Pb} * 1/137.88)$

^cRho is the error correlation defined as the quotient of the propagated errors of the $^{206}\text{Pb}/^{238}\text{U}$ and the $^{207}/^{235}\text{U}$ ratio

^dQuadratic addition of within-run errors (2 SD) and daily reproducibility of GJ-1 (2 SD)

^eCorrected for mass-bias by normalising to GJ-1 reference zircon (-0.6 per atomic mass unit) and common Pb using the model Pb composition of Stacey & Kramers (1975)

Sample	Analysis	U [ppm] ^a	Pb [ppm] ^a	Th/U ^a	RATIOS						AGES [Ma]						Conc.	
					$^{207}\text{Pb}/^{235}\text{U}$ ^b	$2\sigma^d$	$^{206}\text{Pb}/^{238}\text{U}$ ^b	$2\sigma^d$	ρ_{ho}^c	$^{207}\text{Pb}/^{206}\text{Pb}$ ^e	$2\sigma^d$	$^{207}\text{Pb}/^{235}\text{U}$	2σ	$^{206}\text{Pb}/^{238}\text{U}$	2σ	$^{207}\text{Pb}/^{206}\text{Pb}$	2σ	
204/27-1, 2094.65 m	Zircon_sample-007	142	77	0.45	14.10	0.32	0.544	0.009	0.71	0.188	0.003	2757	22	2800	37	2725	26	103
204/27-1, 2094.65 m	Zircon_sample-008	21	11	0.35	13.43	0.45	0.517	0.009	0.53	0.189	0.005	2710	32	2685	39	2729	47	98
204/27-1, 2094.65 m	Zircon_sample-009	73	36	0.65	13.18	0.32	0.500	0.008	0.68	0.191	0.003	2693	23	2614	36	2752	29	95
204/27-1, 2094.65 m	Zircon_sample-010	257	134	0.15	13.57	0.48	0.521	0.017	0.92	0.189	0.003	2720	34	2703	72	2734	23	99
204/27-1, 2094.65 m	Zircon_sample-011	46	25	0.84	14.14	0.44	0.536	0.015	0.90	0.191	0.003	2759	29	2767	62	2754	22	100
204/27-1, 2094.65 m	Zircon_sample-012	608	321	0.48	14.42	0.51	0.528	0.015	0.82	0.198	0.004	2778	34	2733	65	2810	33	97
204/27-1, 2094.65 m	Zircon_sample-013	43	23	0.44	13.74	0.43	0.522	0.006	0.37	0.191	0.006	2732	30	2708	26	2750	48	98
204/27-1, 2094.65 m	Zircon_sample-014	900	334	0.03	9.30	0.51	0.371	0.017	0.83	0.182	0.006	2368	51	2032	80	2670	51	76
204/27-1, 2094.65 m	Zircon_sample-020	121	66	0.73	14.53	0.50	0.544	0.014	0.73	0.194	0.005	2785	33	2800	57	2775	39	101
204/27-1, 2094.65 m	Zircon_sample-021	127	66	0.27	13.54	0.44	0.518	0.014	0.86	0.190	0.003	2718	30	2691	61	2739	27	98
204/27-1, 2094.65 m	Zircon_sample-022	422	156	0.17	9.47	0.27	0.369	0.009	0.87	0.186	0.003	2385	26	2024	43	2710	23	75
204/27-1, 2094.65 m	Zircon_sample-023	193	105	0.24	14.06	0.28	0.542	0.006	0.56	0.188	0.003	2754	19	2793	25	2725	27	102
204/27-1, 2094.65 m	Zircon_sample-024	199	106	0.59	13.98	0.56	0.536	0.019	0.89	0.189	0.003	2748	38	2765	80	2736	30	101
204/27-1, 2094.65 m	Zircon_sample-025	164	73	0.63	11.72	0.39	0.444	0.009	0.58	0.192	0.005	2583	31	2367	38	2757	45	86
204/27-1, 2094.65 m	Zircon_sample-026	36	19	0.62	13.65	0.54	0.527	0.014	0.68	0.188	0.005	2725	37	2730	60	2722	47	100
204/27-1, 2094.65 m	Zircon_sample-027	179	97	1.41	14.40	0.40	0.543	0.013	0.85	0.192	0.003	2777	26	2797	53	2762	24	101
204/27-1, 2094.65 m	Zircon_sample-028	83	42	1.12	13.45	0.46	0.508	0.012	0.71	0.192	0.005	2712	33	2649	53	2759	40	96
204/27-1, 2094.65 m	Zircon_sample-029	1141	293	0.01	5.70	0.18	0.257	0.006	0.76	0.161	0.003	1931	28	1472	32	2467	36	60
204/27-1, 2094.65 m	Zircon_sample-033	148	73	0.29	12.56	0.23	0.490	0.006	0.66	0.186	0.003	2647	17	2569	25	2707	22	95
204/27-1, 2094.65 m	Zircon_sample-034	20	10	0.23	12.80	0.69	0.493	0.020	0.75	0.188	0.007	2665	51	2582	86	2728	58	95
204/27-1, 2094.65 m	Zircon_sample-035	83	41	0.36	13.37	0.54	0.492	0.015	0.74	0.197	0.005	2706	38	2581	65	2801	44	92
204/27-1, 2094.65 m	Zircon_sample-036	47	24	0.75	13.70	0.43	0.517	0.009	0.58	0.192	0.005	2729	30	2687	40	2761	42	97
204/27-1, 2094.65 m	Zircon_sample-037	72	37	0.39	13.05	0.51	0.510	0.012	0.61	0.185	0.006	2683	37	2659	51	2701	51	98
204/27-1, 2094.65 m	Zircon_sample-038	70	36	0.40	13.30	0.51	0.519	0.009	0.46	0.186	0.006	2701	37	2695	39	2706	57	100
204/27-1, 2094.65 m	Zircon_sample-039	28	15	0.71	14.22	0.48	0.537	0.009	0.52	0.192	0.006	2764	32	2769	39	2761	47	100
204/27-1, 2094.65 m	Zircon_sample-041	66	22	0.75	8.59	0.24	0.328	0.008	0.87	0.190	0.003	2296	25	1829	38	2742	23	67
204/27-1, 2094.65 m	Zircon_sample-042	214	113	0.51	13.55	0.58	0.526	0.020	0.87	0.187	0.004	2719	41	2725	83	2715	35	100
204/27-1, 2094.65 m	Zircon_sample-047	318	121	0.25	9.48	0.55	0.381	0.021	0.93	0.180	0.004	2385	53	2080	96	2657	36	78
204/27-1, 2094.65 m	Zircon_sample-048	72	39	1.09	14.69	0.41	0.546	0.008	0.51	0.195	0.005	2796	26	2809	32	2786	39	101
204/27-1, 2094.65 m	Zircon_sample-049	370	157	0.70	10.71	0.45	0.423	0.009	0.53	0.183	0.007	2498	39	2276	43	2684	59	85
204/27-1, 2094.65 m	Zircon_sample-050	284	155	0.26	13.93	0.30	0.544	0.009	0.74	0.186	0.003	2745	20	2801	36	2704	24	104
204/27-1, 2094.65 m	Zircon_sample-051	80	42	2.29	13.60	0.45	0.526	0.012	0.69	0.187	0.004	2722	31	2725	50	2720	39	100
204/27-1, 2094.65 m	Zircon_sample-052	1880	934	0.16	11.88	0.57	0.496	0.017	0.69	0.174	0.006	2595	45	2599	71	2592	58	100
204/27-1, 2094.65 m	Zircon_sample-053	60	31	0.86	13.42	0.56	0.518	0.012	0.53	0.188	0.007	2709	39	2689	49	2724	58	99
204/27-1, 2094.65 m	Zircon_sample-054	113	62	0.85	15.69	0.82	0.554	0.027	0.93	0.205	0.004	2858	50	2843	112	2868	30	99
204/27-1, 2094.65 m	Zircon_sample-055	365	107	0.77	7.20	0.26	0.293	0.008	0.80	0.178	0.004							

Sample	Analysis	U [ppm] ^a	Pb [ppm] ^a	Th/U ^a	RATIOS						AGES [Ma]						Conc.	
					$^{207}\text{Pb}/^{235}\text{U}$ ^b	$2\sigma^d$	$^{206}\text{Pb}/^{238}\text{U}$ ^b	$2\sigma^d$	ρ_{ho}^c	$^{207}\text{Pb}/^{206}\text{Pb}$ ^e	$2\sigma^d$	$^{207}\text{Pb}/^{235}\text{U}$ ^b	2σ	$^{206}\text{Pb}/^{238}\text{U}$ ^b	2σ	$^{207}\text{Pb}/^{206}\text{Pb}$ ^b	2σ	%
2023-1 1642.50 m	Zircon_sample-007	217	106	0.18	13.41	0.45	0.490	0.013	0.78	0.198	0.004	2709	32	2573	56	2812	34	91
2023-1 1642.50 m	Zircon_sample-008	2295	360	0.20	3.05	0.35	0.157	0.015	0.84	0.141	0.009	1420	89	939	85	2240	109	42
2023-1 1642.50 m	Zircon_sample-010	134	71	1.68	13.64	0.64	0.527	0.015	0.61	0.188	0.007	2725	44	2729	63	2722	61	100
2023-1 1642.50 m	Zircon_sample-011	2306	346	0.25	2.93	0.16	0.150	0.005	0.57	0.142	0.006	1389	40	900	25	2247	76	40
2023-1 1642.50 m	Zircon_sample-012	307	155	1.05	12.98	0.37	0.504	0.003	0.22	0.187	0.005	2678	27	2631	13	2714	45	97
2023-1 1642.50 m	Zircon_sample-013	55	30	0.67	15.10	0.76	0.557	0.013	0.45	0.197	0.009	2822	48	2853	53	2799	73	102
2023-1 1642.50 m	Zircon_sample-015	321	171	0.75	14.04	0.93	0.534	0.011	0.31	0.191	0.012	2752	63	2756	45	2749	104	100
2023-1 1642.50 m	Zircon_sample-016	282	99	0.52	9.68	0.35	0.352	0.011	0.86	0.199	0.004	2404	33	1943	52	2822	29	69
2023-1 1642.50 m	Zircon_sample-020	34	19	0.34	14.81	1.00	0.546	0.022	0.59	0.197	0.011	2803	65	2810	91	2797	90	100
2023-1 1642.50 m	Zircon_sample-021	117	63	0.73	14.28	0.98	0.540	0.021	0.58	0.192	0.011	2769	65	2783	89	2758	92	101
2023-1 1642.50 m	Zircon_sample-022	380	183	0.63	12.37	0.76	0.482	0.018	0.61	0.186	0.009	2633	58	2535	79	2710	80	94
2023-1 1642.50 m	Zircon_sample-024	246	98	0.91	10.55	0.74	0.397	0.025	0.90	0.193	0.006	2485	65	2155	115	2767	51	78
2023-1 1642.50 m	Zircon_sample-025	104	56	0.93	14.45	0.66	0.539	0.016	0.64	0.195	0.007	2780	43	2778	66	2781	58	100
2023-1 1642.50 m	Zircon_sample-026	148	78	1.70	13.80	0.38	0.526	0.009	0.63	0.190	0.004	2736	26	2724	39	2744	35	99
2023-1 1642.50 m	Zircon_sample-027	732	293	0.25	10.34	0.60	0.400	0.016	0.68	0.187	0.008	2466	54	2170	73	2720	70	80
2023-1 1642.50 m	Zircon_sample-028	230	85	0.88	9.76	0.84	0.371	0.019	0.59	0.191	0.013	2413	79	2032	89	2751	114	74
2023-1 1642.50 m	Zircon_sample-029	199	52	1.30	7.03	0.56	0.260	0.020	0.97	0.196	0.004	2116	71	1489	103	2796	29	53
2023-1 1642.50 m	Zircon_sample-033	822	193	0.39	2.80	0.18	0.234	0.009	0.61	0.087	0.004	1356	48	1358	48	1353	97	100
2023-1 1642.50 m	Zircon_sample-034	2930	199	0.20	1.68	0.15	0.068	0.006	0.95	0.179	0.005	1001	59	424	36	2648	46	16
2023-1 1642.50 m	Zircon_sample-036	717	105	0.99	3.84	0.46	0.146	0.017	0.98	0.191	0.005	1602	97	878	97	2751	39	32
2023-1 1642.50 m	Zircon_sample-037	85	46	1.24	13.72	0.46	0.533	0.007	0.42	0.187	0.006	2731	32	2754	31	2713	50	101
2023-1 1642.50 m	Zircon_sample-038	431	204	0.91	12.60	0.40	0.473	0.013	0.88	0.193	0.003	2650	30	2496	58	2770	25	90
2023-1 1642.50 m	Zircon_sample-039	873	189	0.86	5.45	0.42	0.216	0.007	0.39	0.183	0.013	1892	66	1261	35	2678	117	47
2023-1 1642.50 m	Zircon_sample-040	238	64	0.50	7.01	0.20	0.267	0.007	0.85	0.190	0.003	2112	26	1527	34	2743	25	56
2023-1 1642.50 m	Zircon_sample-041	377	97	0.83	6.64	0.47	0.258	0.018	0.98	0.187	0.003	2065	63	1478	92	2714	23	54
2023-1 1642.50 m	Zircon_sample-042	290	124	1.03	11.31	0.36	0.428	0.013	0.98	0.192	0.001	2549	29	2297	60	2757	11	83
2023-1 1642.50 m	Zircon_sample-046	21	8	0.41	7.10	0.44	0.390	0.015	0.63	0.132	0.006	2124	56	2122	71	2127	85	100
2023-1 1642.50 m	Zircon_sample-047	114	60	0.49	14.21	1.07	0.528	0.021	0.52	0.195	0.013	2764	71	2734	87	2786	105	98
2023-1 1642.50 m	Zircon_sample-048	175	94	0.40	13.92	0.78	0.534	0.015	0.50	0.189	0.009	2744	53	2759	63	2733	80	101
2023-1 1642.50 m	Zircon_sample-049	261	87	0.50	5.51	0.15	0.332	0.008	0.91	0.120	0.001	1903	24	1850	40	1960	20	94
2023-1 1642.50 m	Zircon_sample-050	216	32	0.91	1.56	0.08	0.149	0.004	0.61	0.076	0.003	954	30	898	25	1086	78	83
2023-1 1642.50 m	Zircon_sample-051	2475	222	0.39	1.51	0.10	0.090	0.005	0.77	0.122	0.005	935	41	553	28	1991	77	28
2023-1 1642.50 m	Zircon_sample-052	1437	126	0.70	2.23	0.11	0.088	0.003	0.70	0.184	0.006	1191	34	544	18	2688	57	20
2023-1 1642.50 m	Zircon_sample-053	113	60	0.37	14.10	0.87	0.534	0.026	0.78	0.191	0.007	2756	58	2760	107	2753	63	100
2023-1 1642.50 m	Zircon_sample-054	1220	181	0.57	3.82	0.31	0.148	0.012	0.96	0.187	0.004	1597	65	892	65	2713	38	33
2023-1 1642.50 m	Zircon_sample-055	1283	178	0.75	3.94	0.15	0.138	0.003	0.61	0.206	0.006	1622	30	836	18	2878	48	29
2023-1 1																		

Sample	Analysis	U [ppm] ^a	Pb [ppm] ^a	Th/U ^a	RATIOS						AGES [Ma]						Conc.	
					$^{207}\text{Pb}/^{235}\text{U}$ ^b	$2\sigma^d$	$^{206}\text{Pb}/^{238}\text{U}$ ^b	$2\sigma^d$	ρho^c	$^{207}\text{Pb}/^{206}\text{Pb}$ ^e	$2\sigma^d$	$^{207}\text{Pb}/^{235}\text{U}$ ^b	2σ	$^{206}\text{Pb}/^{238}\text{U}$ ^b	2σ	$^{207}\text{Pb}/^{206}\text{Pb}$ ^b	2σ	%
206/4-1 4115 m	Zircon_sample-007	203	106	0.77	13.66	0.52	0.524	0.016	0.79	0.189	0.004	2727	36	2715	67	2735	39	99
206/4-1 4115 m	Zircon_sample-009	519	266	0.90	12.92	0.53	0.512	0.019	0.89	0.183	0.003	2674	39	2667	79	2679	31	100
206/4-1 4115 m	Zircon_sample-011	97	51	0.84	13.64	0.40	0.521	0.009	0.59	0.190	0.005	2725	28	2704	39	2741	39	99
206/4-1 4115 m	Zircon_sample-012	128	68	1.04	13.84	0.40	0.533	0.011	0.70	0.188	0.004	2739	27	2755	45	2728	34	101
206/4-1 4115 m	Zircon_sample-013	326	183	0.40	14.44	0.29	0.561	0.006	0.54	0.187	0.003	2779	19	2870	25	2713	28	106
206/4-1 4115 m	Zircon_sample-014	257	136	0.61	13.63	0.32	0.527	0.008	0.64	0.188	0.003	2725	22	2729	33	2721	30	100
206/4-1 4115 m	Zircon_sample-015	749	392	0.39	13.27	0.23	0.524	0.007	0.75	0.184	0.002	2699	17	2714	29	2687	19	101
206/4-1 4115 m	Zircon_sample-016	894	480	0.18	14.14	1.06	0.537	0.024	0.60	0.191	0.011	2759	72	2771	102	2751	99	101
206/4-1 4115 m	Zircon_sample-020	881	478	0.88	14.28	0.56	0.543	0.014	0.66	0.191	0.006	2769	37	2794	58	2750	48	102
206/4-1 4115 m	Zircon_sample-021	121	65	1.18	14.06	0.37	0.540	0.011	0.74	0.189	0.003	2754	25	2783	44	2732	29	102
206/4-1 4115 m	Zircon_sample-022	447	236	0.89	13.38	0.30	0.528	0.008	0.66	0.184	0.003	2707	21	2732	33	2688	28	102
206/4-1 4115 m	Zircon_sample-024	362	192	0.25	13.52	0.41	0.529	0.008	0.48	0.185	0.005	2717	29	2736	33	2702	44	101
206/4-1 4115 m	Zircon_sample-025	179	96	0.74	13.92	0.30	0.538	0.006	0.52	0.188	0.003	2744	20	2773	25	2723	30	102
206/4-1 4115 m	Zircon_sample-026	783	400	0.69	12.99	0.63	0.510	0.013	0.54	0.185	0.007	2679	46	2658	57	2694	67	99
206/4-1 4115 m	Zircon_sample-028	201	108	0.83	13.96	0.33	0.537	0.007	0.55	0.189	0.004	2747	22	2770	29	2730	32	101
206/4-1 4115 m	Zircon_sample-029	186	98	0.48	13.50	0.21	0.524	0.005	0.64	0.187	0.002	2715	15	2716	22	2714	20	100
206/4-1 4115 m	Zircon_sample-033	477	231	0.60	12.33	0.30	0.484	0.002	0.19	0.185	0.004	2630	23	2543	10	2697	40	94
206/4-1 4115 m	Zircon_sample-034	839	435	0.50	12.90	0.58	0.519	0.016	0.68	0.180	0.006	2673	42	2694	67	2657	54	101
206/4-1 4115 m	Zircon_sample-036	169	90	0.63	13.96	0.39	0.533	0.013	0.91	0.190	0.002	2747	26	2755	56	2741	19	100
206/4-1 4115 m	Zircon_sample-037	240	129	0.49	13.98	0.26	0.537	0.005	0.45	0.189	0.003	2749	18	2773	19	2731	28	102
206/4-1 4115 m	Zircon_sample-038	215	114	0.51	13.73	0.30	0.532	0.005	0.44	0.187	0.004	2731	20	2750	21	2718	32	101
206/4-1 4115 m	Zircon_sample-039	351	196	0.68	14.27	0.26	0.559	0.008	0.76	0.185	0.002	2768	17	2864	32	2698	20	106
206/4-1 4115 m	Zircon_sample-040	987	505	0.35	12.88	0.64	0.511	0.024	0.94	0.183	0.003	2671	47	2662	102	2677	28	99
206/4-1 4115 m	Zircon_sample-046	203	111	0.39	14.11	0.30	0.545	0.008	0.67	0.188	0.003	2757	20	2805	32	2722	26	103
206/4-1 4115 m	Zircon_sample-047	400	211	0.41	13.80	0.38	0.526	0.013	0.88	0.190	0.003	2736	26	2725	54	2744	22	99
206/4-1 4115 m	Zircon_sample-050	601	326	0.83	13.60	0.23	0.542	0.006	0.67	0.182	0.002	2722	16	2793	26	2671	21	105
206/4-1 4115 m	Zircon_sample-051	131	71	1.90	14.17	0.25	0.541	0.005	0.51	0.190	0.003	2761	17	2789	20	2741	25	102
206/4-1 4115 m	Zircon_sample-052	157	84	0.62	13.99	0.33	0.537	0.010	0.76	0.189	0.003	2749	22	2771	40	2733	25	101
206/4-1 4115 m	Zircon_sample-053	312	138	0.81	11.30	0.39	0.442	0.012	0.77	0.186	0.004	2548	32	2358	53	2703	37	87
206/4-1 4115 m	Zircon_sample-054	282	148	1.12	13.54	0.20	0.525	0.005	0.68	0.187	0.002	2718	14	2721	22	2717	18	100
206/4-1 4115 m	Zircon_sample-055	202	105	0.65	13.62	0.28	0.521	0.006	0.61	0.190	0.003	2724	19	2702	27	2740	27	99
206/4-1 4115 m	Zircon_sample-059	179	94	0.95	13.72	0.32	0.525	0.008	0.65	0.189	0.003	2730	22	2722	34	2736	30	99
206/4-1 4115 m	Zircon_sample-060	1379	511	0.59	9.42	0.26	0.370	0.009	0.91	0.185	0.002	2380	25	2030	43	2694	19	75
206/4-1 4115 m	Zircon_sample-061	573	315	0.33	14.09	0.22	0.549	0.006	0.72	0.186	0.002	2756	15	2821	25	2708	18	104
206/4-1 4115 m	Zircon_sample-062	61	32	0.81	13.48	0.36	0.525	0.008	0.53	0.186	0.004	2714	25	2720	32	2709	38	100
206/4-1 4115 m	Zircon_sample-063	113	61	1.06	14.45	0.45	0.541	0.010	0.61	0.194	0.005	2779	30	2787	43	2774	41	100
206/4-1 4115 m	Zircon_sample-064	125	71</															

Supplementary files #3 - Basement Lu-Hf Data

LA-MC-ICPMS Lu-Hf isotope data of zircon from basement samples west of Shetland

lab number	$^{176}\text{Yb}/^{177}\text{Hf}$	$\pm 2\sigma$	$^{176}\text{Lu}/^{177}\text{Hf}^a$	$\pm 2\sigma$	$^{178}\text{Hf}/^{177}\text{Hf}$	$^{180}\text{Hf}/^{177}\text{Hf}$	Sig _{Hf} ^b	$^{176}\text{Hf}/^{177}\text{Hf}$	$\pm 2\sigma^c$	$^{176}\text{Hf}/^{177}\text{Hf}_{(t)}^d$	$\varepsilon\text{Hf}(t)^d$	$\pm 2\sigma^c$	T _{DM} ^e	age ^f	$\pm 2\sigma$	
							(V)							(Ga)	(Ma)	
11686_86	0.0125	11	0.00042	3	1.46719	1.88692	15	0.281069	23	0.281048	0.9	0.8	2.89	2739	31	
11686_87	0.0097	8	0.00033	2	1.46715	1.88657	14	0.281060	27	0.281043	0.6	1.0	2.90	2732	36	
11686_89	0.0191	25	0.00064	7	1.46721	1.88687	13	0.281097	18	0.281063	1.3	0.6	2.87	2731	29	
11686_90	0.0168	14	0.00056	4	1.46715	1.88670	12	0.281076	28	0.281046	1.1	1.0	2.89	2749	31	
11686_92	0.0157	13	0.00050	3	1.46720	1.88689	29	0.281095	15	0.281069	1.5	0.5	2.85	2732	32	
11686_93	0.0112	9	0.00039	2	1.46724	1.88670	36	0.281082	28	0.281062	1.1	1.0	2.87	2723	28	
11686_94	0.0165	13	0.00054	3	1.46717	1.88687	31	0.281085	18	0.281057	0.6	0.6	2.89	2712	29	
11686_98	0.0160	14	0.00052	4	1.46719	1.88677	27	0.281094	19	0.281067	1.7	0.7	2.85	2743	35	
11686_100	0.0125	11	0.00044	3	1.46716	1.88658	25	0.281069	23	0.281047	0.7	0.8	2.90	2731	27	
11686_101	0.0115	9	0.00038	2	1.46718	1.88679	30	0.281068	28	0.281048	0.8	1.0	2.89	2733	32	
11686_102	0.0096	8	0.00031	2	1.46723	1.88681	26	0.281078	16	0.281060	4.0	0.6	2.81	2852	101	
11686_103	0.0130	12	0.00041	3	1.46720	1.88685	13	0.281096	21	0.281075	1.7	0.7	2.84	2730	36	
11686_104	0.0124	10	0.00039	2	1.46718	1.88678	13	0.281078	21	0.281057	0.9	0.7	2.88	2726	33	
11686_106	0.0094	8	0.00033	2	1.46717	1.88677	27	0.281062	19	0.281045	0.2	0.7	2.91	2715	32	
11686_107	0.0152	13	0.00049	3	1.46721	1.88671	29	0.281091	17	0.281066	-0.3	0.6	2.90	2658	36	
11686_111	0.0114	10	0.00039	3	1.46723	1.88694	15	0.281096	41	0.281076	1.5	1.4	2.84	2724	33	
11686_113	0.0149	12	0.00050	3	1.46713	1.88662	14	0.281070	24	0.281044	1.0	0.8	2.90	2746	34	
11691-48	0.0127	13	0.00048	4	1.46725	1.88682	16	0.281049	17	0.281024	0.0	0.6	2.94	2738	24	
11691-50	0.0366	60	0.00129	19	1.46730	1.88683	13	0.281091	23	0.281024	0.0	0.8	2.94	2737	30	
11691-51	0.0286	26	0.00102	7	1.46724	1.88672	16	0.281082	21	0.281029	-0.1	0.8	2.94	2722	24	
11691-55	0.0084	8	0.00032	2	1.46725	1.88684	17	0.281027	17	0.281010	-0.9	0.6	2.98	2717	30	
11691-59	0.0108	9	0.00043	3	1.46731	1.88681	19	0.281030	19	0.281007	-0.1	0.7	2.96	2757	26	
11691-60	0.0178	17	0.00070	6	1.46727	1.88692	18	0.281056	19	0.281019	-0.4	0.7	2.95	2728	27	
11691-62	0.0176	17	0.00062	5	1.46732	1.88676	18	0.281044	18	0.281012	-0.9	0.6	2.97	2716	26	
11691-63	0.0169	18	0.00063	6	1.46726	1.88690	17	0.281042	17	0.281009	-0.7	0.6	2.97	2729	37	
11691-64	0.0111	9	0.00039	2	1.46731	1.88689	16	0.281038	16	0.281017	-0.9	0.6	2.97	2709	29	
11691-66	0.0274	27	0.00104	8	1.46726	1.88679	19	0.281065	17	0.281011	-0.8	0.6	2.97	2723	26	
11691-72	0.0266	22	0.00093	6	1.46729	1.88675	14	0.281054	22	0.281005	-0.6	0.8	2.98	2738	27	
11691-73	0.0067	6	0.00024	2	1.46731	1.88670	15	0.281042	23	0.281029	0.1	0.8	2.93	2735	36	
11694-14	0.0155	13	0.00062	4	1.46725	1.88683	38	0.280935	12	0.280903	-3.6	0.4	3.16	2767	20	
11694-24	0.0116	12	0.00041	3	1.46721	1.88688	33	0.280930	12	0.280909	-3.7	0.4	3.16	2751	27	
11694-25	0.0122	10	0.00043	3	1.46723	1.88683	27	0.280957	13	0.280934	-2.3	0.5	3.10	2774	37	
11694-26	0.0076	6	0.00027	2	1.46724	1.88676	29	0.280922	16	0.280908	-3.3	0.6	3.15	2772	26	
11694-28	0.0129	10	0.00045	3	1.46728	1.88691	31	0.280922	12	0.280897	-1.5	0.4	3.13	2865	20	
11694-29	0.0078	6	0.00027	2	1.46731	1.88683	27	0.280919	13	0.280905	-4.6	0.5	3.18	2722	27	
11694-37	0.0099	8	0.00035	2	1.46726	1.88687	25	0.280955	18	0.280937	-3.6	0.6	3.12	2714	43	
11694-38	0.0098	8	0.00035	2	1.46721	1.88698	31	0.280923	13	0.280904	-3.1	0.5	3.15	2786	31	
11694-39	0.0183	16	0.00060	4	1.46723	1.88678	35	0.280961	14	0.280929	-3.2	0.5	3.12	2745	24	
11694-46	0.0165	16	0.00056	4	1.46724	1.88658	14	0.281050	18	0.281020	-0.1	0.6	2.95	2737	31	
11694-50	0.0106	9	0.00037	2	1.46727	1.88670	16	0.280941	18	0.280921	-3.6	0.6	3.14	2738	30	
11694-51	0.0115	10	0.00041	3	1.46715	1.88696	30	0.280932	16	0.280911	-4.7	0.6	3.18	2708	42	
11694-53	0.0154	14	0.00053	4	1.46719	1.88687	24	0.280968	14	0.280940	-3.5	0.5	3.11	2715	46	
11694-54	0.010															

11700-10	0.0087	7	0.00030	2	1.46733	1.88651	14	0.280878	22	0.280862	-5.5	0.8	3.25	2748	32
11700-11	0.0092	7	0.00031	2	1.46724	1.88665	14	0.280880	18	0.280863	-4.4	0.6	3.23	2794	23
11700-13	0.0093	11	0.00032	3	1.46715	1.88688	5	0.280886	36	0.280869	-4.7	1.3	3.23	2771	54
11700-14	0.0095	8	0.00033	2	1.46733	1.88652	11	0.280897	22	0.280879	-4.4	0.8	3.21	2766	26
11700-15	0.0125	12	0.00042	3	1.46728	1.88682	15	0.280900	21	0.280878	-4.8	0.7	3.22	2752	34
11700-20	0.0087	8	0.00031	2	1.46721	1.88663	3	0.281021	25	0.281005	0.4	0.9	2.96	2782	39
11700-21	0.2419	235	0.00555	42	1.46722	1.88675	20	0.280923	26	0.280636	-14.6	0.9	3.71	2703	24
11700-23	0.0109	9	0.00037	2	1.46716	1.88660	12	0.280884	24	0.280864	-4.1	0.9	3.22	2803	26
11700-25	0.0100	10	0.00033	2	1.46734	1.88656	15	0.280875	27	0.280857	-4.6	1.0	3.24	2792	64
11700-27	0.0095	9	0.00033	2	1.46715	1.88674	7	0.280873	30	0.280856	-5.4	1.1	3.26	2761	28
11700-36	0.0111	11	0.00037	3	1.46734	1.88688	12	0.280880	23	0.280860	-4.3	0.8	3.23	2803	29
11705-85	0.0154	13	0.00053	3	1.46725	1.88684	13	0.280966	19	0.280938	-2.5	0.7	3.10	2759	41
11705-87	0.0091	9	0.00036	3	1.46726	1.88678	17	0.280962	19	0.280944	-2.8	0.7	3.10	2740	26
11705-89	0.0096	8	0.00035	2	1.46728	1.88678	14	0.280971	16	0.280953	-2.5	0.6	3.08	2739	29
11705-90	0.0221	18	0.00081	5	1.46727	1.88680	17	0.281004	16	0.280962	-2.7	0.6	3.07	2713	23
11705-92	0.0207	21	0.00085	7	1.46727	1.88674	17	0.281010	16	0.280970	-8.0	0.6	3.17	2477	23
11705-93	0.0170	14	0.00067	4	1.46729	1.88690	18	0.281001	16	0.280967	-2.7	0.6	3.07	2707	30
11705-94	0.0093	8	0.00035	2	1.46728	1.88670	16	0.280960	19	0.280942	-2.5	0.7	3.09	2755	28
11705-98	0.0176	19	0.00061	6	1.46725	1.88670	14	0.281000	18	0.280967	-1.8	0.6	3.05	2744	33
11705-112	0.0090	8	0.00034	2	1.46733	1.88686	17	0.280975	17	0.280957	-2.0	0.6	3.06	2755	31
11705-116	0.0179	21	0.00069	7	1.46732	1.88681	16	0.280994	21	0.280958	-1.9	0.7	3.06	2755	32
11711-07	0.0172	15	0.00065	5	1.46728	1.88666	13	0.281050	18	0.281016	1.0	0.7	2.93	2791	39
11711-08	0.0148	12	0.00057	4	1.46726	1.88678	12	0.281055	19	0.281024	2.3	0.7	2.89	2833	36
11711-09	0.0173	15	0.00061	4	1.46720	1.88657	11	0.281078	20	0.281046	0.7	0.7	2.90	2733	36
11711-12	0.0206	20	0.00079	6	1.46731	1.88664	12	0.281072	22	0.281030	1.4	0.8	2.90	2786	36
11711-13	0.0143	12	0.00055	3	1.46724	1.88672	12	0.281045	22	0.281015	0.8	0.8	2.93	2786	34
11711-14	0.0170	15	0.00065	4	1.46732	1.88667	12	0.281066	21	0.281031	1.6	0.7	2.90	2793	35
11711-15	0.0126	13	0.00046	4	1.46715	1.88697	16	0.281053	25	0.281028	2.0	0.9	2.89	2814	35
11711-36	0.0127	11	0.00049	3	1.46717	1.88671	13	0.281034	23	0.281007	1.8	0.8	2.92	2836	57
11711-37	0.0177	22	0.00065	7	1.46724	1.88651	11	0.281051	25	0.281016	1.2	0.9	2.93	2799	45
11711-38	0.0155	15	0.00057	4	1.46714	1.88663	8	0.281076	24	0.281045	2.6	0.9	2.86	2815	59
11711-42	0.0122	10	0.00047	3	1.46718	1.88697	6	0.281053	27	0.281027	2.2	1.0	2.89	2827	55
Plesovice (n=7)	0.0055	32	0.00014	8	1.46730	1.88670	14	0.282476	20	0.282475	-3.4	0.7	1.17	338	3
GJ-1 (n=7)	0.0076	6	0.00026	0	1.46729	1.88671	9	0.282013	25	0.282010	-13.9	0.9	1.96	606	6
JMC 475 (n=6)					1.46719	1.88669	11	0.282149	8						

Quoted uncertainties (absolute) relate to the last quoted figure. The effect of the inter-element fractionation on the Lu/Hf was estimated to be about 6 % or less based on analyses of the GJ-1 and Plesoviče zircon. Accuracy and reproducibility was checked by repeated analyses (n = 7) of reference zircon GJ-1 and Plesoviče (data given as mean with 2 standard deviation uncertainties)

(a) $^{176}\text{Yb}/^{177}\text{Hf} = (^{176}\text{Yb}/^{173}\text{Yb})_{\text{true}} \times (^{173}\text{Yb}/^{177}\text{Hf})_{\text{meas}} \times (M_{173(\text{Yb})}/M_{177(\text{Hf})})^{\beta(\text{Hf})}$, $\beta(\text{Hf}) = \ln(^{179}\text{Hf}/^{177}\text{Hf}_{\text{true}} / ^{179}\text{Hf}/^{177}\text{Hf}_{\text{measured}}) / \ln(M_{179(\text{Hf})}/M_{177(\text{Hf})})$, M=mass of respective isotope. The $^{176}\text{Lu}/^{177}\text{Hf}$ were calculated in a similar way by using the $^{175}\text{Lu}/^{177}\text{Hf}$.

(b) Mean Hf signal in volt.

(c) Uncertainties are quadratic additions of the within-run precision and the daily reproducibility of the 40ppb-JMC475 solution. Uncertainties for the JMC475 quoted at 2SD (2 standard deviation).

(d) Initial $^{176}\text{Hf}/^{177}\text{Hf}$ and εHf calculated using the apparent Pb-Pb age determined by LA-ICP-MS dating (see column f), and the CHUR parameters:

$^{176}\text{Lu}/^{177}\text{Hf} = 0.0336$, and $^{176}\text{Hf}/^{177}\text{Hf} = 0.282785$ (Bouvier *et al.*, 2008).

(e) two stage model age in billion years using the measured $^{176}\text{Lu}/^{177}\text{Hf}$ of each spot (first stage = age of zircon), a value of 0.0113 for the average continental crust (second stage), and a depleted mantle (DM<, Chauvel *et al.* 2008) $^{176}\text{Lu}/^{177}\text{Hf}$ and $^{176}\text{Hf}/^{177}\text{Hf}$ of 0.0384 and 0.28316, respectively.

(f) apparent Pb-Pb age determined by LA-ICP-MS

GJ1-28-90-100-6	0.0076	6	0.00026	2	1.46727	1.88681	6	0.282027	34	0.282024	-13.4	1.2	1.93	606	9
GJ1-33-90-100-6	0.0075	6	0.00026	2	1.46733	1.88663	6	0.282020	29	0.282017	-13.7	1.0	1.95	606	9
GJ1-33-90-100-6	0.0076	6	0.00026	2	1.46729	1.88649	6	0.282029	21	0.282026	-13.3	0.8	1.93	606	9
GJ1-40-90-100-6	0.0083	7</													